N° d'ordre: 3244

THESIS

Submitted in Fulfillment of the Requirements for the *Degree of PhD*

Research Center: GEOPAC

Research Structure: Laboratory of Geophysics and Natural Hazards

Discipline: Geophysics and Geology

Specialty: Sedimentology and Natural Hazards

Presented and defedend on 23/09/2019 by:

Modeste MELIHO

Soil Erosion Risk Assessment in Relationship to Land Uses and Vegetation Cover through Rainfall Simulations, 137Cs Radioactive Tracer and Modelisation based on GIS and Remote Sensing (High Atlas, Morocco)

JURY

President:

Mohammed FEKHAOUI, PES, Scientific Institute of Rabat, Mohammed V University (Reporter)

Reviewers:

Nadia MHAMMDI, PES, Scientific Institute of Rabat, Mohammed V University (Supervisor)
Abdelfatah TAHIRI, PES, Scientific Institute of Rabat, Mohammed V University (Reporter)
Said LAHSSINI, PH, National School of Forest Engineers of Salé (Reporter)
Abdellatif KHATTABI, PES, National School of Forest Engineers of Salé (Co-supervisor)

Guest:

Asmae NOUIRA, PhD, Researcher, National Center for Energy Sciences and Nuclear Techniques of Rabat

Dedication

I am thankful to my God and my Heavenly Father for giving me all these years to realize without doubt that I am the great sinner and that Jesus Christ is the great Savior.

This is a faithful saying, and worthy of all acceptation, that Christ Jesus came into the world to save sinners, of whom I am the equal first with the Apostle Paul. I give thanks to my Lord Jesus Christ who alone can save such a sinner as me.

Glory be to my Heavenly Father for calling me to do this work, not because the doctoral degree was something in itself, but to give me the opportunity to experience the immensity of his grace for me in Jesus Christ.

Blessed be the God and Father of my Lord Jesus Christ for using the years I have spent doing this work to teach me to count on His grace in Christ, to realize the full sufficiency of His grace for me in His Son Jesus Christ.

Now unto the King eternal, immortal, invisible, the only wise God, be honour and glory forever and ever. Amen.

Father, we shall understand, before Your face above,
Your great goodness for Your elect;
In the ages without end we will bless Your grace
Manifested to us in the work of Jesus.

Without Your sovereign plan, we would not have life,
Through faith which grasps eternal salvation;
We glorify that infinite grace
Which has foreknown us and chosen us for heaven.

Oh wonderful design of the only-wise God:
You desire us in the glory with the First-born!
To surround Your Son and bear His image
Your unsearchable love has predestinated us.

What treasures are hidden in that divine mystery
Which we will sound throughout eternity;
In the perfect happiness of the Father's house
May Your name, our God, be forever exalted!

I found it, I found it, Ineffable happiness! I am saved, I am saved, O inexpressible joy! All my sins are blotted out: The blood of Christ cleanses me. The days of slavery to sins have passed away: I am no longer a slave! To God only wise, be glory through Jesus Christ for ever. Amen.

Acknowledgements

I am very grateful to my thesis supervisor, Mrs. Nadia MHAMMDI, Professor at the Scientific Institute of Rabat, who has agreed to lead my thesis and give me the opportunity to pursue my doctoral studies. I would like to express my sincere thanks for his scientific rigor, his excellent academic orientation and his useful advice to overcome various obstacles during my research. His explanations, suggestions and useful conversations have been important in improving the quality of this thesis. I am honored by the extraordinary kindness I received from her and grateful for all the support she has given me.

All my gratitude and thanks go to my co-supervisor Mr. Abdellatif KHATTABI, Professor at National School of Forest Engineers of Salé, for having granted me the immense privilege of working with him. It has been a great pleasure and a great honor to work with him. I am very grateful to him for having trusted me when I was not worthy. He has always been interested in my work and has followed the progress of my research. He has not stopped providing me with advice, criticisms and judgments that are essential to the progression of my dissertation. He was generous to me infinitely beyond what I could think or imagine. He took care of me as a father takes care of his child. May he find here the testimony of my deep respect and gratitude!

I would like to thank Mr. Mohammed FEKHAOUI, Director of the Scientific Institute of Rabat, for the great honor, he gives me by accepting to be the president of the jury and having accepted to be rapporteur of this work despite all his commitments and his numerous occupations.

Table of content

List of figures

List of tables

List of acronyms

A: Clay

A: Average soil loss

AUC: Area under curve

MBM II: Mass balance model II

BD10: Bulk density between 0 and 10cm

BD20: Bulk density between 10 and 20cm

BD30: Bulk density between 20 and 30cm

C: Cover and management practice factor

C (%): soil organic carbon

CF: Coarse fraction

D: detachability

FC: woodland

FD: dense forest

FMD: moderately dense forest

FR: frequency ratio

H10: humidity at 0-10cm

H20: humidity at 10-20cm

H30: humidity at 20-30cm

GIS: Geographic information system

If: infiltration

InfVal: Information value

K: Soil erodibility factor

Kr: runoff coefficient

L: Silt

LS: Topographic factor

M: scrubland

m: mean

MO: organic matter

MWD: mean weight diameter of soil aggregates

NDVI: Normalized difference vegetation index

P: Conservation support practice factor

P10: porosity at 0-10cm

P20: porosity between 10 and 20cm

P30: porosity between 20 and 30cm

PDM: Profile distribution model

PEN: penetration resistance

Pi: initial abstraction

ROC: Receiver operating characteristic

RUSLE: Revised universal soil loss equation

R: Rainfall erosivity factor

R (%): Surface roughness

S: Sand

SC: covered soil surface

sd: standard deviation

SD: hard substrate (pink granite, andesite, migmatite)

SO: non-crusted soil surface

SOC(t/ha) : Soil organic carbon

SPI: The stream power index

SS: shear strength

ST: soft substrate (red sandstone, red marl, flysch shale and sandstone)

TC: cropland field

TSAVI: Transformed soil adjusted vegetation index

TWI: Topographic wetness index

Xe: thorny xerophytes or bare non-forest land

Abstract

Soil erosion is a major problem around the world because of its effects on soil productivity, nutrient loss, siltation in water bodies, and degradation of water quality. Assessment of soil erosion is useful in planning and conservation works in a watershed or basin. Like the other areas of the High Atlas of Morocco, the Ourika watershed characterized by a very rugged topography, friable substrates, a harsh and brutal climate, a sparse vegetation cover and an increasing human impact, is particularly exposed to the phenomena of soil erosion. The purpose of this study is to study soil erosion using rainfall simulations, fallout radionucleide Cesium-137, RUSLE model and bivariate statistical methods and to highlight the role of landuse and vegetation cover in the control of soil erosion.

The average annual rate of soil erosion in Morocco was estimated at 22.24 t/ha/yr with standard deviation of 78.70 t/ha/yr. The results show that 79.14 % of the country area has low risk of soil erosion, 10.27 % moderate risk, 7.55 % high risk and 3.04 % very high risk. The main predisposing factors of Morocco to water erosion were topography and rainfall erosivity. The results obtained through rainfall simulations show that total infiltration was negatively correlated with penetration resistance ($r = -0.81$) and was positively correlated with both covered and non-crusted soil surfaces ($r = 0, 84$ and $r = 0.83$ respectively), thus confirming the importance of vegetation cover with respect to mitigating runoff and consequently water erosion. A strong correlation was observed between ^{137}Cs and either soil organic carbon or slope gradient, in uncultivated area. However, there was no correlation for cultivated terraces. Indeed, the net erosion rates were estimated about 8.5 and 6.0 t ha^{-1} yr^{-1} in cereal crop and arboriculture agrosystems, respectively, whereas in forest, the net erosion rate was of about 4.2 t ha^{-1} yr^{-1}. The results of gully susceptibility prediction showed that barren and sparse vegetation lands and slope gradient above 50% were very susceptible to gully erosion. The analysis confirms that the frequency ratio model (AUC = 80.61 %) shows a better accuracy than information value model (AUC = 52.07 %).

As the effectiveness of forests and arboriculture in reducing soil erosion has been proven, more efforts need to be made to preserve forests in the upslope sections of the region and encourage arboriculture agrosystems.

Key words: Soil erosion, Rainfall simulations, Cesium-137, RUSLE model, bivariate statistical methods, Landuse, vegetation cover, Morocco.

Résumé

L'érosion des sols est un problème majeur dans le monde entier en raison de ses effets sur la productivité des sols, la perte d'éléments nutritifs, l'envasement et la dégradation de la qualité de l'eau. L'évaluation de l'érosion des sols est utile pour la planification et la conservation dans un bassin versant. Comme les autres régions du Haut Atlas marocain, le bassin versant de l'Ourika, caractérisé par une topographie très accidentée, des substrats friables, un climat rude et brutal, une couverture végétale éparse et un impact humain croissant, est particulièrement exposé aux phénomènes d'érosion des sols. Le but de cette étude est d'étudier l'érosion des sols à l'aide de simulations de pluie, du radioélément césium-137, du modèle RUSLE et de méthodes statistiques bivariées, et de mettre en évidence le rôle de l'utilisation des sols et de la couverture végétale dans le contrôle de l'érosion des sols.

Le taux annuel moyen d'érosion des sols au Maroc a été estimé à 22,24 t/ha/an avec un écart type de 78,70 t/ha/an. Les résultats montrent que 79,14% de la superficie du pays présentent un faible risque d'érosion du sol, 10,27% un risque modéré, 7,55% un risque élevé et 3,04% un risque très élevé. Les principaux facteurs prédisposant le Maroc à l'érosion hydrique sont la topographie et l'érosivité des pluies. Les résultats obtenus lors de simulations de pluie montrent que l'infiltration totale est corrélée négativement avec la résistance à la pénétration (r = -0,81) et positivement avec les surfaces de sol couvertes et ouvertes (r = 0, 84 et r = 0,83 respectivement), ce qui confirme l'importance de la couverture végétale pour atténuer le ruissellement et par conséquent l'érosion hydrique. Une forte corrélation a été observée entre le 137Cs et le carbone organique du sol et le gradient de la pente, sur les terrains non cultivés. Cependant, il n'y avait pas de corrélation sur les terrasses cultivées. En effet, les taux d'érosion nette ont été estimés à environ 8,5 et 6,0 t ha^{-1} an^{-1} dans les agrosystèmes de cultures céréalières et arboricoles, respectivement, alors que dans les forêts, le taux d'érosion nette est d'environ 4,2 t ha^{-1} an^{-1}. Les résultats de la susceptibilité au ravinement ont montré que les sols nus et à végétation claire, les pentes supérieures à 50% sont très sensibles au ravinement. L'analyse confirme que le modèle du rapport de fréquence (AUC = 80,61%) montre une meilleure précision que le modèle de la valeur de l'information (AUC = 52,07%).

Comme l'efficacité des forêts et de l'arboriculture dans la réduction de l'érosion des sols a été prouvée, des efforts supplémentaires doivent être consentis pour préserver les forêts dans les parties montagneuses de la région et encourager les agrosystèmes arboricoles.

Mots clés : Erosion des sols, Simulations de pluie, Césium-137, Modèle RUSLE, Méthodes Statistiques Bivariées, Utilisation des sols, Couvert Végétal, Maroc.

General introduction

1 Thesis motivation and context

In the Mediterranean region, soils are a fragile component of ecosystems. They are sensitive to the risk of erosion due to being exposed to strong and intense rain, causing a marked runoff phenomenon. This is especially accelerated by hilly or mountainous topography (Albergel et al. 2010). With increasing food requirements due to population growth and declining productivity of high-potential land, it is imperative to work on land that is less suitable for agriculture, characterized by unfavorable climatic conditions (Roose 1993). A result of this is the accentuation of vulnerability of the Mediterranean region to water erosion.

Water erosion is the main cause of soil degradation in Morocco. It is a multidimensional natural hazard and an environmental challenge for the ecosystem. Indeed, it is among the most worrying phenomena in water and soil conservation. Water erosion is a very complex phenomenon related to natural and anthropogenic factors that are difficult to control over space and time. Some parts of Morocco are subjected to water erosion during periods of torrential rains, which affect either the topsoil or the surface layer. In Morocco, modeling of water erosion has been the subject of numerous studies based on different approaches, at different scales and requiring significant data for the main factors related to erosion. Several researchers have taken an interest in studying water erosion using several research methods including experimental plots under natural or simulated rainfall (Nafaa 1997; Sabir et al 2004; Laouina et al. 2004; Al Karkouri et al 2000; Sabir et al 2007). Additionally, mapping of erosion has been done using the USLE / RUSLE model (eg Sadiki et al. 2004; Elbouqdaou et al. 2005; Yjjou et al. 2014; Markhi et al. 2015) and radioactive markers (Bouhlassa et al. 2000; Nouira et al. 2003; Sadiki et al. 2007; Benmansour et al. 2013; Damnati et al. 2013).

The High Atlas is the highest mountain range in Morocco, with its highest peak being Mount Toubkal at an altitude of 4167 m. This mountain range is structured in a multitude of watersheds that constitute a veritable water tower for the surrounding arid plains (Boudhar et al. 2007). Nevertheless, the different mountainous areas of the High Atlas are subject to considerable pressures that negatively affect their hydrological functioning and render the High Atlas particularly sensitive to human activity (Maselli 1993; Alifriqui et al. 1993). These include a particularly rugged topography, areas subject to severe erosion, a harsh and brutal climate, vegetation cover often low in density, and increasing human impact. Indeed, in the Atlas mountainous areas, which is with limited resources in the same extent as the High Atlas, man draws directly from the natural environment the resources necessary for his survival. This often leads to a reasonably advanced degradation of these resources (Montes 1999). For instance, the

silvopastoral ecosystems of the Moroccan High Atlas are characterized by significant degradation of their vegetation cover due to an overgrazing which far exceeds the production potential of these environments (Alifriqui 1993; Aderdar, 2000).

The Ourika watershed is a sub-watershed of the larger Tensift basin that lies on the northwestern side of the High Atlas and is one of the most important watersheds in this mountain range (Ouhammou 1986). Thanks to its great geographical, geological and climatic diversity, this watershed is home to a remarkable diversity of forest and pre-forest ecosystems, mainly distinguished by holm oak, cedar, juniper as well as oleo-lentic species (Ouhammou 1986; Achhal 1986). However, the natural ecosystems of this watershed have undergone, during their history, important changes over space and time under the action of several driving factors, notably anthropogenic and ecological factors (Achhal 1986; Ouhammou 1986; Maselli 1993; Alifriqui et al. 1993; El Qayedy 2008). The latter are illustrated by the unfavorable topo-edapho-climatic conditions prevailing in the region (Hammi et al. 2007). Furthermore, the excessive human pressure observed in these regions stems from the fact that the population has not had resources other than the quasi-autarkic exploitation of their environment over an extended period of time: culture under irrigation in the lower valleys as well as pastoralism on the slopes, which is currently aggravated by population growth, in a bioclimatic context that does not allow for optimal plant productivity. Beyond this proven anthropogenic impact, the amplifying effect of climate changes is an added factor whose effect is increasingly apparent (Mateh 1998; Bedhri 2000). These imbalances generate a series of ecological and socio-economic consequences such as the degradation of natural resources and immigration to urban centers.

Similarly to the other areas of the High Atlas, the Ourika watershed perfectly illustrates the problem of the degradation of natural resources and raises many questions regarding the rationality of the management of its resources in the current state as well as in the future. The pressures to which Ourika watershed is subjected: rugged topography, friable substrates, harsh and brutal climate, sparse vegetation cover, and increasing human impact considerably expose the area to the phenomenon of water erosion (Ouhammou 1986; Alifriqui et al. 1993; Hammi 2003; El Qayedy 2008; Cheggour 2008; Meliho 2015). The current state of these ecosystems shows that they have been shaped by both the ancestral and recent human impact, and may evolve in a regressive manner in the context of global climate change. This change is characterized by an increase in temperature, significant reduction in rainfall and the multiplicity of environmental disasters such as acute droughts and catastrophic floods (Mateh 1998; Bedhri 2000).

Economic and social development remain dependent on the rational use of water, whose mobilization and use require greater control. Additionally, the preservation of soil becomes a priority (Cheggour, 2008). However, the sustainable management of these two fundamental resources is threatened by water erosion. Hence, an in-depth study of erosion in the Ourika watershed area, with a view to a better orientation of the land uses for a better management of the soil is of great importance. Nevertheless, water erosion in the Ourika watershed has never been quantified with respect to the different land uses in order to orient the uses of the space for a better conservation of the soil resources of the watershed, of which depend also on the water resources.

The development of a natural resource conservation strategy for the Ourika watershed, the restoration and development of these resources and the adoption of appropriate mechanisms for adapting to the context of climate change require a better understanding of erosion control as a function of the different land uses and density of the vegetation cover in the context of climate change.

2 Thesis objectives

The overall objective of this research is to assess the risks of water erosion in the Ourika watershed using several erosion models and to highlight the role of land use in the control of water erosion.

The specific objectives assigned to this study are:

- Risk mapping of water erosion in Morocco using the RUSLE empirical model, GIS and remote sensing;

- Research and identification of potential indicators of runoff risks and erosion in the Ourika watershed

- Highlighting the relationships between indicators of runoff and erosion risks;

- Quantification of water erosion using ^{137}Cs in the Ourika watershed;

- Quantification of water erosion in the Ourika watershed using the RUSLE model with the accurate determination of the factors of the model.

- Gully erosion susceptibility mapping using GIS and bivariate statistical methods in the Ourika watershed.

- Comparison of the results of the RUSLE model with results obtained using the ^{137}Cs.

- Study of the impact of land use on soil erosion

3 Thesis structure

The thesis begins with a general introduction that includes the specific purpose and objectives of the research, a short bibliographic review and a presentation of the study area. Subsequently, the results are presented in the form of independent chapters, each chapter being the subject of an article published or in the process of being published. The chapters are presented as follows:

Chapter 1. Spatial assessment of Soil erosion risk in Morocco

Chapter 2. Effects of land use and cover type on the risks of runoff and water erosion: Infiltration tests in the Ourika watershed (High Atlas, Morocco)

Chapter 3. Assessment of soil redistribution rates by ^{137}Cs in typical Moroccan High Atlas cultivated and uncultivated soils

Chapter 4. Assessment of the effect of vegetation cover on potential soil erosion risk in a mountainous watershed of Morocco

Chapter 5. A GIS-based approach for gully erosion susceptibility modelling using bivariate statistics methods in the Ourika watershed, Morocco

4 Water erosion: a brief state of knowledge

Water erosion is a complex phenomenon that exceptionally threatens soil and water potential. It is defined as the detachment and transport of soil particles from its original location by different agents to a place of deposit. Thus, the three stages through which erosion occurs are detachment, transport and sedimentation (Laflen and Roose 1997). Rain and surface runoff are responsible for the detachment, transport and deposition of particles. However, it must be pointed out that soil erosion can also be caused by intensification of land use, tillage, construction structures, overgrazing, land use and deforestation (Roose et al. 1993). Either incisions or sediments commonly recognize soil erosion on the surface of the soil.

4.1   Origin and mechanism of water erosion

Soil erosion is a process of stripping the soil surface, whereby soil particles are torn off, transported and deposited elsewhere (Morgan 1995). It is a complex phenomenon that results from three phases: detachment, transport and deposition, caused by the generally combined action of rainfall and runoff.

4.2   Detachment

When considering the mechanism of water erosion, one of the essential actions of atmospheric precipitation is the formation of fine elements that are likely to be carried away by water (Loch & Silburn 1996).). Soil aggregates are usually too large to be easily carried away by runoff. However, raindrops, characterized by their kinetic energy, exert a mechanical effect on these previously moistened aggregates at their point of impact (Boiffin 1976; Boiffin 1984). This effect is manifested by moistening under the effect of raindrops and runoff. The phenomenon begins with bursting, cracking of aggregates and reduction of attractive forces between colloidal particles resulting in detachment by the splash effect (Le Bissonnais 1995). The impact of raindrops can fragment aggregates and especially detach particles from their surface. This mechanism requires rain of a certain energy, which is variable according to the soils. The kinetic energy of the drops is no longer absorbed but is transformed into a shear force that causes detachment and splash.

The energy of a single drop of rain causes erosion by splashing or spilling that can move the particles over tens of centimeters. This distance depends on the mass of the particles and the angle of incidence of raindrops relative to the surface (Leguedois et al. 2005). There is a difference between the splash effect and the structural disaggregation because the former can move aggregates without structural disaggregation in some cases.

The very fine soil particles that are detached from the surface by the impact of the drops are trapped between the coarser elements and can clog the pores of the upper layer of soil. This significantly reduces the rate of infiltration and consequently increases the risks to erosion and surface runoff. Silty soils are particularly affected by this phenomenon. When the crust is formed, subsequent rains, even if they are of low intensity, will generate runoff (Le Bissonnais et al. 2005).

Soil erosion develops when rainwater, which can no longer infiltrate the soil, dribbles over the parcel carrying away the soil particles. This refusal of the soil to absorb the excess water appears either when the intensity of the rains is greater than the infiltrability of the soil surface

(Hortonian runoff), or when the rain arrives on a surface that is either partially or totally saturated by a water table (saturation runoff). It should be noted that detachment by runoff occurs when the friction force of the water on the soil particles is greater than the soil resistance to shear.

Detachment is influenced by several rain-related parameters such as rainfall intensity, speed, shape, diameter, and kinetic energy of raindrops (Lajili 1999). Soil parameters influencing detachment include aggregate stability and diameter, bulk density, matrix potential, and soil shear strength (Gerits et al. 1990).

4.3   Transport

The surface runoff, which provides the transport, is generated either by saturation of the soil porosity or by infiltration refusal resulting from rain whose intensity is greater than the infiltration capacity of the soil surface (Leguedois 2003). Both raindrops and runoff ensure transport. However, it should be noted that the splash transport mode is generally negligible except on a steep slope. On the other hand, runoff is most responsible for transporting loose soil particles. The main variables controlling the action of runoff on detachment and particle transport are slope, velocity and flow thickness (Gimenez and Govers 2002).

4.4   Sedimentation

Particles removed from the soil settle between the origin and the downstream depending on their size, density and the carrying capacity of the runoff or stream. Sediment deposition occurs when the current is no longer able to hold the particles in suspension and results in a slowing of the flow rate, the causes of which can be multiple (Cheggour, 2008).

4.5   Types of water erosion

Water erosion is a process that is manifested by the detachment of soil particles caused largely by the impact of raindrops and the transport of soil particles mainly by runoff (Ellison, 1944, Goldman et al. 1986). It involves a complex and interdependent set of processes that cause the detachment and transport of soil particles. Water erosion is defined as the loss of soil due to water that tears and transports the earth to a place of deposit. Several forms of erosion can be observed.

4.5.1 Splash effect

This is the first stage of water erosion that occurs when soil is directly exposed to the impacts of raindrops and soil particles are disintegrated (Le Bissonnais 1995). Splash is directly related to the intensity of the rains and the size of the raindrops. The manifestation of erosion by splash is subtle and only differs in certain rather peculiar circumstances: a soil subject to strong erosion and which is covered by places of pebbles. The impact of raindrops on the surface loosens the sediment from the soil matrix and transports it to the air where the majority of the splash, and thus the solid transport, is directed down the slope. In general, splash is important for sediment detachment in diffuse erosion but carries relatively little sediment compared to diffuse or concentrated runoff.

4.5.2 Sheet erosion

Sheet erosion is characterized by runoff water with no visible claws or channels. Under the effect of the raindrops (splash effect), the particles are torn off and transported. This phenomenon is observed on weak slopes, where the concentration of water is impossible. Initially, it is the impact of the drops that will tear off the particles. The beat of raindrops will send droplets in all directions. Only under the effect of gravity will the droplets have a greater speed downstream than upstream. From there, the formation of puddles and overflow of non-infiltrated water from one puddle to another occurs, which will cause a runoff in a sheet.

Soil erosion depends on the maximum intensity of rainfall that triggers the runoff, on the kinetic energy of the rains that detach the particles and on the duration of the rains and/or moisture before the rains (Roose 1994). When the intensity of precipitation becomes greater than the infiltration of the soil, sheet erosion takes place. When this occurs, the particles initially move by "splash" effect at a short distance and then by the sheet runoff. The dropping of raindrops sends droplets and particles in all directions. In fact, it is only after formation of puddles and overflowing of the non-infiltrated water from one puddle to another, that the sheet runoff occurs (Goldman et al. 1986). This form of erosion may be significant for soils such as loams that are characterized by low erosion resistance and consist of relatively fine particles that are easy to remove and transport.

Sheet erosion results in a reasonably uniform removal of a thin layer of soil because the energy of the raindrops is applied to the entire soil surface, with the transport of loose material being carried out by sheet runoff (Cheggour 2008). Sheet erosion leads to the leveling of the soil surface through clod degradation and cavity filling. Moreover, skeletonization of the surficial

horizons occurs through selective loss of organic matter and clays, leaving in place a layer of sand and gravel. Stripping of the humus horizon also occurs, revealing the underlying mineral horizon to open air (Roose 1994).

4.5.3 Linear erosion

Linear erosion begins when the flow is concentrated in reasonably large channels and the kinetic energy of the runoff is sufficient to detach the sediments from the soil surface. When the intensity of the rains exceeds the infiltration capacity of the soil surface, the formation of puddles occurs. Subsequently, these puddles disseminate by streams of water and when these streams reach a speed of about 25 cm/s, they acquire their own energy that will create a limited erosion in space by flow lines Hjulström (1935). This energy is no longer scattered over the entire surface of the soil, but is rather focused on lines of steeper slope.

Linear erosion is an indication that runoff has become organized. That it has gained speed and acquired kinetic energy capable of slicing the soil and carrying larger and larger particles: not only clays and silts such as selective sheet erosion, but gravel or pebbles and even blocks. All the linear digs that cut the surface of the ground in various shapes and sizes (claws, channels, gullies, etc) express linear erosion. In fact, it occurs when the sheet runoff is organized, digging deeper into forms. When the small channels are a few centimeters deep they are referred to as claws. On the other hand, when the channels exceed 10 cm of depth but are still erasable by the cultural techniques, they are referred to as gullies. In fact, on a watershed or a plot, rill erosion replaces sheet erosion where concentration of the runoff in the troughs. At this stage, the channels do not converge but form parallel streams.

4.5.4 Gully erosion

Gullying occurs when water flows in narrow channels during or immediately after heavy rain or slush. Gully erosion is the culminating form of soil erosion. The damage caused is all the more important as the stabilization and repair of this form of erosion are the most costly of all erosion control works. Gully formation is a complex process that is not yet understood (Goldman et al. 1986). The deepening of the gullies rises up from the bottom to the top of the slope (regressive erosion). This form of erosion can transform the landscape into badlands.

4.6   Evaluation of water erosion

In general, the quantification of erosion is difficult and depends on both the spatial and temporal scales considered. Erosion can be measured directly in the field or is estimated based on either

soil analysis or empirical or physical models that take into account the impact of all water erosion variables.

4.6.1 Topographic measurements

They are based on monitoring the topographic evolution of the soil surface. Among these, measurements using a rugosimeter consist of estimating the variation of the height of the ground relative to a reference plane (Roose 1994).

4.6.2 Measurements by plots under natural rainfall

Erosion can be measured on experimental plots in the order of 1 to 200 m^2 under natural rainfall (Wischmeier and Smith 1978; Roose 1981; Rishirumuhirwa 1997). The erosion plot is a natural object, isolated in space by arbitrary boundaries, forming closed pseudo-rectangular surfaces, leading downstream to tanks for the storage of water and sediments, allowing the quantification of both runoff and erosion from their genesis and over a determined distance corresponding to the length of the plot (Cheggour 2008). With the upstream runoff being cut off, this setup provides only a local representation of the actual functioning of the environment and, thus, raises the question of the representativity of the measurements. Nevertheless, this remains an essential tool for comparing situations of the same order of magnitude and especially for the dynamics of infiltration and the risks of runoff and erosion (Cheggour 2008).

4.6.3 Measurements by rain simulation

The spatio-temporal variability of erosive rains prompted researchers to develop rain simulators. These are mobile devices capable of producing quantities of rains similar to natural rains at will. Currently, hydrodynamic soil behavior studies can be done in the field by adopting experimental devices whose feasibility depends on the means used. It has become possible to shorten observation times in the field and to simulate high-intensity showers that rarely occur and cause the most damage. It aims to determine the hydrodynamic characteristics of soils studied at a small scale and under various conditions. The setup consists of the artificial creation of falling drops of water with combinations of different parameters characterizing a rain. These combinations are defined by research objective and are simulated at the local natural conditions of the experimental site (Sabir 1986). There are several methods of implementing these simulations. In fact, several types of rain simulators that can be used, among which include the SWANSON simulator, the ORSTOM mini-simulator and the manual boom irrigator.

4.6.4 Measurements by the study of solid transport

The measurement of homogeneous dissolved concentrations in one section allows for the study of solid transport. These concentrations can be determined indirectly by the measurement of conductivity, which is easily measurable in situ. The joint measurement of flow rates and sediment concentration makes it possible to evaluate the volume of fine materials eroded and exported in a watershed. Moreover, these hydrometric and water quality measurements at the outlet of small watersheds must span several years to achieve temporal representativeness (Mabit et al. 2002).

4.6.5 Measurements by study of sedimentation in reservoirs

The determination of sediment density and volume allows for the estimation of the amount of sediment deposited in a reservoir. The sediment density is variable with respect to time and depending on the position in the reservoir. In addition, it varies according to particle size, mineralogical composition, deposit depth, water level in the reservoir and age of deposits. In general, knowledge of data from the measurement of exports at the outlet is insufficient since it neither allows locating the source zones of sediment nor make it possible to evaluate the losses of earth in the plots constituting these source areas (Boiffin 1994).

4.6.6 Modeling

Models for estimating soil erosion can be divided into three categories: empirical models, physical models, and conceptual models. Empirical models are developed from statistical analysis of information obtained from experimental measurement or field measurement and are specifically used to identify sediment sources (Merritt et al. 2003). Therefore, empirical models are widely used at the watershed scale as they are applied uniformly across the region. However, they are unable to analyze the dynamics of sediment and sediment erosion in the watershed. These models are less demanding with regards to input data. As for physical-based models, they are developed based on the law of conservation of mass and energy for using differential equations to describe the runoff and sediment transport induced by independent rain events in the watershed. They are mainly used to describe the effect of factors such as topography, slope, vegetation, soil characteristics as well as climatic parameters including precipitation, temperature and evaporation (Legesse et al. 2003). The disadvantage of this type of model is the requirement of a large amount of data. On the other hand, conceptual models, which are a mixture of empiricism and physical models, provide an indication of quality as well as

quantitative processes in a watershed without considering interactions between said processes. The most widely used empiric models are: Musgrave equation (Musgrave 1947), USLE (Wischmeier and Smith 1978), SLEMSA (Elwell 1978), RUSLE (Renard et al. 1996), SEDNET (Prosser et al. 2001), RUSLE2 (Foster et al. 2002), PESERA (Kirkby et al. 2004), etc.

Several physical-based models are used in the literature: ANSWERS (Beasley et al. 1980), CREAMS (Knisel 1980), GUESS (Rose et al. 1983), EPIC (Williams et al. 1984), WEPP (Nearing et al. 1989), EROSION2D (Schmidt 1991), KINEROS2 (Smith et al. 1995), EUROSEM (Morgan et al. 1998), etc.

As for the conceptual models, the most widely used are Sediment concentration graph (Johnson 1943), Renard-Laursenn model (Renard and Laursen 1975), Unit Sediment Graph (Rendon-Herrero 1978), Instantaneous Unit Sediment Graph (Williams 1978), AGNPS (Young et al. 1989), etc.

4.6.7 Remote sensing and Geographic Information System

In recent decades, studies have shown the value of GIS in monitoring and quantifying water erosion (Cheggour 2008). Remote sensing and GIS are used to evaluate erosion factors. The use of these systems provides a simple, fast and efficient way for planning and decision-making studies. GIS and remote sensing remain a privileged source of information for the spatialization of erosion on a large scale. Several researchers (eg: Pandey et al. 2007; Efe et al. 2008, Kouli et al. 2009, Benzer 2010; Prasannakumar et al. 2012; Alexakis et al. 2013; Saygin et al. 2014, Farhan and Nawaiseh 2015) have used this technique. However, very few of these results have been validated because it is difficult to measure soil losses across large areas over long periods. As a result, the validity and accuracy of these maps are often questioned (Bonn 1998). Thus, this approach cannot be used in place of field studies to establish an understanding of the phenomenon and establish relationships between spectral information and reality in the field.

4.6.8 Radioactive tracers

Radioactive tracers are a promising approach for studying erosion and soil degradation. Their use in the study of erosion dynamics in the continental environment goes back to the 1960s with the advent of the "nuclear" era (AIEA 2014). Of the wide range of radioactive isotopes present in the environment, only a small number can serve as markers of soil particle displacements. These markers must be characterized by a high chemical affinity for soil particles allowing them to follow the latter in their movement through the landscape (Sogon 1999; AIEA 2014):

- A radioactive half-life sufficiently long to be detected between the sampling and the measuring phase;
- Specific characteristics to obtain information on the origin of the particles transported and the processes involved during erosive episodes (Wallbrink and Murray 1993) and;
- Type of radiation. Gamma emitters are preferable to alpha and beta, for their ease of detection and analysis (Baskaran et al. 1993).

The radionuclides thus retained for the study of the transfers of soil particles are mainly ^{137}Cs and ^{7}Be, ^{210}Pbexe, 134Cs and ^{40}K. Only ^{137}Cs was used in this study.

- Origin of Cesium-137

Cesium (Cs) is the 55th element of Mendeleev's Periodic Table. The electronic configuration of this element gives it great potential reactivity. Its atomic mass is variable, from 125 to 145. Only the stable isotope ^{133}Cs exists naturally. The most common radioactive isotopes are ^{137}Cs and ^{134}Cs with half-lives of 30 years and 2 years respectively. The ^{137}Cs derives from the fission of uranium-235, uranium-238 and other fissile materials. It is derived from gaseous precursors, represented by the following reaction:

$$^{137}I \rightarrow ^{137}Xe \rightarrow ^{137}Cs \rightarrow ^{137}mBa \rightarrow ^{137}Ba$$
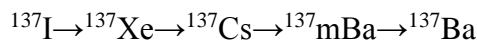
^{137}mBa (meta-stable form), formed from ^{137}Cs, has a half-life of 2.57 minutes and produces stable ^{137}Ba with emission of a γ-ray with an energy release of 661 KeV. This radiation is measured and used to quantify ^{137}Cs. The ^{137}Cs precursor is therefore ^{137}I while the end product of the disintegration chain is ^{137}Ba.

The introduction of this isotope into the environment began in 1945. However, the fallout did not become significant, on a planetary scale, until the advent of thermo-nuclear devices in 1952. These devices were powerful enough to propel radioactive debris into the stratosphere, where it circulated the globe, only to gradually to return to the ground with rain. Thus, between 1954 and 1962, 5.18.1017 Bq of ^{137}Cs was released into the atmosphere (AIEA 2014). The maximum fallout was recorded in 1963. The significance of these fallout events particularly affected the hemisphere, since most atmospheric nuclear tests took place below mid-northern latitudes. After the 1963 Test-Ban Treaty, the fallout from radioactive fallout was considerably reduced, despite some significant fallout in 1971 and 1974, following the numerous nuclear tests of the non-treaty countries.

Overall, the importance of fallout over a territory is proportional to annual local rainfall. The impact of the fallout from the Chernobyl accident on 26 April 1986 in Chernobyl, Ukraine, was estimated at an environmental injection of 100 PBq (1 PBq = 1 Petabecquerel = 1015 Becquerels) of ^{137}Cs. The fallout from this accident was not as far reaching as that from the atomic tests of the 1950s and 1960s. They were more localized and strongly influenced by the circulation pattern of the radioactive cloud and rainfall in the few weeks following the accident.

- Environmental behavior of ^{137}Cs

Radioactive cesium that has fallen back to the ground alongside rain is quickly and strongly adsorbed by soil particles, especially by fine fractions. Indeed, the clay-humic complex strongly adsorbs ^{137}Cs. The direct fallout of ^{137}Cs on plants can be adsorbed on the surface of tissues or absorbed. The adsorbed portion is generally leached by subsequent rainfall and thus returns to the soil. In a study to quantify this phenomenon, 93% of ^{137}Cs applied to grass was found on the ground after one year (Zapata, 2002). Absorption of cesium by transfoliar penetration may occur. This absorbed cesium is released into the soil when the vegetation dies and decomposes. In addition, the uptake by the plant from the soil is very low, so that the export of ^{137}Cs out of agrosystems by harvests is very small (AIEA 2014). The movements of this isotope in the environment (water and soil) are therefore made by physical processes such as tillage and erosion, which redistribute it within agrosystems and agrosystems respectively to hydrosystems.

- Estimation of water erosion

In order to estimate soil movement from ^{137}Cs measurements, the soil cesium stock must be measured at both study sites (erosion or deposit zones) and non-eroded reference sites. The latter are located near the study site, in areas considered free from erosion or deposit after the first introduction of radio-cesium into the environment (forest environment or old uncultivated grasslands since the 60s). The degree of soil movement is estimated by comparing the specific ^{137}Cs (Bq/m^2) activity of the study sites to that of non-eroded control sites. Activity lower than that of the control sites is interpreted as reflecting a net loss of soil, while higher activity indicates net soil gain.

- Advantage of marking by ^{137}Cs

^{137}Cs is particularly well suited for erosion studies for a variety of reasons (AIEA 2014):

- Due to its universal fallout nature, this isotope is easily detectable anywhere and allows the quantification of erosion at spatial scales ranging from the plot to the watershed;
- The first results can be obtained fairly quickly after a simple sampling campaign;
- Present for 50 years in our environment, tracing by ^{137}Cs allows for the estimation of average erosion rates in the long term and, therefore, takes into account the influence of extreme events;
- The technique also allows to provide the net rate of erosion and the percentage of sediment delivered;
- The evaluation of soil redistribution integrates all the processes leading to the movement of soil particles: water erosion, wind erosion, redistribution due to the plowing effect.

In addition, measurements of ^{137}Cs make it possible to estimate all the movements of the soil, which are erosion as well as deposit. It is possible not only to have an overall quantification at a specific location, but also to spatialize the movements of the soil and their importance by sampling a territory in a reasonably systematic way.

- Limitations of the method

Like all techniques, the ^{137}Cs method has its limitations and some aspects still need to be clarified (AIEA 2014). In addition to the choice of the interpretation model itself, the problem raised by the importance of the Chernobyl fallout must be taken into account where these benefits have been significant. Nevertheless, this accident has had a minimal effect out of Europe, with Morocco being spared from its fallout. The selective nature of erosion is another issue. It is well known that eroded sediments are enriched in fine particles compared to the soils in place from which they are derived. Conversely, the deposits that are initially affected are the coarsest fractions first. ^{137}Cs is retained mainly by the finest fractions of the soil. Therefore, the eroded soil has higher cesium levels than the soils of the cultivated plots, while the redeposited soil should be poorer. Ignoring this aspect when transposing ^{137}Cs measurements in terms of soil movement results in overestimation of sediment departures and underestimation of arrivals.

- Conversion models

Several models of interpretation of ^{137}Cs soil activity fluctuations have been proposed. In this study, models for conversion of ^{137}Cs activity to soil redistribution rates used are models: Proportional model (PM), simplified mass balance model (MBM1), mass balance model version 2 (MBM2) and mass balance model version 3 (MBM3) for cultivated sites and profile distribution model (PDM) and dissemination and migration model (DMM) for the forest site.

The application of these models was performed using Csmodel1 software (Walling et al. 2002; Walling et al. 2014).

4.6.9 Bivariate statistics method

Several models have been developed for gully erosion. However, only a few authors have focused on mapping susceptibility to erosion (eg, Bou Kheir et al. 2007; Conoscenti et al. 2008; Gómez Gutiérrez et al. 2009; Krishna Bahadur 2009; Pike et al. 2009; Conforti et al. 2010; Conoscenti et al. 2014). Statistical methods are appropriate for detecting quantitative estimates of the location of future events, since the sensitivity assessment ought to be as objective as possible. The estimation of the contribution of each predisposing factor makes it possible to divide the area into zones characterized by different susceptibilities. All these statistical techniques, which are seldom used in ravine erosion research, can be grouped into bivariate and multivariate methods (Gómez Gutiérrez et al. 2009; Lucà et al. 2011).

Bivariate statistical approaches rely on the calculation of gully density weighting values for each class of causal factors (Yalcin 2008). Approaches based on bivariate statistics are easier to use than multivariate statistical methods. However, bivariate statistics methods have the disadvantage of not taking into account the mutual interrelationships between different causal factors. Among the existing bivariate statistical methods for the quantitative assessment of susceptibility, the information value method and the frequency ratio are the most commonly used statistical methods (Pardeshi et al. 2013).

5 Study area

5.1   Geographic, administrative and forestry frameworks

5.1.1 Geographic framework
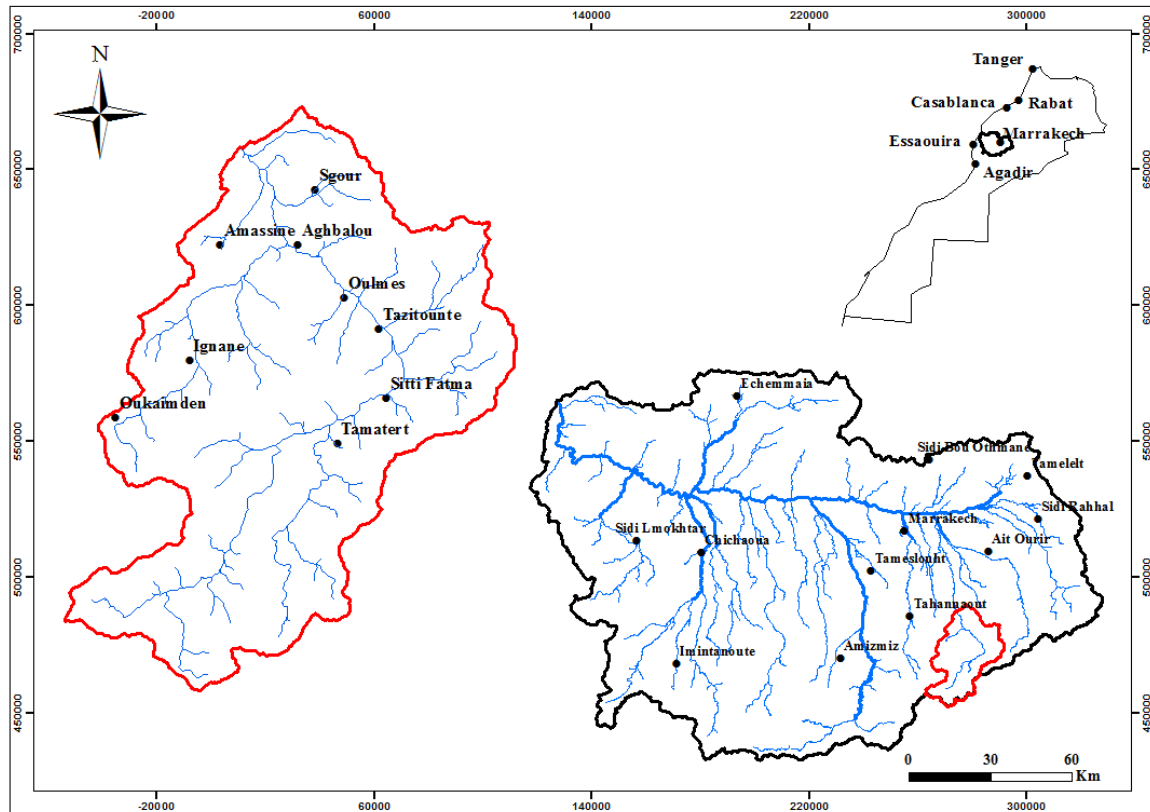
Figure 1. Geographic location of the Ourika watershed

The Ourika River watershed, which is a sub-basin of the Tensift basin, covers an area of 57600 ha. It is located in the High Atlas region of Marrakech, between latitudes 31° and 31°20'North, and longitudes 7°30' and 7°60' West (Figure 1). The main wadi originates from the high foothills of the High Atlas Mountains. Hard crystalline rocks upstream together with the more friable sedimentary formations downstream have shaped its current course with valleys and steep slopes. The Ourika watershed is bounded to the North by the Haouz plain, to the South by the Oued Souss watershed, to the East by the Oued Zat watershed and to the West by Oued Rheraya and Oued Issil watersheds. It is characterized by three main physiographic units namely i) the Piedmont areas at altitudes of around 900 m, ii) the valleys of Oued Ourika and its tributaries, iii) the high mountain areas and plateaus.

5.1.2 Administrative framework

Administratively, the area falls within the territory covering three provinces:

- Al Haouz Province: 90% of the area
- Ouarzazate and Taroudant Provinces: 10%

The following rural communes are part of the administrative division of the watershed:

- Iguerferouane, Ourika, Tighdiouine, Setti Fadma, Oukaimden (Al Haouz Province)
- Igherem N'Ougdal, Tidili (Ouarzazate Province)
- Toubkal (Taroudant Province)

Sur le plan administratif, la zone relève du territoire de trois provinces :
- Province d'Al Haouz : 90 % de la superficie
- Provinces d'Ouarzazate et de Taroudant : 10%

Les communes rurales suivantes font partie du découpage administratif du bassin versant :
- Iguerferouane, Ourika, Tighdiouine, Setti Fadma, Oukaimden (Province d'Al Haouz)
- Igherem N'Ougdal, Tidili (Province d'Ouarzazate)
- Toubkal (Province de Taroudant)

5.1.3 Forestry framework

The management structure of the Ourika watershed is the DREF of the High Atlas region, to which the Provincial Water and Forest Service of Marrakech belongs. The three corresponding units are Asgaouar, Dar Louriki and Agaiouar.

5.2 Physical environment

5.2.1 Hypsometry

The Ourika massif is formed by rocky slopes characterized by steep slopes, where most of the summits exceed 2000 m. These high altitudes in the upstream section of the valley favor the installation of a cold and humid climate, which bring about significant snow cover in winter. This climate, among other factors contribute to the formation of a large water reservoir.
The topography of the region is not favorable for large-scale use of these water resources by the local population, excluding the piedmont where they accumulate in rivers and depressions, given the impermeability of crystalline soils.

The distribution elevations in the Ourika basin shows the predominance of land between 1600 and 3200 m (75%) where the average altitude is 2500 m. The highest point of the basin is at an altitude of 4001 m while the lowest point is at 852 m (using a 10m DEM).

5.2.2 Slope

The erosive or sedimentary phases of a watercourse are determined by the type of slope. In the high altitude areas, rivers often contribute to the erosion of the substrate on which they flow whereas in the plain, sedimentation is predominant. At the Ourika watershed, the slopes are generally steep, giving the wadi a rather violent and torrential character.

5.2.3 Morphology and hydrology of the basin

- Morphological context of the watershed

With a surface area of 576 km^2, the Ourika watershed, which extends to Aghbalou, has a substantially elongated shape. Moreover, it is characterized by a compactness index of 1.3. Its main watercourse, which is characterized by a NE and NW beyond the town of Setti Fadma, crosses a long valley to which converges, on both banks, a succession of valleys and ravines/tributaries. This phenomenon provides an explanation to why the flood waves of the Ourika wadi grow downstream, as they are fed by the tributaries.

The Gravelius compactness index is of the order of 1.58, which explains the relatively elongated shape of the basin. The main course forms a linear valley that is fed on both banks by a succession of tributaries. This situation allows the flood waves to grow downstream as they are fed by the tributaries.

- Hydrology of the watershed

Oued Ourika is a tributary of the Lahjar wadi, which, in turn, is a left bank tributary of Oued Tensift. It is divided into two distinctly opposite sections on both sides of Ait Barka's elbow. The length of the Ourika, from its sources to the outlet of Aghbalou watershed, is about 41.5 km. Additionally, the hydrographic network of the Ourika basin is quite dense and fairly branched.

5.2.4 Geologic aspect

The Ourika watershed is one of the basins of the Atlas Mountains (High Atlas of Marrakech), extending from the Atlantic Ocean in the west to Tunisia in the east. It is a typically intracratonic chain that is substantially elongated in an ENE-WSW to an E-W direction. The Ourika region

is divided into four structural zones, parallel to the Atlas axis. They are, from South to North (Saadi & Baou 2005), as follows:

- Axial zone, which corresponds to the highest section of the High Atlas, with Jbel Toubkal culminating at 4165 m. It is mainly composed of pink granite and Toubkal andesite rocks of the Precambrian era.
- High plateaus zone such as Adrar Yagour, Timenkar and Tizrag located at about 2500 m. This corresponds to a Permo-Triassic unit, generally consisting of sandstone, conglomerate and red marl formations. Nevertheless, the dominant formations are the pink granite biotite.
- Piedmont Zone: It is characterized by a subatlantic zone formed, due to the corresponding hills, of basins and plateaus. There is a dominance of conglomerate formations dating from the Lias to Cretaceous era, Visean flyschs, limestone, and friable sandstone (1st Permo-Triassic unit)
- Haouz plain zone.

These four zones are morphologically, geologically and structurally very different from each other. From a structural point of view, this basin is affected by major reverse faults, oriented around N70. This orientation is parallel to the direction of the atlasic chain. The areas between these reverse faults are in turn affected by normal NNE-SSW sedimentary, infracambrian, and Permo-Triassic faults with the basement, to the north by other faults related to the North Atlas accident which resulted in the overlapping and folding of the Carboniferous and post-Atlas secondary covers.

5.2.5 Soil aspect

Different soil types derive from substrates that are influenced by climatic factors and vegetation. The four main types of parent rocks result in the following soil types:

- Soils on eruptive rocks: the magmatic rocks are alterable and most often result in deep and rich soils;
- Soils on schist-sandstone flysch: the evolution of these types of soil remains linked to ecological conditions, and their alteration gives rise to a zonal ground that can lead to the formation of soils;
- Shallow humeral brown forest hummocks on wet slopes where the bedrock is being altered;

- Crude minerals (lithosols) on dry slopes, with outcropping of substrates;
- Permo-Triassic soils of red sandstone and marl nature: this type of soil extends over a fairly large area at the basin level. These formations consist of very soft argillites that are exploited at a large scale for agricultural purposes, thus easily being subjected to runoff (gully). When subjected to more xeric conditions, the alteration of the sandstones gives rise to the formation of a clay-sandy layer which, in turn, result in fersialitic soils;
- Soils on limestone: under vegetation, true or browned rendzines are observed until the formation of a calcareous brown soil. At the shady (north) slope and on steep slopes, these limestones dry the area. On deep marl-limestone colluvium, fersialitic soils, characterized by the presence of rock salt (alluvium, colluvium, verticles), are formed.

5.2.6 Climatic context

The region is characterized by its particularly harsh climate. This is due to the orientation of the reliefs, which are generally inclined in a NE-SW direction. As a result, the region receives not only humid ocean currents arriving from the NW, but also arid Saharan currents deriving from the SE (Saadi & Baou 2005). The climate analysis in the Ourika watershed is based upon its main characteristics of which data (records) are available. As such, the choice of weather stations for the study was done at Agouns, Amenzar, Aghbalou, Tazitount and Tourcht.

The observation periods correspond to the following series: Agouns (1996-2011), Amenzar (1996-2011), Aghbalou (1968-2011), Tazitount (1998-2011) and Tourcht (1996 -2011). The distribution of rainfall amounts in the area is highly dependent on geographical position and altitude, and to some extent aspect. The highest annual rainfall was observed at the Aghbalou station in the Ourika watershed (541.46 mm) while the lowest records were observed at Agouns (321.09 mm). The study of seasonal mean rainfall patterns consists of classifying the seasons in order of decreasing rainfall. This refers to drawing up the precipitation balances obtained during each season. The analysis of these data showed that for the upstream stations with higher altitudes (Agouns and Amenzal), the seasonal regime is of the P.A.H.E. (Spring- Autumn- Winter- Summer). On the other hand, for those in both moderately high altitudes (Tourcht and Tazitounte) and downstream (Aghbalou), it is of type P.H.A.E (Spring- Winter- Autumn- Summer).

The lowest temperatures (4.1 °C in January) are observed at the higher elevations, upstream of Oued Ourika (Agouns). These go up and reach the highest recorded values (25.2 °C) at the lower elevations, downstream of Oued Ourika (Aghbalou).

5.3   Land uses

Thanks to the classification of satellite images of the area as well as validation by field data, the following types of land cover can be distinguished:

- Forest: 35% of the extent of the watershed

- Cropland: 7%

- Non-forested open areas and matorral: 50%

- Bare ground and buildings: 8%

5.4   Flora and vegetation

5.4.1 Natural Vegetation

According to Ouhammou (1986), the main plant formations found in the Ourika watershed are as follows:

From downstream to the higher altitudes upstream:

- Thuja (*Tetraclinis articulata*) stand in association with juniper (*Juniperus phoenicea*) and holm oak (*Quercus rotundifolia*) stands. They occupy the subatlasic zone as well the front-upstream.

- Juniper stand comprised of Phoenicean juniper in internal domains

- Bushy *Genista spp*. formations*: Retama dasycarpa* and *Adenocarpus anagyrofolius* replace the Phoenicean juniper upstream of the inner valleys.

- Holm oak covers the upper upstream, the oceanic spacing of the first Permo-Triassic unit and some northern slopes of the inner domains.

- *Juniperus thurifera* stands are mainly present in the upper parts of the inner valleys. Its rarity and in some case absence is observed on the northern slope of the oceanic escarpment reliefs. Holm oak forms the treeline at this level.

- Spiny xerophyte formations and altitude grass characterize the high mountain area

Alyssum is the xerophyte that covers the largest area, in areas ranging from 2050 m to 3600 m in altitude. Moreover, it is dominant on the northern slopes. The other forest species found in the other formations include the carob tree (*Ceratonia siliqua*), the olive tree (*Olea europaea europaea sylvestris var.*), with the latter being found in isolated stands or in bouquets, mainly on the hot slopes. The undergrowth species consist of lentisk (*Pistacia lentiscus*), wicker (*Phillyrea spp*.) and rockrose (*Cistus spp*.). The natural riparian vegetation of the watershed is

composed of *Fraxinus angustifolia*, white poplar (*Populus alba*), black poplar (*Populus nigra*), and olive-leaf willow (*Salix atrocinerea*).

5.4.2 Artificial forest stands

Reforestation of Aleppo pine (*Pinus halepensis*), the Canary pine (*Pinus canariensis*), *Eucalyptus camaldulensis* and *Eucalyptus gomphocephala* is being done to cope with the decline in the area under the both holm oak and junipers, as well as reducing the extent of the non-forested area.

Chapter 1

Spatial assessment of Soil erosion risk in Morocco

Spatial assessment of Soil erosion risk in Morocco

Abstract

Soil erosion is the most important natural hazard in land degradation in the world. Natural climatic, edaphic and topographic conditions and human activities have made Morocco particularly prone to water erosion. Rainfall, soil properties, topography and land use/land cover data have been used to compute the RUSLE model's factors and their integration in GIS environment made it possible to estimate the average annual soil loss of Morocco.

The average annual rate of soil erosion in Morocco was estimated at 22.24 t/ha/yr with standard deviation of 78.70 t/ha/yr. The results show that 79.14 % of the country area has low risk of soil erosion, 10.27 % moderate risk, 7.55 % high risk and 3.04 % very high risk. The main predisposing factors of Morocco to water erosion were topography and rainfall erosivity. The topographic factor was strongly correlated with soil loss with correlation coefficient of more than 0.90 in Morocco's biogeographical, bioclimatic, agroecological regions, regional soil and water conservation systems and vegetation levels. Soil erosion management should focus particularly on topographic factor within different regions of Morocco. While the used empirical model helps to map areas of soil erosion risk, the methodology could be improved by obtaining data that are more accurate for RUSLE factors in Morocco.

Keywords: Soil erosion, RUSLE model, GIS, Morocco

1 Introduction

Soil erosion and degradation of associated land are spatio-temporal phenomena that take to scale in several countries (Hoyos 2005; Bini et al. 2006; Fernandez & Nunez 2011; Xu et al. 2011). Soil erosion is an inevitable natural phenomenon, which becomes a serious environmental and economic problem when accentuated by human activities (Lal 1998; Del Mar López et al. 1998; Rozos et al. 2013). Water erosion has increased all over the world (De Graaf 1996; Lal 2006; IAEA 2014). Population pressure agriculture expansion by various human activities, agricultural practices, forest exploitation, grazing, construction of roads and buildings; associated with the amplifying effects of climate change, have led to the exposure of land to runoff, and thus to soil degradation by water erosion (Vezena & Bonn 2006 ; Wachal 2007).

In North Africa, the phenomenon of water erosion is also widespread, with the majority of watersheds being characterized by important soil losses exceeding 2000 t/ km^2/year, resulting in average annual siltation of dam reservoirs of 125 million m^3 (Remini and Remini 2003). According to FAO studies (FAO 1990), 40 % of land is affected by water erosion in Morocco, 35% in Greece, 45% in Tunisia and 50% in Turkey.

In Morocco, the problems of water erosion have increased in recent decades due to demography, clearing and overgrazing leading to land cover degradation and subsequently increased soil erosion. Soil losses exceed 20 t/ha/year in the Rif in the north, between 10 and 20 t/ha/year in the Pre-Rif, between 5 and 10 t/ha/year in the Middle and High Atlas and less than 5 t/ha/year in other regions (Ghanam 2003). The inappropriate intensification of agriculture in natural areas has accentuated the phenomenon. More than 15 million hectares of agricultural land is threatened, with an estimated 100 million tons of soil lost annually (HCEFLCD, 2012). Human well-being remains largely dependent on rational use of two main resources, water whose mobilization and especially the use requires to be further mastered and extended, and the soil whose preservation is urgent. These two potentialities are threatened by water erosion. The consequences of soil erosion in downstream areas are costly for the national economy as reservoirs siltation is estimated at 75 million m3 annually, which corresponds to a 0.5% decrease in storage capacity or a loss in irrigation of 60000 ha/year (Comité national MAB, 1990).

The accelerated increase in the extent of soil erosion has led to the development of several models (Bou Kheir et al., 2008). Quantitative and spatial information on soil loss are of great practical importance to manage, conserve and control soil erosion (Prasannakumar et al. 2011, 2012). Soil erosion models can integrate the complex relationships and interactions between the predisposing factors to soil erosion. Several researchers have used GIS technologies to model soil erosion (eg: Pandey et al. 2007; Efe et al. 2008, Kouli et al. 2009, Benzer 2010; Prasannakumar et al. 2012; Alexakis et al. 2013; Saygin et al. 2014, Farhan and Nawaiseh 2015). RUSLE model has proven to be the most widely used methodology in the world because its applicability and the reliability of the results are indisputable (Lee 2004; Lu et al. 2004). This is because RUSLE is considered simple and integrates readily available and accessible data.

In order to provide spatial modelling of erosion in Morocco, a need was identified to estimate soil erosion risk on a national scale. The study aims to assess the spatial soil erosion indicators

in Morocco on a national scale, including rainfall erosivity, soil erodibility, topography and vegetation cover. This study provides a new national datasets on soil erosion factors and potential soil loss, which are not available until now. The results will be useful to decision-makers and planners in implementing appropriate land management measures in Morocco.

2 Material and methods

2.1 Study area

Located between the Atlantic and the Mediterranean between latitudes 21 ° to 36 ° N and longitudes 1 ° to 17 ° W, Morocco is at the extreme north-west of the African continent (Fig 1). Only the Strait of Gibraltar separates it from the European continent. The closest points between Morocco and Spain are 14 km away. Due to its large extension in latitude, it benefits from an important facade on the Atlantic Ocean (2 934 km), to which are added, to the North, 512 km of coasts on the Mediterranean Sea. This situation gives it a geographical and strategic position of the first order.

The Moroccan territory covers an area of 710,850 km^2. The situation of Morocco between two climate belts, and between the Azores anticyclone in the West and the Saharan depression in the Southeast, causes a great spatial and temporal variability of the climate inducing a considerable impact on the water resources, agricultural production and plant cover of the country.

Morocco is characterized by a very significant spatial and temporal variability of rainfall. The northwest is on average, more watered than the rest of the Kingdom. And even in this region, the average annual cumulative rainfall varies considerably. For example, it can reach more than 800 mm on the reliefs, while it does not exceed 300 mm on the surrounding plains. In fact, coastal areas enjoy a temperate climate, while the climate is desert in the south and east of the country.

In Morocco, soils have been shaped by a long evolution, under the combined action of climatic factors and vegetation cover, characterized historically by cyclical variations. These factors operate, of course, taking into account topography and geology data. The diversity of all these factors explains the wide variety of soils that result. But on the whole, soils are vulnerable and land is often degraded, vulnerability becoming worse with steep slopes and declining vegetation cover. Soil erosion is the principal factor of soil degradation in the country.

Figure 1.1. Location of Morocco

2.2 RUSLE factors generation

The annual soil loss can be assessed as follows (Renard et al. 1997):

A = R*K*LS*C*P

where

A: average soil loss (t/ha/year),

R: rainfall erosivity factor (MJ mm/ha/h/year),

K: soil erodibility factor (t ha h/ha/MJ/mm),

LS: topographic factor,

C: cover and management practice factor,

 P: conservation support practice factor.

The Figure 1.2 summarizes the methodology used in the study.
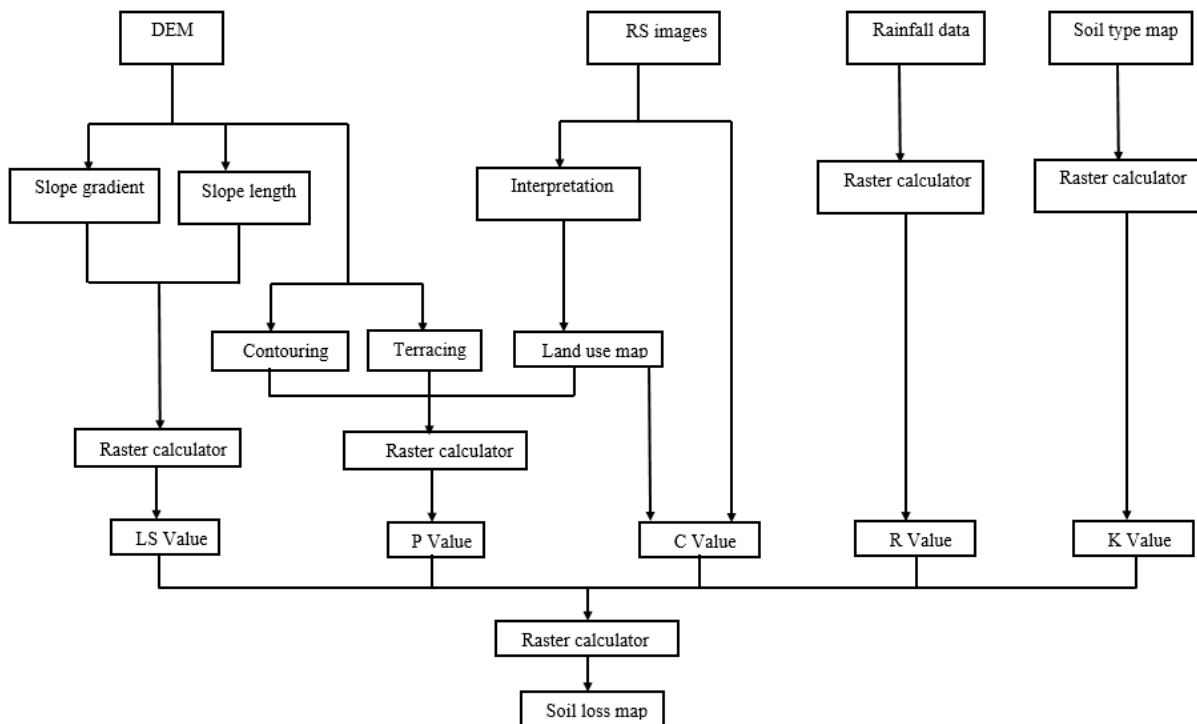
Figure 1.2. Methodology for RUSLE model

2.2.1 Rainfall erosivity factor (R)

The records of monthly rainfall data were used to assess the R factor. The Rango & Arnoldus formula (1987) was applied:

Log R = 1.74 * log Σ (Pi² / P) + 1.29

Where:

R is rainfall erositivity factor in MJ mm/ha/h/year, Pi monthly rainfall and P annual rainfall in mm.

R factor have been calculated for 31 climatic stations (1988-2011) and a continue surface was produced using the point data of the stations. The inverse distance weighted method was used to produce the final erosivity map (Figure 1.3).

2.2.2 Soil erodibility factor (K)

The soil erodibility map (Figure 1.4) was obtained by attributing to the different soil types, using FAO soil data, the corresponding K values (Table 1.1). The corresponding K values for the soil types were identified based on texture and organic matter content using a table proposed by Roose (1996).

Table 1.1. Soil types and their K Values

Class	Sand %	Silt %	Clay %	Organic carbon %	K value
1	81.6	6.8	11.7	0.44	0.05
2	40.2	50.3	9.6	1.09	0.34
3	48.5	30.8	20.7	1.74	0.34
4	39.1	26.5	34.6	1.46	0.33
5	58.9	16.2	24.9	0.97	0.2
6	39.6	39.9	20.6	0.65	0.34
7	70.8	12.8	16.5	1.15	0.14
8	39.1	37.0	23.9	1.93	0.34
9	16.5	48.9	34.4	1.5	0.35
10	36.7	40.3	23.1	2	0.26
11	64.3	12.2	23.5	0.63	0.2
12	70.6	14.1	15.4	0.57	0.05
13	68.3	15.1	16.6	0.5	0.14
14	55.4	20.4	24.2	0.65	0.2
15	24.6	14.4	61.0	0.68	0.24
16	76.6	10.3	13.1	0.46	0.05
17	61.4	21.9	16.7	1.25	0.14
18	72.8	10.5	16.8	0.36	0.05
19	48.7	29.9	21.6	0.64	0.34
20	49.2	26.0	24.8	0.33	0.2
21	50.4	29.0	20.6	0.33	0.34
22	63.5	17.9	18.7	0.26	0.14
23	49.2	26.0	24.8	0.41	0.2
24	47.8	8.5	43.8	0.38	0.2
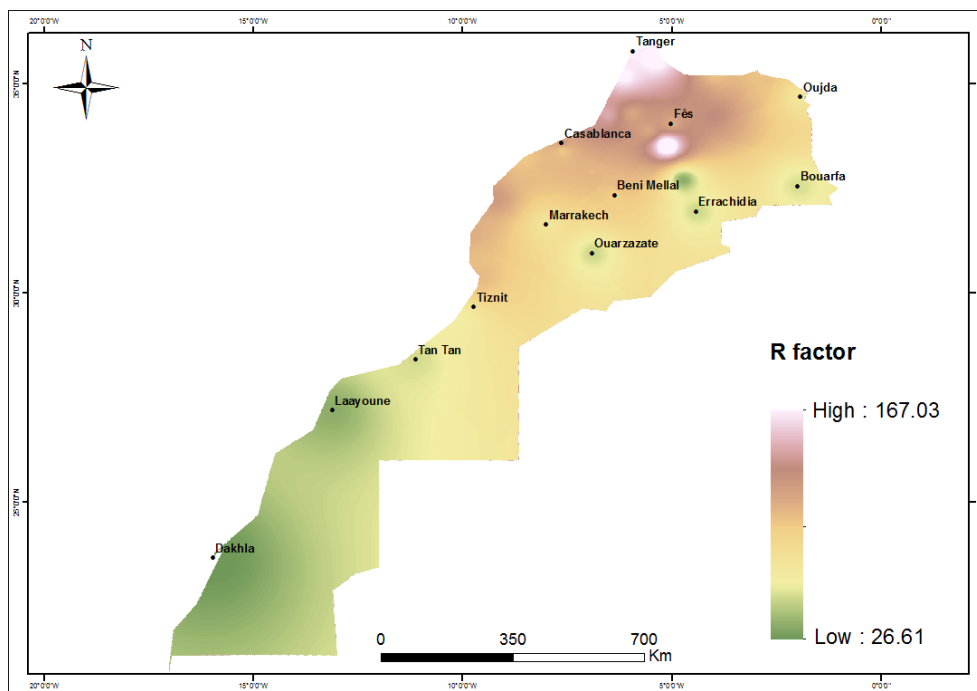
Figure 1.3. Spatial distribution of the R factor in Morocco
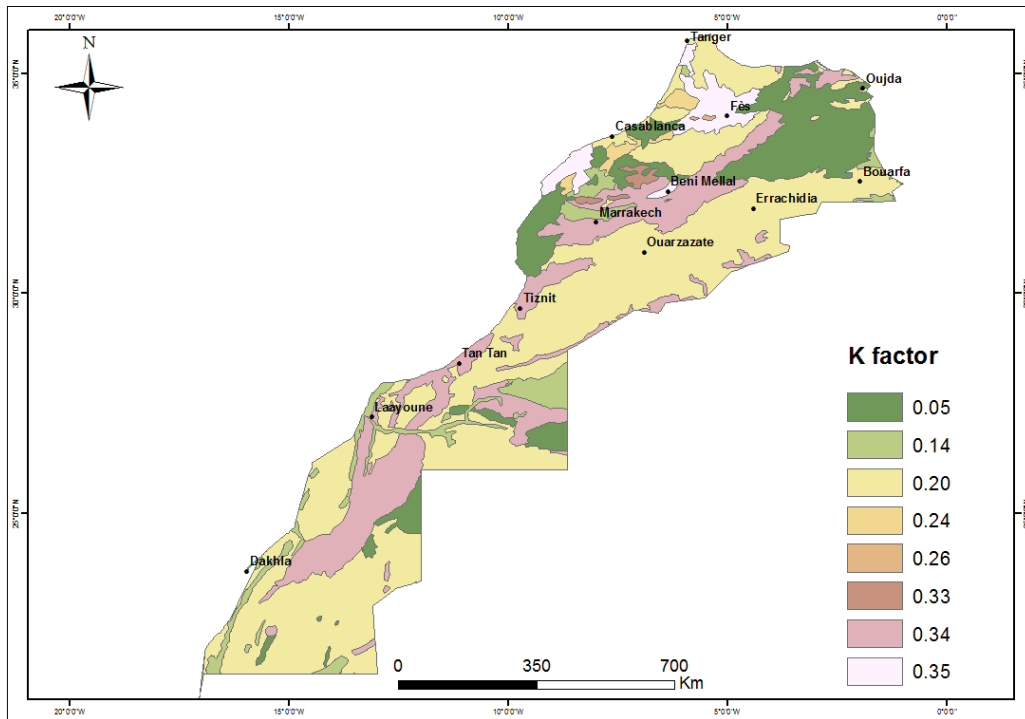
Figure 1.4. K Factor map in Morocco
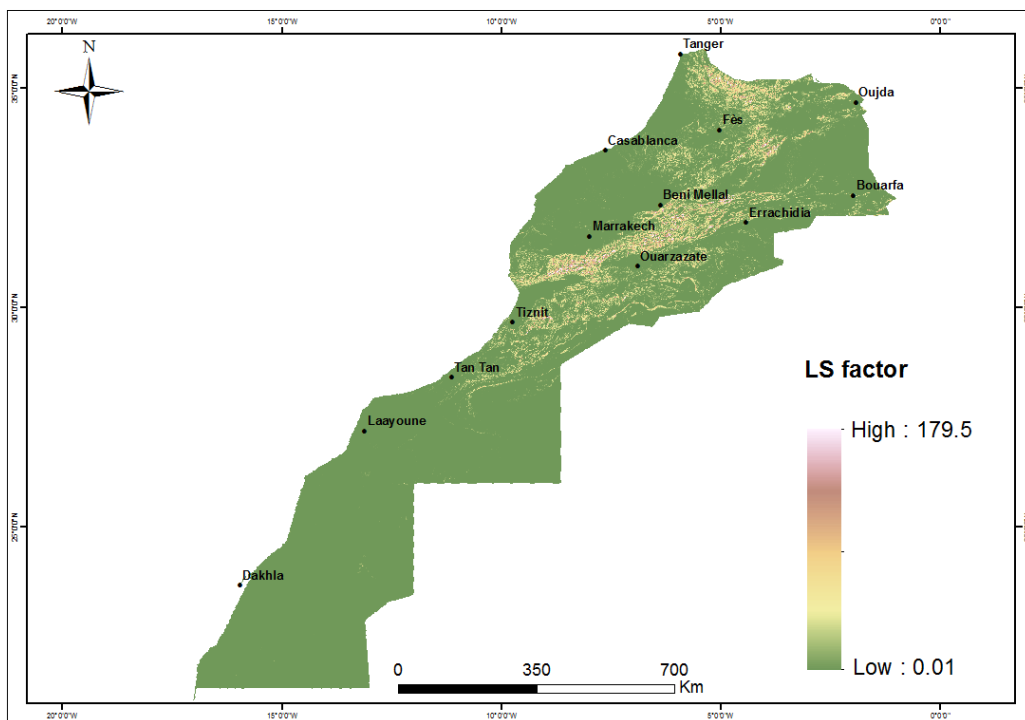
Figure 1.5. LS Factor map in Morocco
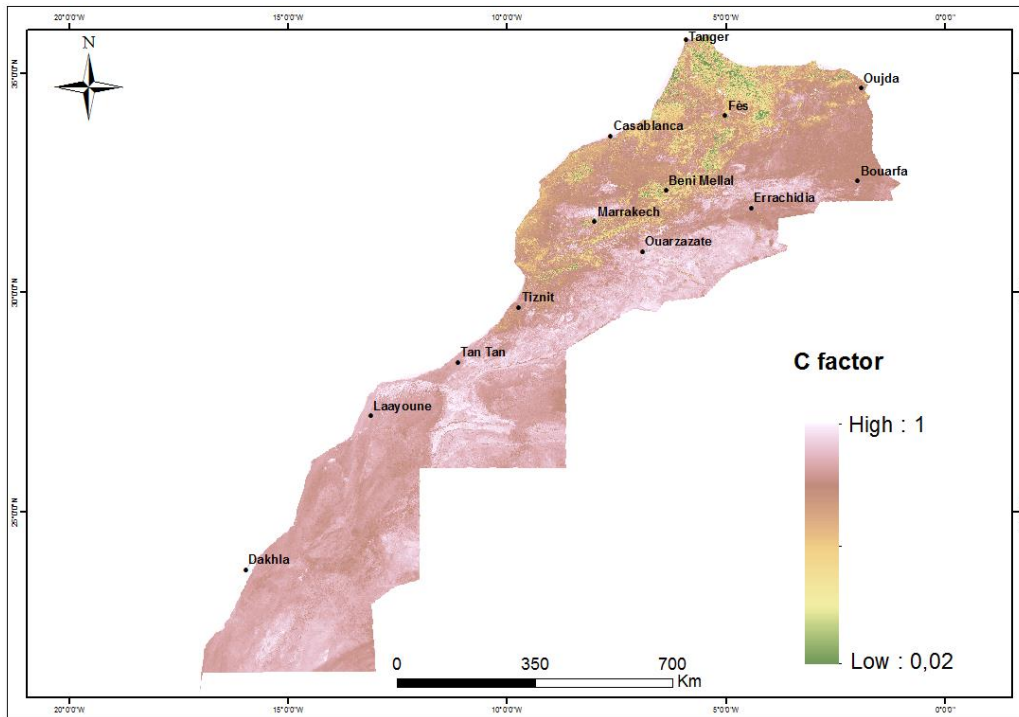
Figure 1.6. C factor map in Morocco

Table 1.2. Conservation practice factor (P) values in Morocco

LULC classes	P factor values
Herbaceous cover	1
Cropland	0.45
Mosaic natural vegetation / cropland	0.5
Tree cover	1
Mosaic tree and shrub / herbaceous cover	1
Shrubland	1
Grassland	1
Sparse vegetation (tree, shrub, herbaceous cover)	1
Urban areas	1
Bare areas	1
Water bodies	0
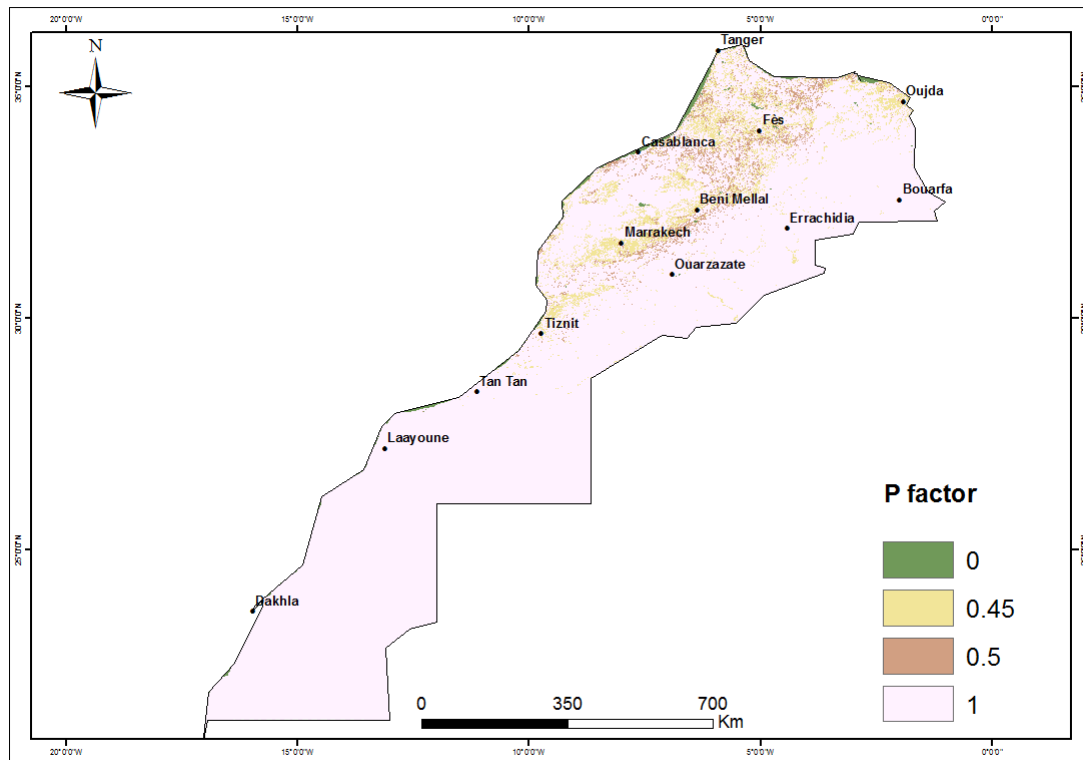
Figure 1.7. P factor map in Morocco

3 Results and discussion

The raster map of the soil loss is obtained after the multiplication of the five factors of the model (R, K, LS, C and P), organized in a grid format with a cell size of 30 m x 30 m. The resulting soil erosion map was reclassified into four classes (Figure 1.8 and Table 1.3), according to FAO (FAO, 1979).

Table 1.3. Proportion of each soil loss category

Soil loss (t/ha/yr)	Erosion risk	Area (%)
< 10	Low	79.14
10 - 50	Moderate	10.27
50 - 200	High	7.55
> 200	Very high	3.04
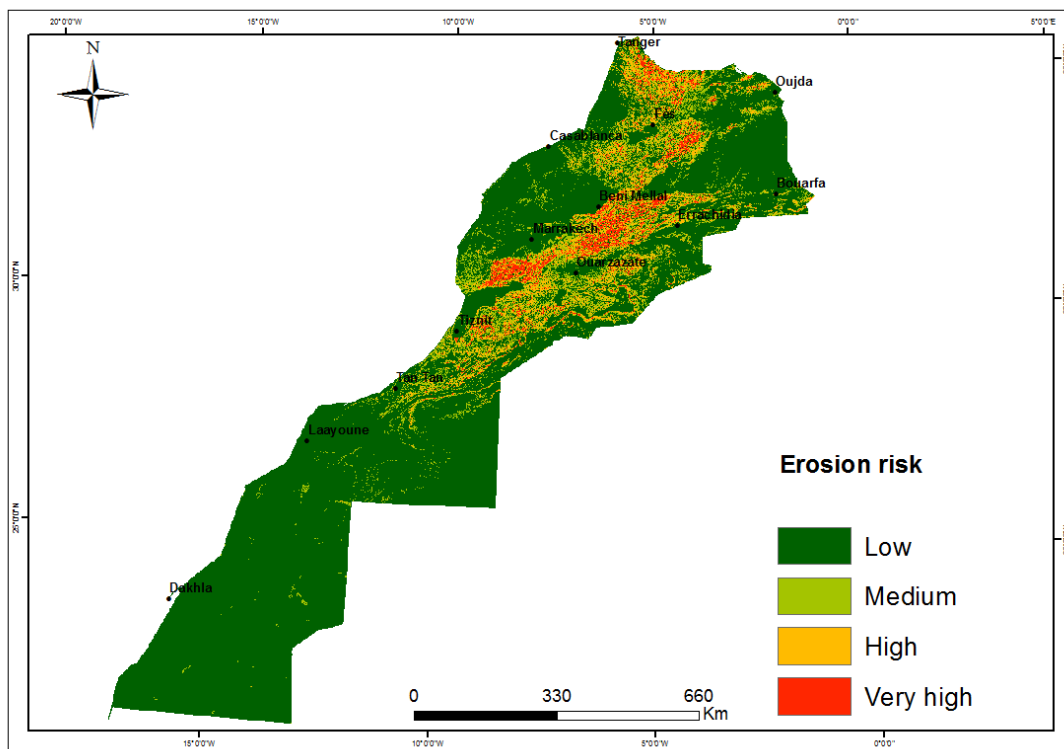
Figure 1.8. Spatial distribution of soil losses in Morocco

Table 1.4. Soil erosion and biogeographical regions

Biogeographical regions		Soil loss (t/ha/yr)		Soil loss categories [t/ha/yr (area %)]			
	Area (%)	Mean	Std	Low < 10	Moderate 10 - 50	High 50 − 200	Very high > 200
Anti-Atlas	5.11	56.50	85.52	2.32	15.50	18.11	11.12
Saharan Atlas	1.60	14.19	36.17	1.49	2.65	1.76	0.40
High Atlas	5.58	147.90	204.96	1.68	11.64	21.52	48.06
Mediterranean coastline	0.73	36.32	74.37	0.54	1.53	1.58	1.06
Middle Atlantic Morocco	10.75	9.79	43.02	11.66	10.05	4.98	3.75
North Atlantic Morocco	6.26	29.09	58.01	4.71	12.81	13.28	4.96
Saharan Morocco	56.74	4.57	23.51	66.14	27.30	17.38	6.78
Eastern Morocco Mountains	0.60	25.60	51.34	0.44	1.59	1.03	0.39
Middle Atlas	2.38	96.15	174.94	0.99	5.92	9.08	10.69
Plains and plateaus of eastern Morocco	8.35	8.49	47.63	9.42	6.32	2.82	2.31
Rif	1.91	100.23	132.01	0.60	4.68	8.45	10.48

Table 1.5. Soil erosion and bioclimatic regions

Bioclimatic regions	Area (%)	Soil loss (t/ha/yr)		Soil loss categories [t/ha/yr (area %)]			
		Mean	Std	Low < 10	Moderate 10 - 50	High 50 − 200	Very high > 200
Arid	11.24	20.62	49.17	9.98	19.26	16.21	6.89
Humid	2.11	101.02	178.17	0.91	5.06	7.78	10.85
Per-humid	0.31	113.81	134.07	0.07	0.75	1.71	1.90
Saharan	49.16	1.51	11.80	59.02	11.32	4.43	1.28
Semi-arid	27.83	27.75	75.27	25.06	44.12	40.70	33.01
Subhumid	9.36	92.02	167.15	4.97	19.50	29.17	46.07

Table 1.6. Soil erosion and regional systems of water and soil conservation

Regional systems of water and soil conservation	Area (%)	Soil loss (t/ha/yr)		Soil loss categories [t/ha/yr (area %)]			
		Mean	Std	Low < 10	Moderate 10 - 50	High 50 − 200	Very high > 200
Arid mountains	4.95	39.29	80.64	3.63	10.16	10.57	8.87
Atlas semi-arid Mountains	5.59	141.01	209.22	2.15	11.09	18.36	46.21
Eastern semi-arid Rif Mountains	1.29	80.53	115.82	0.51	3.59	4.81	5.60
Subhumid Mountains (Rif, Middle Atlas)	5.56	72.34	136.20	2.66	14.38	19.99	17.44
Atlantic and Mediterranean plains	8.08	12.61	37.22	7.83	9.34	6.96	2.23
Steppes (Atlantic and Eastern)	13.47	8.26	41.42	15.17	9.86	5.36	3.78
Desert areas (Presahara and Sahara)	61.05	8.32	34.04	68.05	41.57	33.95	15.88

Table 1.7. Soil erosion and agroecological regions

Agroecological regions	Area (%)	Soil loss (t/ha/yr)		Soil loss categories [t/ha/yr (area %)]			
		Mean	Std	Low < 10	Moderate 10 - 50	High 50 − 200	Very high > 200
Favorable	9.25	45.60	104.76	6.42	17.53	20.81	17.20
Intermediate	2.94	4.59	17.62	3.32	2.11	0.93	0.10
Mountains	4.77	63.90	137.45	3.11	9.32	12.70	14.43
Unfavorable Oriental	11.26	19.57	70.18	11.20	13.04	10.70	8.76
Unfavorable South	5.74	17.00	67.89	5.96	6.23	2.93	4.95
Saharan	66.04	17.82	70.85	70.00	51.78	51.92	54.56

Table 1.8. Soil erosion and vegetation levels

Vegetation levels		Soil loss (t/ha/yr)		Soil loss categories [t/ha/yr (area %)]			
	Area (%)	Mean	Std	Low < 10	Moderate 10 - 50	High 50 – 200	Very high > 200
Infa-Mediterranean	10.41	12.02	35.89	10.72	12.31	9.17	2.96
Meso-Mediterranean	12.29	41.43	101.22	9.86	21.59	23.86	23.90
Mediterranean Mountains	1.34	169.15	229.12	0.42	2.25	5.54	13.12
Morocco saharan	47.53	2.08	15.45	56.68	12.10	5.89	2.56
Oromediterranean	0.74	208.34	251.86	0.19	1.14	2.78	9.34
Supra-mediterranean	3.59	111.42	182.19	1.61	7.60	12.45	22.93
Thermo-mediterranean	24.09	27.81	67.92	20.52	43.01	40.33	25.19

Table 1.9. Pearson correlation between soil loss and RUSLE factors

Types of regions	Equation	R^2
Biogeographical regions	A = 12.79*LS - 4.52	0.92
Bioclimatic regions	A = 1.61*R - 86.00	0.91
	A = 10.39*LS + 6.13	0.93
	A = -350.49*C + 308.65	0.87
	A = -660.28*P + 656.10	0.92
Regional systems of water and soil conservation	A = 11.89*LS - 0.54	0.90
Agroecological regions	A = 14.91*LS - 5.19	0.96
Vegetation levels	A = 15.92*LS - 8.97	0.99

The results show that the average soil loss in Morocco is 22.24 t/ha/yr with standard deviation of 78.70 t/ha/yr. This was consistent with values obtained in the eastern and the western Mediterranean with similar environmental conditions and agricultural landscapes (Irvem et al. 2007; Efe et al. 2008; Panagopoulos and Ferreira 2010; Demirci and Karaburun 2012; Alexakis et al. 2013; Saygin et al. 2014; Farhan and Nawaiseh 2015). In the country, 79.14 % of the area

has a low risk of erosion, 10.27 % moderate risk, 7.55 % high risk and 3.04 % a very high risk (Figure 1.8 and Table 1.3).

The average soil loss obtained at national scale (22.24 t/ha/yr) is close to the values obtained by Sadiki (2009) and Zouagui et al. (2012) respectively in the Central Rif and Western Rif regions of Morocco (Table 10). However, it is less than the majority of the values reported in different regions of Morocco (Poesen and Lavee 1994; Merzouk et al. 1996; Ait Brahim et al. 2003; Al Karkouri 2003; Sadiki 2004; Moukhchane et al. 2005; Sadiki 2009; Tribak et al. 2012; Khali Issa et al. 2014; Tahiri et al. 2014; Yjjou et al. 2014; Markhi et al. 2015; Khali Issa et al. 2016; Meliho et al. 2016).

There is a significant difference between the average soil loss obtained in this study (22.24 t/ha/yr) and the value reported by Gourfi et al. (2018) (5.06 t/ha/yr) in Morocco. This could be explained by the resolution and the precision of the data used in the study. The low soil loss value reported by these authors could be explained by the underestimation of some factors such as the K an LS factors. The RUSLE model is very sensitive to data resolution and precision.

Biogeographic regions are areas, which ecologically, are relatively homogeneous with common characteristics in terms of species. Morocco is subdivided into eleven biogeographical regions (Benabid and Fennane 1994, 1999) (Table 1.4). The relationship between soil erosion and biogeographic regions (Table 1.4) revealed that the highest average soil loss values were obtained in the High Atlas, Rif, Middle Atlas and Anti-Atlas with average losses of 147.90, 100.23, 96.15 and 56.50 t/ha/yr, respectively (Table 1.4). The higher average soil loss values obtained in these biogeographic regions could be explained by the strong correlation between soil loss and LS factor ($R^2 = 0.92$) (Table 1.9). Saharan Morocco, the plains and plateaus of eastern Morocco and the Moroccan Middle Atlantic are less vulnerable to water erosion because of their low LS values. The topographic factor was the determining factor in the vulnerability of Morocco's biogeographical regions to soil erosion by water (Table 1.9).

Bioclimatic regions designate areas with a specific climate that determines fauna and flora. Morocco is subdivided into six bioclimatic regions (Benabid and Fennane 1994, 1999) (Table 1.5). The bioclimatic regions most vulnerable to water erosion are Per-humid, Humid and Subhumid regions with average soil losses of 113.81, 101.02 and 92.02 t/ha/yr, respectively, while the Saharan and Arid are the bioclimatic regions least vulnerable to water erosion (1.51 and 20.62 t/ha/yr, respectively) (Table 1.5). This could be explained by the fact that soil loss was strongly correlated with R, LS, C and P factors (R^2 of 0.91, 0.93, 0.87 and 0.92 respectively)

within bioclimatic zones (Table 1.9). Effective soil and water conservation measures can be adopted within Moroccan bioclimatic zones by focusing interventions on topographic, crop management and conservation practices.

The water and soil conservation regions have been delineated in Morocco based on relief, rainfall, soil depth, agro-pastoral vocation and degree of intensification of agricultural land (Laouina, 2010) (Table 1.6). The relationship between water erosion risk and regional soil and water conservation systems reveals that the most vulnerable areas that require the most intervention in terms of water and soil conservation measures are Atlas semi-arid Mountains, Eastern semi-arid Rif Mountains and Subhumid Mountains (Rif, Middle Atlas) (Table 1.6). The topographic factor was the principal predisposing factor in the vulnerability of Morocco's regional soil and water conservation systems to water erosion (Table 1.9).

Morocco has been classified into six agro-ecological zones based on rainfall and temperature (Table 1.7) (Balaghi et al., 2013). The agroecological regions most vulnerable to water erosion are the Mountain and the Favorable regions with average soil losses of 63.90 and 45.60 t/ha/yr, respectively (Table 1.7). Despite the fact that agroecological regions have been delineated based on rainfall and temperature, the principal predisposing factor to water erosion was topographic factor (Table 1.9).

A vegetation level has a complex and diversified meaning but defines a geographical area located in an altitudinal interval, with a defined climate and characterized by a specific vegetation. Morocco is characterized by seven vegetation levels (Benabid and Fennane 1994, 1999) (Table 1.8). The Oromediterranean, Mediterranean Mountains and Supra-Mediterranean are the vegetation levels most vulnerable to water erosion with average soil losses of 208.34, 169.15 and 111.42 t/ha/yr, respectively (Table 1.8). Soil erosion was strongly correlated with topographic factor within vegetation levels (Table 1.9). Soil erosion management should focus specially on topographic factor within different regions of Morocco.

The results of the study of the correlation between sensitivity to soil erosion and RUSLE factors are consistent with the findings of Gourfi et al (2018). They find that the factor controlling the most soil erosion in Morocco is the LS-factor.

4 Conclusion

In this study, an empirical RUSLE model integrated with RS and GIS was used to predict water erosion risk in order to adopt effective strategies for soil and water resources preservation in

Morocco. The model took into account precipitations, soil properties, topography and land use/land cover. The average annual rate of soil erosion in Morocco was estimated at 22.24 t/ha/yr, with 79.14 % of the country area having low risk of erosion, 10.27 % moderate risk, 7.55 % high risk and 3.04 % very high risk. Morocco's vulnerability to soil erosion was mainly due to the influences of topography and rainfall erosivity. The topographic factor was strongly correlated with soil loss with correlation coefficient of more than 0.90 in Morocco's biogeographical, bioclimatic, soil and water conservation, agroecological regions and vegetation levels. The predicted amount of soil loss and its spatial distribution can provide a basis for overall management and sustainable land use in Morocco. Areas of high to extremely high soil erosion rates deserve special intervention for the implementation of soil erosion control measures. While the current analytical model helps to map areas of soil erosion risk, the methodology could be improved by obtaining data that are more accurate for RUSLE factors in Morocco.

Chapter 2

Effects of land use and cover type on the risks of runoff and water erosion: Infiltration tests in the Ourika watershed (High Atlas, Morocco)[1]

Effects of land use and cover type on the risks of runoff and water erosion: Infiltration tests in the Ourika watershed (High Atlas, Morocco)

Abstract

The upstream section of the Ourika watershed is located in the northwest slopes of the High Atlas Mountains of Morocco. It is characterized by rugged topography and sparse vegetation, and is under increasing human induced pressures, exacerbated by climate variability and change. Its vulnerability to water erosion is high and, thus, wadi flows with significant solid loads are a constant risk. Infiltration measures through rain simulations, using a simple irrigator ramp, were carried out as part of an investigation to highlight the role of vegetation cover in mitigating soil erosion in the watershed. The methodology assessed the effect of land use and cover type on the soil surface state and properties, on $1m^2$ plots. Seventeen experimental sites were considered with reference to both land use and plant cover, with 3 test plots per site, making it a total of 51 test plots for the rainfall simulations. Soil samples were collected at different depths from each site to determine soil properties.

Results obtained show that dense forests protect the soil, produce organic matter improving soil aggregation and hence ensuring adequate infiltration. In woodlands, bare soil is susceptible to crusting, runoff and water erosion. In overgrazed scrublands, soil compaction due to animal trampling, induces significant runoff. Croplands are poor in organic matter and are consequently very susceptible to crusting, losing infiltration capability.

Infiltration was positively correlated with initial abstraction (r = 0.71), covered and non-crusted soil surfaces (r = 0.84 and r = 0.83 respectively), organic matter content (r = 0.62) and aggregate soil stability (r = 0.69). By contrast, it was negatively correlated with soil detachability (r = -0.65), penetration resistance (r = -0.81) and shear strength (r = -0.64). However, a weak correlation between infiltration and either of bulk density, total porosity or texture was observed. Findings showed that total infiltration was not correlated with the physical parameters of the soil but rather with the surface state of soils. Covered surface greatly decreased runoff and soil erosion by increasing the surface roughness and decreasing the runoff velocity in the study zone.

Keywords: Land use, Vegetation cover, soil surface state, soil properties, Water erosion, rainfall simulations, Ourika watershed, Morocco.

1 Introduction

Land degradation has been gaining momentum, globally, on more than 20% of cultivated lands, 30% of forested areas and 10% of meadows (Bai et al. 2008). The main culprit has been water erosion, with over 56% of the degradation directly linked to it (Pimentel et al. 1995; Nanna 1996; Flanagan 2002). Water erosion exacerbates the loss of land productivity (Elirehema 2001), thus negatively affecting both agricultural and forest productivity, water quality, and infrastructure (Vrieling 2006). Several studies have highlighted the effects of plant cover in mitigating soil erosion, showing that it is the most important factor in reducing soil erosion (Alejandro and Kenji 2007). Additionally, they have shown that soil erosion is more influenced by land use than other environmental features at both plot and watershed scales (Valentin et al. 2008). In the Mediterranean regions, soil remains a fragile component of ecosystems and, if exposed to high and intense rainfall, becomes susceptible to erosion, which is aggravated by hilly or mountainous topography associated with low plant cover (Albergel et al. 2010).

In Morocco, soil erosion has been increasing annually. Indeed, in recent decades, the countryside has undergone considerable changes, with specific degradation varying from region to region and ranging from 5 to 20 t/ha/an (Ghanam 2003). In addition, water reservoirs such as dams have been associated with the accumulation of sediments which results in an annual loss of storage capacity equivalent to 75 million m^3. This corresponds to an irrigation potential of around 5-6000 ha/year (Sabir et al. 2007).

Rainfall simulations have being used since the 1930s to study soil erosion and soil hydrology (Martínez-Murillo et al., 2013). Indeed, they have been successful in hydrology and many other disciplines. During the course of the last 80 years, more than 100 rainfall simulators with plot areas of less than 5 m^2 have been developed (Iserloh et al., 2010). Rainfall simulation contributes to the knowledge of water erosion processes under different environmental situations (Torri et al., 2012). It allows for the exploration of processes which are difficult to detect in natural context during rainfall events (Yair et al., 2013).

The Ourika watershed, located northwest of the High Atlas is characterized by rugged topography, friable substrates, harsh and brutal climate, sparse vegetation and an increasingly human activity, which render it particularly vulnerable to soil erosion (Meliho et al 2016a, b, c). A loss of forest cover or density, and any changes in land uses may induce modifications in the quality and quantity of soil organic matter (Kocyigit and Demirci 2012; Riezebos and Loerts

1998). Other soil properties are equally altered (Tesfahunegn 2013; Wang et al. 2011). Indeed, land use change influences water infiltration (Lal 1988).

Land use, particularly the surface state of the soil (covered soil surface, non-crusted soil surface, penetration resistance, shear strength and surface roughness) are significant factors that affect soil erosion by water effect. Thus, variations in soil physical properties (bulk density, total porosity, humidity and texture) and chemical properties (organic matter content, structural stability of aggregates) may be responsible for the risks of runoff and soil erosion in the upstream section of the Ourika watershed.

This study deals with the effects of different land uses on soil infiltration capacity depending on both physical and chemical parameters, and their interactions in order to identify the main factor of runoff and water erosion risks in the Ourika watershed. To assess erosion risk indicators, rainfall simulations offer an interesting alternative and involve the application of infiltration tests on 1 m^2 plots with the help of a simple irrigator ramp (Roose and Smolikowski 1997).

2   Materials and methods

2.1   Study area
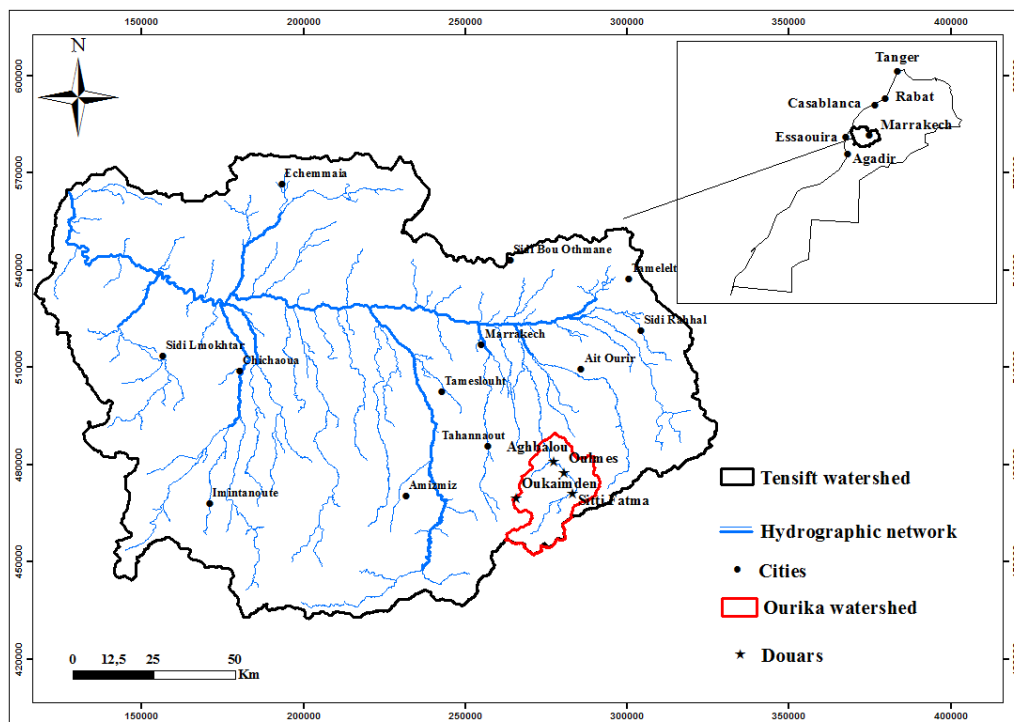
Figure 2.1. Location of the Ourika watershed

The upstream section of the Ourika watershed, covering an area of 576 km² and located in the High Atlas region of Marrakech, is a sub-watershed of the larger Tensift basin (Figure 2.1). The average altitude of the watershed is 2,500 m with a predominance of altitudes (75%) ranging from 1,600 and 3,200 m. Its slopes are generally steep, intensifying runoff and erosion (Meliho et al 2016a, b, c). Geologically, two types of facies characterize the watershed: a hard bedrock (igneous or metamorphic rock) located upstream and a soft to moderately soft substrate of Permo-Triassic and Quaternary deposits located at lower altitudes. Its climate is characterized by high spatial and temporal variability. Annual rainfall averages 500 mm, increasing with altitude, with about 400 mm/year in the foothills while exceeding 700 mm/year in the highest peaks. Ourika watershed shelters a remarkable diversity of forest and pre-forest ecosystems characterized mainly by the holm oak, cedar, juniper as well as oleo-mastic species.

2.2 Experimental design

Land use types in the Ourika watershed were grouped into six classes (croplands, woodlands, moderately dense forests, dense forests, scrubland and bare non-forest lands). The choice of the experimental sites was solely based on Ourika watershed's substrates and land uses as there are no pedological maps available for the region. Superposition of the watershed land use (Meliho et al 2016b) and substrate maps was used to identify homogeneous units (experimental sites) from which the experiment tests were carried out.

Seventeen stations were chosen based on both land use and the nature of the underlying substrate (Figure 2.2). For each station, three replicates were performed, giving 51 rain simulation tests. Indeed, 15 repetitions were carried out in croplands (cereals, fallow, arboriculture), 9 in woodlands, 9 in moderately dense forests, 6 in dense forests, 9 in scrublands and 3 in bare non-forest lands (thorny xerophytes).

Consolidation of land use into six classes, irrespective of substrate and slope, was a result of substrate and slope not significantly influencing infiltration, initial abstraction or runoff coefficient at the chosen 5% significance level. However, substrate had a significant effect on soil detachability.
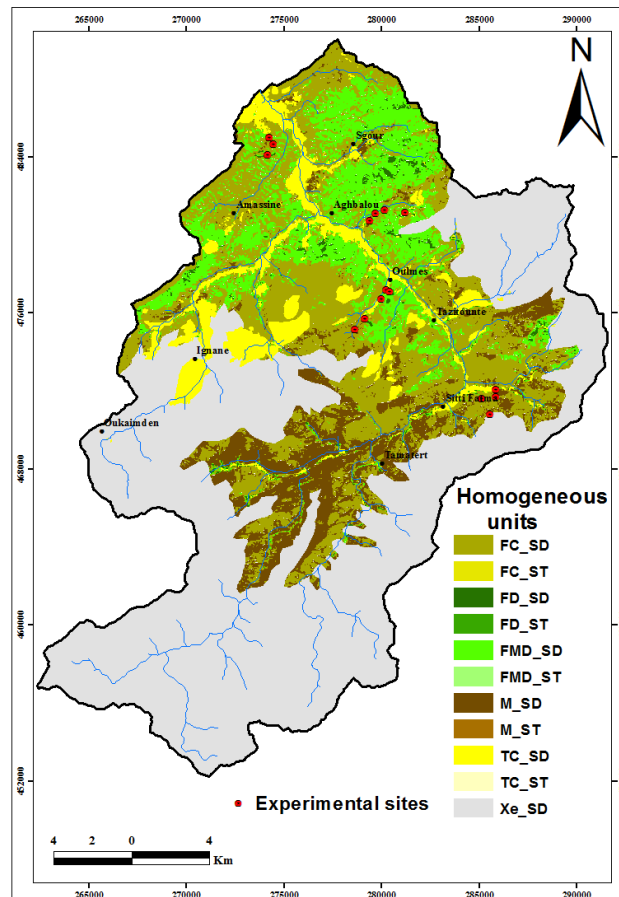
FC: woodland; FD: dense forest; FMD: moderately dense forest; M: scrubland; TC: cropland field; Xe: thorny xerophytes or bare non-forest land; SD: hard substrate (pink granite, andesite, migmatite); ST: soft substrate (red sandstone, red marl, flysch shale and sandstone).

Figure 2.2. Homogeneous units and experimental sites in Ourika basin.

2.3   Description of soil surface state

Measurement of soil surface state was effected using the quadrat method (Roose 1996). Covered soil surface (SC %) included litter, vegetation and pebbles not integrated into the soil mass whereas non-crusted soil surface (SO %) were largely made up of cracks and clods forming traps that facilitate infiltration. After setting up the diagonals of each plot, a pencil was allowed to descend systematically, without aiming, at regular intervals every 2 cm along the line. At the point of contact with the ground, the surface state observed was noted. It is from these readings that the proportion of each surface state was calculated. The formulae are as follows:

- % of bare soil surface = (number of points with bare land) / (total number of points along the two diagonals)

- % of covered soil surface = 100% - % of bare soil surface
- % of non-crusted soil surface = (number of points where the soil is not crusted) / (total number of points observed along the two diagonals)
- % of crusted soil surface = 100% -% non-crusted soil surface

Penetration resistance (PEN) and shear strength (SS) were measured using a pocket penetrometer and a scissometer respectively. Ten measurements were realized for each plot. Penetration resistance (kg/cm²) provides information on soil compaction while shear strength (kg/cm²) gives an idea of the force used by water to detach aggregates from the soil.

Employing the chain method (Roose 1996), soil surface roughness index (R %) was determined. It corresponds to the difference between the expanded chain length and the plot width, divided by the plot width. Three repetitions were done for this parameter.

2.4   Rainfall simulations

Rainfall simulation is one of several methods used to study soil hydrodynamics (Roose and Smolikowski 1997; Roose 1996). Installation of the rainfall simulator consisted of placing two 1.66 m long metallic rods in the direction of the slope (Figure 2.3). A parallel orientation of the two side rods of the equipment's frame, with a width 0.6 m separating them, was maintained. These rods were driven 5 cm below the ground using a hammer to prevent lateral losses of water. A triangular metal platform was then placed downstream to ensure that the dripping water together with the sediments would be directed towards the receptacle.

Figure 2.3. Rainfall simulator

The equipment was installed on a 50 cm wide watering ramp connected by a hose to a tank filled with water holding up to 60 liters. This was located a few meters above the upstream section of the plot (Figure 2.3). The intensity of the simulated rain was maintained at an average of about 80 mm/h by a valve located at the tank's outlet.

Using the rainfall simulator, a simple manual irrigator, allowed drops with relatively low energy to be projected onto a surface of 1m² (Roose 1996). Watering commenced at an average height of 50 cm above the surface with a regular distribution all over the plot. The moment in which run-off is observed is noted since it allows for the determination of initial abstraction (Pi in mm), which simply translates to the height of water infiltrated before the occurrence of run-off. The quantity of water from runoff, measured every five minutes at the lower end of the plot, allowed for measurement of both runoff and infiltration. Moreover, its collection enabled the determination of overall solid load in grams per liter for the period of the experiment.

2.5   Soil sampling

Soil samples, from each site were used for the determination of structural stability, particle size distribution and organic matter content. Others were taken at various depths (0-10, 10-20 and 20-30 cm), using a 10 cm long cylinder with a diameter of 4 cm, to determine bulk density (BD), total porosity (P %), humidity (H %) and soil detachability (D). Measures were taken to protect the samples from external heat before transporting them to the laboratory for analysis. Particle size distribution was determined using Meriaux's densimeter (Meriaux 1954), aggregate stability by Le Bissonnais and Le Souder method (Le Bissonnais and Le Souder 1995) whereas organic matter content was estimated by employing the Walkley-Black method (Walkley and Black 1934).

2.6   Statistical tests

One way analysis of variance was used to determine the differences in effects of land use on soil physical parameters, soil surface state parameters and soil hydrological parameters. The soil surface state parameters examined were both covered and non-crusted soil surfaces, penetration resistance, shear strength and surface roughness. The hydrological parameters considered were total infiltration, initial abstraction, run-off coefficient and soil detachability.

The relationships between the different soil parameters were determined through Pearson correlation test. All the tests were carried out using SPSS software.

3 Results

The results of soil particle distribution, obtained by Meriaux's densimetric method are presented in Table 2.1. They show that the soil texture was loamy and sandy loam under cropland, sandy loam under woodland, loam and sandy loam under moderately dense forest, loamy fine sand under dense forest, sandy loam in scrubland and fine sand under bare non-forest land.

Table 2.1. Soil texture according to USDA classification for the study sites

Land Use	Stations	%Clay	%Silt	%Sand	Texture
Cropland	S1	5	76	19	Silt Loam
	S2	12	40	48	Loam
	S3	10	28	62	Sandy Loam
	S4	12	29	59	Sandy Loam
	S5	7	12	81	Loamy Fine Sand
Woodland	S6	10	32	58	Sandy Loam
	S7	15	0	85	Sandy Loam
	S8	14	13	73	Sandy Loam
Moderately dense forest	S9	18	33	49	Loam
	S10	11	21	68	Sandy Loam
	S11	22	16	62	Sandy Clay Loam
Dense forest	S12	7	10	83	Loamy Fine Sand
	S13	9	6	85	Loamy Fine Sand
Scrubland	S14	13	34	53	Sandy Loam
	S15	15	14	70	Sandy Loam
	S16	14	5	81	Sandy Loam
Bare non-forest land	S17	5	7	89	Fine Sand

3.1 Effects of land use on soil physical parameters

Under all land uses, bulk density increased with depth as total porosity decreased (Table 2.2 and Table 2.3). Compaction, regardless of depth, was pronounced under bare non-forest land, scrubland and woodland, moderate under cropland and low in moderately dense and dense forests.

Table 2.2. Effect of land use on bulk density as a function of soil depth in the Ourika watershed

Land Use	BD_{10} (g/cm³)		BD_{20} (g/cm³)		BD_{30} (g/cm³)	
	m	sd	m	sd	m	sd
Cropland	1.44a	0.17	1.47ac	0.13	1.60a	0.21
Woodland	1.47a	0.10	1.52a	0.09	1.55a	0.17
Moderately dense forest	1.35a	0.26	1.36ac	0.17	1.36ab	0.19
Dense forest	1.26ab	0.44	1.30ac	0.40	138ab	0.33
Scrubland	1.53a	0.21	1.65abc	0.21	1.78ac	0.16
Bare non-forest land	1.78ac	0.26	1.96ab	0.01	-	-

BD10 : Bulk density between 0 and 10cm ; BD20 : Bulk density between 10 and 20cm ; BD30 : Bulk density between 20 and 30cm ; m : mean ; sd : standard deviation. Means followed by the same letter do not significantly differ from each other (P <0.05).

Table 2.3. Effect of land use on porosity as a function of soil depth in the Ourika watershed

Land Use	P_{10} (%)		P_{20} (%)		P_{30} (%)	
	m	sd	m	sd	m	sd
Cropland	45.76a	6.42	44.65ac	4.98	39.59a	7.81
Woodland	44.64a	3.70	42.64a	3.26	41.61a	6.49
Moderately dense forest	49.21a	9.74	48.65ac	6.39	48.64ab	7.24
Dense forest	52.39ab	16.48	50.89ac	15.18	47.87ab	12.49
Scrubland	42.15a	7.91	37.59abc	7.88	32.81ac	6.10
Bare non-forest land	32.89ac	9.83	26.43ab	0.54	-	-

P10 : porosity at 0-10cm ; P20 : porosity between 10 and 20cm ; P30 : porosity between 20 and 30cm ; m : mean ; sd : standard deviation. Means followed by the same letter do not significantly differ from each other (P <0.05).

Values obtained for both bulk density and porosity at 10 cm of depth (Table 2.2 and Table 2.3), varied significantly, at the 5% significance level, between dense forests and bare non-forest lands. At 20 cm, there were significant variations in bulk density between croplands and bare non-forest lands. A similar trend was observed for low-density forests and bare non-forest lands. Additionally, in the bare non-forest lands, the parent rock is encountered at 30 cm depth. As for total porosity, there was a significant variation observed between dense and moderately dense forests, and scrubland.

Table 2.4. Effect of land use on moisture as a function of soil depth in the Ourika watershed

Land Use	H_{10} (%)		H_{20} (%)		H_{30} (%)	
	m	sd	m	sd	m	sd
Cropland	22.33a	13.44	29.67a	12.09	37.53a	15.01
Woodland	16.78ab	8.67	28.44a	10.55	34.22a	8.06
Moderately dense forest	20.78ab	7.61	29.22a	4.99	36.78a	5.91
Dense forest	30.83a	8.21	38.67a	13.63	49.00ab	15.58
Scrubland	16.22ab	13.53	28.00a	14.81	29.75ac	13.80
Bare non-forest land	0.00b	0.00	11.50a	0.71	-	-

H_{10} : humidity at 0-10cm ; H_{20} : humidity at 10-20cm ; H_{30} : humidity at 20-30cm ; m : mean ; sd : standard deviation. Means followed by the same letter do not significantly differ from each other (P <0.05).

Soil samples were collected in March 2016. This was during spring, a period characterized by relatively humid soil, and thus could explain the relatively high moisture content values. Indeed, moisture content values generally are a function of the sampling period. They are high in both winter and spring, when rain is at its most abundant, in the Ourika watershed.

For this period, during which the samples were collected, moisture increased with depth in all land uses (Table 2.4). At a depth of 10 cm, there was a significant difference in moisture, at the 5% significance level, between dense forest and bare non-forest land. However, no significant differences were observed at 20 cm while, at 30 cm, there was a significant difference was noted between dense forest and scrubland. Additionally, no significant difference in soil moisture was observed between moderately dense forest, woodland, cropland and scrubland.

3.2   Effects of land use on soil surface state

Surface state relates to covered soil surface (SC %), non-crusted soil surface (SO %), penetration resistance (PEN %), shear strength (SS %), and the surface roughness index (R %). The highest proportions of covered soil surface were observed in both dense and moderately dense forests (78.33% and 96% respectively). In both cropland and scrubland surface cover was moderate (59% and 52.22% respectively) whereas both bare non-forest land and woodland registered low values (38.33 and 44.44% respectively) (Table 2.5). Plant cover in both dense and moderately dense forests was significantly higher than in scrubland, cropland, woodland and bare non-forest land, at the chosen 5% significance level.

Non-crusted surface proportions were generally low under most of the land uses characterizing the watershed. The highest values were observed under dense forests (41.67%) and cropland (20.60%) while lower proportions were observed in moderately dense forest (13.44%), bare non-forest land (3.67%), scrubland (2.89%) and woodland (2%). Moreover, the non-crusted soil surface proportion observed under dense forest, at a 5% significance level, was significantly higher than the rates observed at other land uses. The values observed under cropland, at a 5% significance level, were higher than those observed under other land uses. They were equally higher than values observed under moderately dense forests, however, not statistically significant.

Table 2.5. Effect of land use on the covered and non-crusted soil surfaces in the Ourika watershed

Land Use	SC %		SO %	
	m	sd	m	sd
Cropland	59.00a	18.15	20.60a	9.13
Woodland	44.44bc	7.07	2.00bc	1.12
Moderately dense forest	78.33bd	7.07	13.44ab	1.94
Dense forest	96.00bd	1.55	41.67bd	6.83
Scrubland	52.22abc	7.55	2.89bc	1.76
Bare non-forest land	38.33abc	2.89	3.67b	1.53

SC%: covered soil surface; SO%: non-crusted soil surface; m: mean; sd: standard deviation. Means followed by the same letter do not significantly differ from each other (P <0.05).

Table 2.6. Effect of land use on soil surface parameters in the Ourika watershed

Land Use	PEN (Kg/cm²)		SS (Kg/cm²)		R %	
	m	sd	m	sd	m	sd
Cropland	1.29a	0.46	1.20abc	0.31	3.42ab	1.42
Woodland	2.62b	0.64	1.50ab	0.40	2.80a	0.80
Moderately dense forest	1.23a	0.81	0.94ac	0.42	3.97ab	1.07
Dense forest	0.21a	0.14	0.35acd	0.11	4.86b	1.18
Scrubland	3.04b	1.93	1.77ab	1.17	2.96a	0.81
Bare non-forest land	0.85a	0.05	0.23ac	0.03	2.36a	0.14

PEN: penetration resistance of the soil surface (kg/cm²); SS: shear strength of the soil surface (kg/cm²); R%: surface roughness; m: mean; sd: standard deviation. Means followed by the same letter do not significantly differ from each other (P <0.05).

Both penetration resistance and shear strength were greater under scrubland (3.04 Kg/cm² and 1.77 Kg/cm² respectively) than at other land uses (Table 2.6). The values observed for the former, under scrubland were higher than those observed under other land uses, with the exception of woodland, at a 5% significance level. As for shear strength, the observed values under scrubland were similarly greater than those observed under other land uses, but with the exception of both woodland and cropland. The highest values for surface roughness were observed under both forests (4.86% in dense forest, 3.97 in moderately dense forest) and cropland (3.42%). Additionally, there was a significant difference in surface roughness between dense forest and the other land uses, with the exception of moderately dense forest and cropland.

3.3   Effect of land uses on hydrological parameters

The hydrological properties considered were final infiltration If (mm/h), initial abstraction Pi (mm), runoff coefficient Kr (%) and soil detachability D (g/m²/h). Data for final infiltration, measured by rainfall simulation, showed three distinct homogeneous groups. Final infiltration was very high in dense forest (all simulated rain was infiltrated, 80 mm/h), high in both moderately dense forest and cropland (64.14 and 63.73 mm/h respectively), and low in bare non-forest land, scrubland and woodland (50.62, 44.69 and 36.17 mm/h respectively) (Table 2.7 and Figure 2.4).

Table 2.7. Effect of land use on soil hydrological parameters in the Ourika watershed

Land Use	If (mm/h)		Pi (mm)		Kr (%)		D (g/m²/h)	
	m	sd	m	sd	m	sd	m	sd
Cropland	63.73a	7.70	6.03a	2.62	16.20a	9.86	19.12a	15.61
Woodland	36.17bc	8.27	1.98bc	0.67	50.16bce	11.56	40.55b	28.88
Moderately dense forest	64.14a	8.06	4.76ab	2.03	10.99abd	9.05	5.73ac	4.97
Dense forest	80.00bd	0.00	80.00cd	0.00	0.00bd	0.00	0.00ac	0.00
Scrubland	44.69bc	8.30	2.75b	1.87	40.97bc	9.54	30.25ab	16.60
Bare non-forest land	50.62abc	1.07	3.78abc	1.26	30.55abc	1.04	61.93b	10.49

If (mm/h): final infiltration; Pi (mm): initial abstraction; Kr: runoff coefficient (%); D (g/m²/h): detachability; m: mean; sd: standard deviation. Means followed by the same letter do not significantly differ from each other (P <0.05).

There was a significant difference in infiltration between dense forest and all other land uses. Indeed, infiltration was highest in the forest, increasing with the density of the canopy. The

runoff coefficient, on the other hand, was null under dense forest (Table 2.7), low in moderately dense forest (10.99 %), and high in other land uses (50.16% in woodlands).

Initial abstraction (Table 2.7) was very high in dense forest (80.00 mm). In dense forest, the absence of runoff implied it being equal to the height of the simulated rain. Indeed, the entire volume of water from the simulation was infiltrated during the experiment.

Detachability was absent in dense forest, owing to the absence of runoff. However, it was low in moderately dense forest (5.73 $g/m^2/h$), high in cropland (19.12 $g/m^2/h$), woodland (30.25 $g/m^2/h$) and scrubland (42.55 $g/m^2/h$), and very high in bare non-forest land (61.93 $g/m^2/h$).
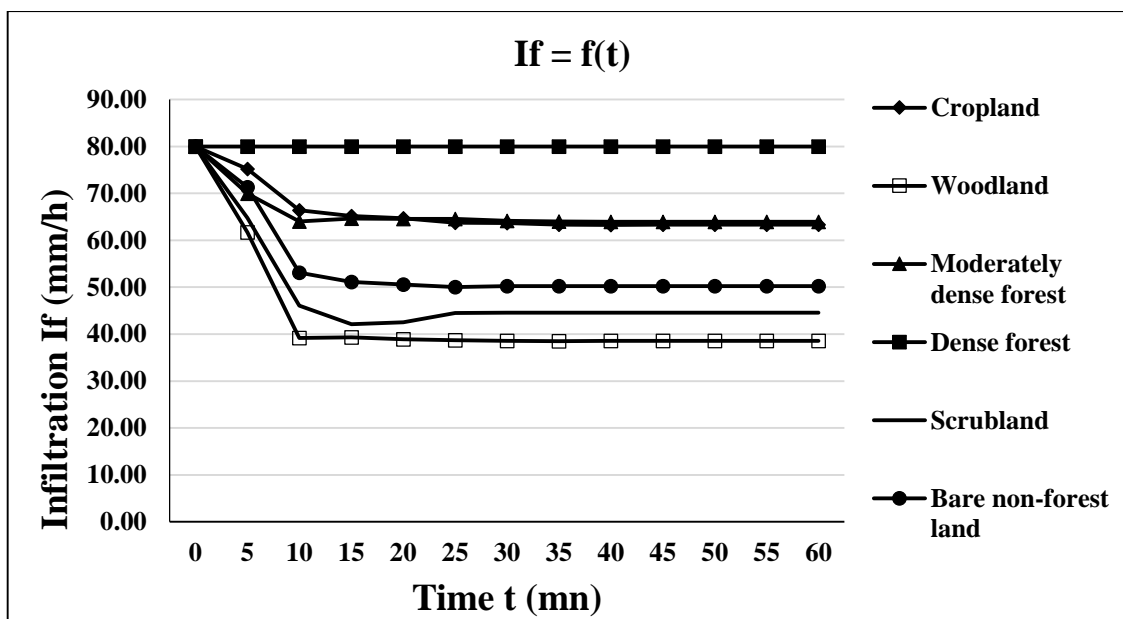
Figure 2.4. Evolution of infiltration measured by rain simulation (80 mm/h) based on different land uses in the Ourika watershed

3.4 Effect of land use on the organic matter content, soil structural stability, and the relationship between them.

Organic matter content was high in the forest (11.81%) compared to other land uses (lower than 6%). Indeed, the forest floor was covered by a surface litter, rich in organic matter and had stable macro-aggregates [mean weight diameter (MWD = 2.3 mm)] compared to scrubland (MWD = 1.06 mm) and cropland (MWD = 1.13 mm). Structural stability of macro-aggregates varied similarly to organic matter in the different land uses and was closely correlated with soil organic matter content ($R^2 = 0.87$) (Figure 2.5).
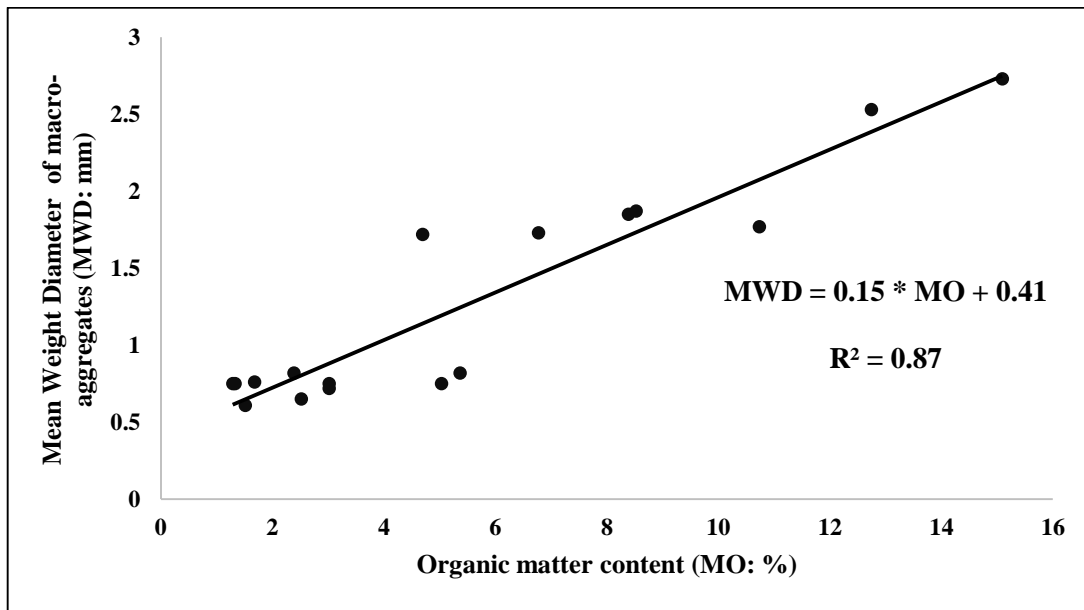
Figure 2.5. Relationship between organic matter content and structural stability of soil aggregates

3.5 Relationship between hydrology, physical, chemical and soil surface state parameters

The study of the relationships between hydrological (If, Pi, Kr, D) and physical (BD_{10}, BD_{20}, BD_{30}, P_{10}, P_{20}, P_{30}, H_{10}, H_{20}, H_{30}, MWD and texture), surface state (SC, SO, PEN, SS, R), chemical (MO) parameters was done by the Pearson correlation test. Our findings are presented in Table 2.8.

Infiltration was positively correlated with both initial abstraction (r = 0.71), covered and non-crusted soil surfaces (r = 0.84 and r = 0.83 respectively), organic matter content (r = 0.62), aggregate stability (r = 0.69), surface roughness (r = 0.53), humidity at 20 and 30 cm depth (r = 0.63 and 0.69, respectively). By contrast, it was negatively correlated with the runoff coefficient (r = -0.99), soil detachability (r = -0.71), penetration resistance (r = -0.81) and shear strength (r = -0.64).

As for initial abstraction, it was positively correlated with infiltration (r = 0.71), covered and non-crusted soil surfaces (r = 0.62 and 0.78 respectively), humidity at 20 and 30 cm depth (r = 0.57 and 0.56, respectively) and negatively correlated with runoff coefficient (r = -0.65).

Table 2.8. Pearson correlation coefficients between the soil hydrological properties and other soil properties

	Soil parameters	If (mm/h)	Pi (mm)	Kr (%)	D (g/m^2/h)
Hydrological parameters	If	1			
	Pi	0.71**	1		
	Kr	-0.99**	-0.65*	1	
	D	-0.65**	-0.19	0.68**	1
Surface state parameters	SC	0.84**	0.62**	-0.84**	-0.81**
	SO	0.83**	0.78**	-0.78**	-0.47
	PEN	-0.81**	-0.46	0.81**	0.37
	SS	-0.64**	-0.46	0.64**	0.11
	R	0.53*	0.44	-0.55*	-0.60*
Chemical parameters	MO	0.62**	-0.31	0.28	0.36
Physical parameters	MWD	0.69**	-0.35	0.42	0.48
	BD$_{10}$	-0.42	-0.32	0.45	0.30
	BD$_{20}$	0.28	0.31	-0.28	-0.36
	BD$_{30}$	0.42	0.35	-0.41	-0.47
	P$_{10}$	0.42	0.31	-0.44	-0.29
	P$_{20}$	0.30	0.38	-0.26	-0.36
	P$_{30}$	0.14	0.37	-0.10	-0.22
	H$_{10}$	0.21	0.42	-0.20	-0.14
	H$_{20}$	0.63**	0.57*	-0.57*	-0.40
	H$_{30}$	0.69**	0.56*	-0.67**	-0.56*
	A	-0.38	-0.35	0.34	0.06
	L	0.19	-0.25	-0.23	-0.21
	S	-0.10	0.34	0.15	0.19

* indicates significant relationship p<0.05
** indicates significant relationship p<0.01
If: infiltration (mm/h), Pi: initial abstraction (mm), Kr: runoff coefficient (%), D: detachability (g/m^2/h), SC: covered soil surface (%), SO: non-crusted soil surface (%), PEN: penetration resistance (Kg/cm²), SS: shear strength (Kg/cm²), R: Surface roughness (%), MO: organic matter (%), MWD: mean weight diameter of soil aggregates (mm), BD$_{10}$: Bulk density between 0 and 10cm (g/cm³) ; BD$_{20}$: Bulk density between 10 and 20cm (g/cm³) ; BD$_{30}$: Bulk density between 20 and 30cm (g/cm³), P$_{10}$: porosity at 0-10cm (%) ; P$_{20}$: porosity between 10 and 20cm (%) ; P$_{30}$: porosity between 20 and 30cm (%), H$_{10}$: humidity at 0-10cm (%) ; H$_{20}$: humidity at 10-20cm (%) ; H$_{30}$: humidity at 20-30cm (%); A: Clay (%) ; L: Silt (%) and S: Sand (%).

The runoff coefficient, on the other hand, was positively correlated with detachability (r = 0.68), penetration resistance (r = 0.81) and shear strength (r = 0.64), and negatively correlated with infiltration (r = -0.99), covered and non-crusted soil surfaces (r = -0.84 and r = -0.78 respectively), surface roughness (r = -0.55), humidity at 20 and 30 cm depth (r = -0.57 and -0.67, respectively).

Detachability was positively correlated with the runoff coefficient (r = 0.68) and negatively correlated with infiltration (r = -0.65), covered soil surface (r = -0.81) and humidity at 30 cm depth (r = -0.56).

These findings clearly showed that surface state was the determinant factor with respect to the soil's hydrological behavior in the Ourika watershed (Table 2.8). Among soil physical properties, only soil humidity below the depth of 10 cm was correlated with the hydrological properties of the soil. This could be explained by the increase in soil humidity in highly covered surfaces. Total infiltration was also correlated with the aggregate stability.

4 Discussion

Vegetation improves both physical and surface properties of the soil by creating cavities in it, as it does soil structure through the incorporation of organic material, thus decreasing bulk density, penetration resistance and shear strength. It equally increases porosity and surface roughness. Tillage, on the other hand, results in rapid loss of organic matter either by mineralization, erosion or through the destruction of aggregates (Sabir et al 2007). In our study, the dominance of sandy soil, coupled with low vegetation cover, in bare non-forest lands could explain the high bulk density and low porosity values observed (Table 2.2 and Table 2.3). In scrubland, soil compaction was probably a result of animal trampling. Under dense and moderately dense forests, the soil was, for the most part, loose on the surface and less dense with increasing depth compared to other land uses. Moreover, the highest macrospore presence was observed in the top 10 cm under dense forests, which could be explained by the abundance of plant cover and consequently litter in the surface horizon (Table 2.3). As for porosity, it plays a very important role in the proportion and circulation of water and air in the soil for plants. Forest soil is rich in litter and consequently better aerated due to root systems and soil animal dynamics. Despite the tillage in croplands, porosity remained lower than in forests. The absence of moisture at the 10 cm depth in the bare non-forest lands (Table 2.4) could be attributed to both the sandy texture of the soil and the low plant cover. By contrast, the high moisture content in forests confirmed the importance of vegetation, which limits the drying effect of sunlight to the soil. This was not the case for either croplands or scrubland whose soil is generally subjected to the direct effects of solar radiation.

Field observations showed that the high surface cover in forests was a direct result of dense vegetation and, consequently, litter accumulation. In croplands, residues of previous crops were

responsible for most of the cover. In scrubland, herbaceous and to some extent scrub vegetation provided soil cover, while pebbles were, for the most part, responsible for the observed cover in both bare non-forested lands and woodlands.

Despite a general environmental degradation, surface cover rate was high under all soil types. Indeed, even when vegetation was scarce, pebbles were present and, to a lesser extent, played a role in protecting the soil surface. Non-crusted surfaces did not account for significant portions of the watershed, with the highest rates being observed under forest and croplands. This could be attributed to the presence of cracks created by root systems and soil animal activity in the forest, and by clods because of ploughing in croplands.

Under forests and bare non-forest lands, very low values of both penetration resistance and shear strength were observed (Table 2.6). This could be attributed to the high litter and, thus, organic matter content in the forest, which attenuate the prevalence of these parameters. By contrast, the low values obtained in bare non-forest lands were most likely a result of the sandy texture of the soil. Under scrubland, woodlands and croplands, these soil properties become more notable. This could be a result of animal trampling in scrubland, the presence of crusts in woodlands and tillage in cropland, which result in loss of soil cohesion as well as crusting. Surface roughness was significant in both forests and croplands, and was mainly attributed to litter originating from abundant vegetation in forests and plough tracks in croplands. To a lesser extent, it could also have been a result of the presence of both herbaceous plants and tiny pebbles, which enable its presence in scrubland, woodlands and bare non-forest lands.

Vegetation cover, upon improving the physical properties and surface state of the soil, facilitates water infiltration into the soil, thus, reducing the risk of runoff and erosion. Several authors have shown that it is the most significant factor with respect to improving soil water infiltration and, consequently, mitigating runoff risks (Roose, 1996; Al Karkouri et al 2000; Sabir et al 2004; Sabir et al 2007 She et al., 2014 ; Liu et al., 2014).

As for total infiltration, it was negatively correlated with both the runoff coefficient ($r = -0.99$) and penetration resistance ($r = -0.81$). By contrast, it was positively correlated with both covered and non-crusted ($r = 0, 84$ and $r = 0.83$ respectively) soil surfaces, thus confirming the importance of plant cover with respect to mitigating runoff and consequently water erosion. Indeed, infiltration in the Ourika watershed is a function of soil surface states. Some authors (Sabir et al 2007, Sabir et al 2004; Al Karkouri et al 2000) have observed similar results in various regions of Morocco. They found final infiltration to be closely related to surface states,

and particularly surfaces covered with crusts as well as those characterized by compacted areas. Additionally, they showed that it was equally correlated with aggregate stability, which itself is a function of organic matter content in the topsoil. The runoff coefficient values observed in this study ranged from 0 (dense forest) to 50.16 % (woodland). These are fairly similar to values obtained in the Western Mediterranean regions (4.7 to 47.4%) (Martínez-Murillo et al., 2013). High runoff coefficient values varying from 25.35 (straw covered soil) to 65.15 % (bare soil) were observed by other authors in Mediterranean vineyards (Prosdocimi et al., 2016).

Detachability, on the other hand, was negatively correlated with the covered soil surface (r = -0.81), with bare soils being the most susceptible to runoff and erosion. Our findings are in tandem with those obtained by another author (Cheggour 2008) in the Rheraya basin, wherein, an exponential relationship between turbidity and bare soil was observed. Factors such as the covered soil surface (vegetation, litter, rocks) probably masked the effect of texture on soil detachability. In our study, soil detachability values ranged from 0 to 61.93 g/m²/h. These values are lower than those obtained in the Western Mediterranean badlands environments (14.1 to 1045.1 g/m²/h) (Martínez-Murillo et al., 2013).

Interestingly, significant correlations between infiltration and soil physical parameters were not observed. This could probably have been due to low variations in these parameters within the studied plots. These results point in the same direction as those obtained by other authors (Sabir et al 2007, Sabir et al 2004; Al Karkouri et al 2000) who performed similar infiltration tests, but on more developed soils of the central Rif in Morocco. Their findings showed that total infiltration was not correlated with the physical parameters of the soil but rather with the surface state of soils.

Soil hydrodynamic parameters and physical properties were weakly correlated (Table 2.8). Infiltration was weakly correlated with bulk density (r = -0.42, r = -0.28 and r = -0.42 at depths of 10 cm, 20 cm and 30 cm respectively), total porosity (r = 0.42, r = 0.30 and r = 0.14 at depths of 10 cm, 20 cm and 30 cm respectively). In the same manner, there was no strong correlation between infiltration and the proportions of clay (r = -0.38), silt (r = 0.19) or sand (r = -0.10). Similar weak correlation relationships were observed for initial abstraction (Table 2.8). These findings could be explained by the fact that the effect of soil physical properties on hydrodynamic parameters seemed to be masked by that of surface state, which was the determining factor. However, in the high non-crusted soils (forest dense and moderately dense, cropland), the correlation between Infiltration and soil physical properties such as bulk density

and total porosity in the first 10 cm of the soil significantly increased (r = - 0.56 and r = 0.56, respectively). Infiltration was also significantly correlated with clay proportion in the soil (r = - 0.76). This points to the fact that in non-crusted soils, soil physical properties improved soil hydrodynamic properties.

5 Conclusion

Results of this study show that infiltration tests make it possible to identify the factors responsible for runoff and therefore water erosion. Despite the simplicity of the experimental device used, results obtained are useful for understanding runoff and erosion risks in semi-arid mountainous areas. It provides important information with regards to runoff and erosion risks, as a product of land use patterns.

In this regard, dense to moderately dense forests, characterized by high organic matter, provide adequate cover for soils and improve their aggregation, thus, resulting in excellent infiltration. In woodland areas, bare soil is exposed to runoff risks and crusting whereas scrublands, associated with overgrazing, cover much less soil and experience significant runoff, but with reduced solid loads. Croplands, on the other hand, are generally associated with reduced plant cover. This coupled with low organic matter content results in them being highly susceptible to crusting, and results in them losing the ability for infiltration.

Infiltration is a function of hydrological parameters (initial abstraction, runoff coefficient, and detachability) and surface state parameters (covered soil surface, non-crusted soil surface, penetration resistance and shear strength). It is equally dependent on soil structural stability determined by the content on organic matter. On the other hand, no relationship between infiltration and soil physical properties such as bulk density, total porosity, soil moisture and texture was observed in the study area. Infiltration was negatively correlated with soil detachability (r = -0.71), which, in similar fashion, was negatively correlated with covered soil surface (r = -0.81). Thus, the degradation of the vegetation, leading to a diminished cover, results in an increase in soil detachability and consequently runoff. The increase in both runoff and detachability resulted in increased risk of erosion and, as such, showed that infiltration could be used as an applicable indicator of runoff and erosion risks.

Finally, the highlighted relationships allow for a preliminary analysis of dominant processes of water erosion in both the Ourika watershed and the Marrakech High Atlas region as a whole. Indeed, they would be useful for the calibration of water erosion hydrological models as well as serve as a

Chapter 3

Assessment of soil redistribution rates by ^{137}Cs in typical Moroccan High Atlas cultivated and uncultivated soils[2]

[2] Meliho M., Nouira A., Benmansour M., Boulmane M., Khattabi A., Mhammdi N., Benkdad A. (2019) Assessment of soil erosion rates in Mediterranean cultivated and uncultivated soils using fallout 137Cs. *Journal of environmental radioactivity*, 208, 106021.

Assessment of soil redistribution rates by ^{137}Cs in typical Moroccan High Atlas cultivated and uncultivated soils

Abstract

Soil degradation, particularly water erosion is considered the major environmental threat affecting soil and water resources management in Morocco. However, there is still only limited data available on soil erosion rates necessary for optimizing strategies for soil conservation. In this study, ^{137}Cs technique was used to assess soil erosion magnitude in Moroccan High Atlas and to study the effectiveness of terrace cultivations. Indeed, in the high atlas, particularly, the Ourika watershed, terraces agriculture is under two differents crops systems; cereal crop and arboriculture. Studied cultivated areas were chosen under increasing anthropic pressure, making them especially vulnerable to water erosion. Representative forest fields were also studied to compare, in term of soil degradation, agroforestry to terraces agriculture. The transect approach was adopted for sampling to study the spatial redistribution of ^{137}Cs and its inventory was determined by gamma spectrometry. Collected sampling points were cut each 10 cm to explore the correlation between land use and soil characteristics.

A strong correlation was observed between ^{137}Cs and either SOC or slope gradient, in uncultivated area (forest). However, there was no correlation for cultivated terraces. Regarding the soil erosion rates, the main results indicate that the cultivated terraces are relatively more eroded than the natural forest and the soil erosion rates associated with cultivated terraces under cereals are higher than those corresponding to terraces under arboriculture. Indeed, the net erosion rates were estimated about 8.5 and 6.0 t ha^{-1} yr^{-1} in cereal crop and arboriculture agrosystems, respectively, whereas in forest, the net erosion rate was of about 4.2 t ha^{-1} yr^{-1}.

The net erosion rate observed on agricultural terraces is not significant compared to the acceptable threshold for soil loss set for Morocco (< 7 t ha^{-1} yr^{-1}). In addition, the rate of erosion on arboriculture terraces is close to that of the forest. Terraced arboriculture systems should be encouraged for better soil preservation against water erosion in the Ourika watershed.

Key words: ^{137}Cs technique, cultivated terraces, uncultivated land, soil erosion, SOC, high atlas, Morocco.

1 Introduction

Soil erosion and the subsequent sedimentation linked to it are natural processes, which are accentuated by human activities such as changes in land use, inappropriate management of farmlands, deforestation and overgrazing. This greatly hampers both production and conservation of natural resources (Lal, 2000; Walling, 2001, Dercon et al., 2012). Soil erosion and related processes not only affect the eroded site, leading to loss of fertility (Schmitter et al., 2010), but also causes off site events such as mobilization and transport of sediments and contaminants to reservoirs and water bodies (Dercon et al., 2012).

Soil degradation affects about 1.9 billion hectares worldwide land, with an increase of 5 to 7 million hectares annually (IAEA, 2014). Around the world, approximately 80% of agricultural lands is suffering from moderate to severe erosion (IAEA, 2014). Indeed, the annual soil loss cost worldwide has been estimated to US $400 billion per year (Lal, 2006).

In the Mediterranean region, soils are a fragile component of ecosystems. They are particularly sensitive to risks of erosion, because of Mediterranean rainfall regime (intensive rainfall) which provokes a marked run-off event. This phenomenon is accelerated by rugged or mountainous topography (Albergel et al., 2010). With increasing food demand, linked to population growth and declining productivity of previously high-potential land, it became imperative to cultivate land less suitable for agriculture and whose climatic conditions are less favorable (Roose, 1993). This, however, particularly exacerbates the vulnerability of the Mediterranean region to water erosion.

Soil erosion is not a recent phenomenon in Morocco. Indeed, it has taking on an increasingly greater scale with every passing year in the sense that, over the last few decades, the Moroccan natural landscape has undergone considerable alterations. Agriculture plays an important socio-economic role in Morocco, with the sector accounting for more than half of the labor force and contributing to more than 17% to the gross domestic product (HCEFLCD, 2012). However, the acceleration of soil erosion threatens the sustainability of this sector. Moreover, the inappropriate intensification of agriculture in natural areas has accentuated the phenomenon. More than 15 million hectares of agricultural land is threatened, with an estimated 100 million tons of soil lost annually. Dam reservoirs, through accumulation of sediments, lose the equivalent of 75 million m^3 of their storage capacity annually. This corresponds to an irrigation potential of 5000 to 6000 ha/year (HCEFLCD, 2012).

Several methods are used in the investigation of water erosion. However, the wide use of these methods has shown their limitations due to various factors including spatial and temporal variability, operational difficulties, cost and reliability of results (IAEA, 2014). Because of limitations associated with the conventional methods of quantifying erosion as well as the generated uncertainties, techniques using radioactive elements have been adopted as an alternative approach.

Several radioactive elements have been used in the study of soil erosion and sedimentation. The main elements used include ^{137}Cs, ^{210}Pb and ^{7}Be (Zapata, 2002). Among the various isotopes tested since the early 1960s, ^{137}Cs, due to its properties and environmental behavior, has proven to be a particularly reliable tracer for measuring soil erosion at different scales, and has been widely adopted (AIEA, 2014).

In the Mediterranean region, Cs-137was used in several erosion studies (eg: Navas and Walling, 1992; Quine et al., 1994; Porto et al., 2001 ; Navas et al., 2007; Porto and Walling, 2012; Porto et al., 2016), thus demonstrating its effectiveness in this regional context. In Morocco, since the mid-1990s, several studies have been carried out using Cs-137 as a tracer of soil erosion in watersheds. These studies were realized in the northern and western regions of Morocco (eg: Bouhlassa et al., 2000; Nouira et al., 2003;Sadiki et al., 2007; Benmansour et al., 2013; Damnati et al., 2013). However, this technique was not used in the High Atlas Mountains of Marrakech. A very rugged topography, friable substrates, a harsh and brutal climate, a low-density plant cover and an increasingly growing human impact characterize the watersheds of these mountainous regions, including Ourika. This exposes them to water erosion. Thus, the Ourika watershed is plagued with the problem of forest degradation and the extension of terraces (Meliho et al., 2016, 2017).

In the High Atlas region of Morocco, farmers have dissected the original long hillslope into several slope segments to minimize soil loss by water and facilitate field management operations. The effectiveness of the resulting terraces in reducing soil erosion by water is well recognized, but studies on soil erosion within them remain a rarity (Zhang et al., 2012). Despite the problem of soil erosion, there are still only limited datasets available regarding the actual status of soil and water resources sustainability. The existing studies on soil erosion in the Ourika Watershed focus on the use of the experimental runoff plots technique and RUSLE model (Meliho et al., 2016, 2017). However, fallout radionuclides such as Cesium-137 can be an excellent alternative for the studies of soil erosion compared to traditional investigation

methods (Zupanc and Mabit, 2010). Reliable data about soil erosion is essential in order to evaluate the severity of the phenomenon and to design effective strategies for soil conservation and sustainable crop production.

The aim of this study is to evaluate the effectiveness of terrace cultivations under different crops and their comparison to natural forest, in term of soil erosion, in Ourika region. Transect approach was used to quantify the spatial soil redistribution, to estimate erosion or deposition rates on a representative cultivated (terraces) and uncultivated (forest) field, with the goal of proposing measures for the conservation and sustainable management of soils.

2 Material and method

2.1 Study area

The Ourika watershed is a well-individualized hydro system of the High Atlas of Marrakech, between 31° and 31°20' North and between 7°30' and 7°60' West (Figure 3.1). The main wadi has its sources in the high foothills of the High Atlas Mountains. The climate of the Ourika watershed is highly variable in time and in space. Annual precipitation averages 500 mm (1976-2011). This increases with altitude and is of the order of 400 mm in the foothills while exceeding 700 mm on the high peaks of the watershed. Average temperatures range from 21.5 to 32°C and 4 to 5.7 ° C for maxima and minima respectively. July and August are the hottest months of the year, while December and January are the coldest. The temperature varies between 48.2°C and -7.2°C, with an average of 27.8 ° C. The region of Ourika is famous for its high and complex reliefs. Seventy-five percent of the watershed's area is between 1600 and 3200 m of altitude with the average of about 2500 m. The slopes are generally steep. A slope gradient greater than 50% characterizes more than 50% of the watershed area. The slopes are low downstream and very high upstream of the watershed. The Ourika watershed is made up of magmatic and metamorphic rocks in the upper zone, and Permo-Triassic and Quaternary Age deposits are located at lower altitudes. The soils are mainly skeletal and rocky. Forest and pre-forest ecosystems in the watershed are generally degraded and sparse. The populations live mainly from terraced farming and extensive livestock farming depending on natural forest ecosystems marked by the presence of *Quercus rotundifolia, Tetraclinis articulata* and *Juniperus* species.
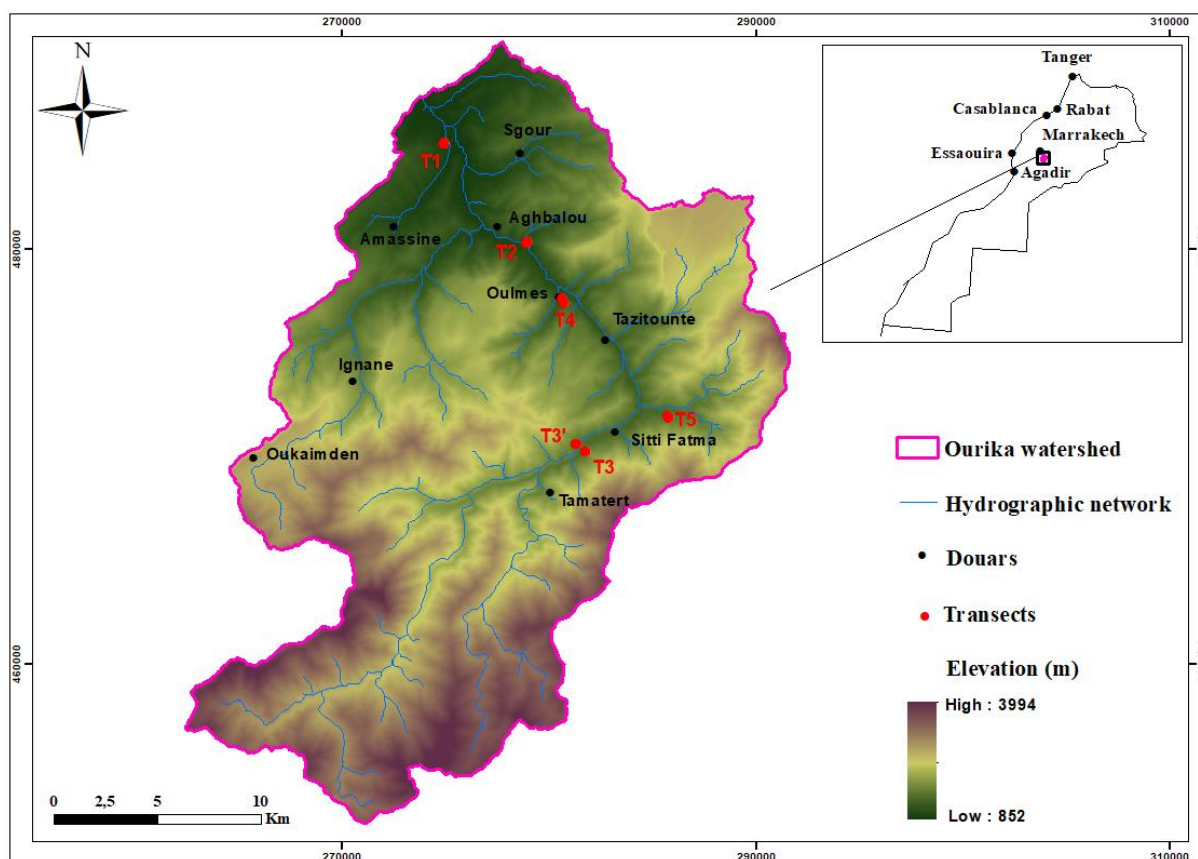
Figure 3.1. Location of the watershed Ourika

2.2 Sampling strategy

In the Ourika watershed, cultivated lands represent 7% of the area, forest 35%, thorny xerophytes 50% and bare soil/buildings represented 8%. On cultivated lands two agricultural systems are commonly adopted in Ourika; cereals and arboriculture in terraces. The construction of the terraces pre-dated the main period of Cs-137 fallout in the late 1950s and the 1960s. There were no specific and regular maintenance of the terraces through time. The upstream section, composed of thorny xerophytes is referred as "non-forest empty land" under pink granite, representing 50% of the total area of the watershed. Those are mainly uncultivated lands, which were almost barren.

To study the efficiency of soil management systems developed in the valley of ourika, 5 homogeneous units have been established taking account of soil texture, slope and cover. The five homogeneous units, were considered during sampling. From each unit only one transect was taken

- Soil type 1 (S1): Loamy soil over sedimentary rock with two land uses, cultivated terraces (grain farming) land (T1) and uncultivated (forest) land (T2),

- Soil type 2 (S2): Sandy loam soil over igneous rock with two land uses, cultivated terraces (arboriculture) land (T3 and T3') and uncultivated (forest) land (T4),

- Soil type 3 (S3): Sandy soil over igneous rock with one land use, uncultivated non-forest empty land (T5).

In S2, because of the topography difficulty, there were no accesses to the top with the material transported on the mule. Therefore, sampling stopped before to reach the top (Figure 3.2). Another transect was chosen from another same site which is transect T3'. The samples, were then collected from six transects (T1, T2, T3, T3', T4 and T5) from the upslope to the downslope and along terraces in cultivated sites (Figure 3.2). Despite the relatively small number of samples, because of the expensive analysis cost, transects were chosen to represent the soil particle behavior (in water flow direction). On terraces, samples were collected from the middle of the terraces. The distance between sampling points depends on both the length of the slopes and the spacing between terraces. Cores were extracted using a core motor consisting of a 9 cm wide and 1 m long cylindrical tube. Each collected point was incremented to 10 cm up to depth 30cm in order to study the ^{137}Cs depth distribution for the different land uses. In each sampling point, coordinates and altitude were recorded using a GPS whereas slope was measured using a clinometer.

Two reference sites were selected next to studied sites with same altitude, precipitation and soil texture. The First reference site (Ref 1) is composed of shrub formation, which was abandoned for over 100 years, composed of *Pistacia lentiscus* and free of any disturbance adjacent to the sampling sites. This one was used to calculate soil erosion assessments for T1 and T2. The second reference site (Ref 2) was used for T3, T3', T4 and T5 erosion rate calculation. It is a plateau at the mountaintop composed of sparse green oak (*Quercus rotundifolia*) and *Cistus sp* vegetation. The two reference sites are flat, with slope gradient varying from 0 to 1%. In each reference site, 12 samples were collected at a depth 30 cm based on grid approach. To determine ^{137}Cs depth distribution in reference sites, an extracted soil core from each reference site was incremented each 4 cm.

The bulk soil samples were clipped to a 0-10, 10-20 and 20-30 cm depth, in each ^{137}Cs sampling point, using a cylinder of 10 cm in height and 4 cm in diameter to investigate some physicochemical parameters of soil. Bulk density was determined by classical method. Particle

size distribution was defined using Meriaux's densimetric methods (Meriaux, 1954) whereas organic matter by the Walkley-Black method (Walkley and Black, 1934).
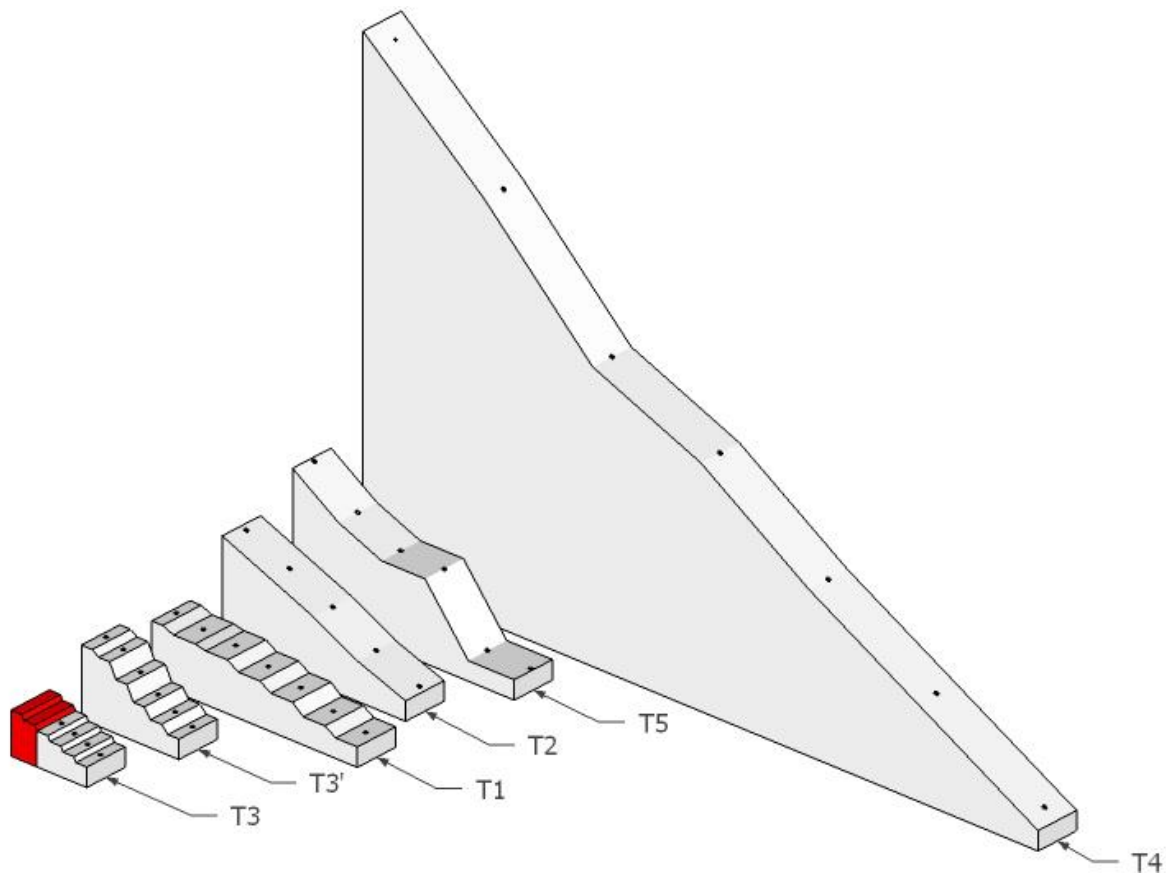
Figure 3.2. The sampling procedure using the transect approach

2.3   Gamma spectrometry

Soil samples were dried at 80°C for 24 h, disaggregated, passed through a 2 mm sieve, homogenized and weighed. Soil coarse fraction (> 2 mm) was determined. Bulk soil samples were placed in 500 ml Marinelli beakers whereas the incremental samples were prepared in 175 ml and 75 ml cylindrical containers.

Two high purity coaxial germanium detectors (30% efficiency, 1.8 keV resolution) coupled to a multichannel analyzer system were used for ^{137}Cs concentration measurements. The detection systems were calibrated using certified multi-gamma source IAEA reference materials (IAEA 327, IAEA 375).[137]Cs activity was determined from the net peak areas of gamma (γ) rays at 661.66keV. Samples radioactivity was counted for 12–24 h with a precision lower than 10% at

the 95% level of confidence. Calibration and quality control of the gamma spectrometry analysis were performed using control charts (efficiency, resolution and background), certified reference materials and through regular participation in inter-comparison exercises and proficiency tests organized by the IAEA (Shakhashiro and Mabit, 2009).

2.4   Conversion models

Mass balance model II (MBMII) was used for estimating long-term (50 years) rates of water-induced soil erosion for cultivated sites. This model takes account of both time-variant fallout ^{137}Cs input and fate of the freshly deposited 137Cs fallout before its incorporation into the plough layer by cultivation (Walling et al., 2002; Walling et al., 2014). Thus, the model results are more likely to be realistic.

The equation of Mass Balance II model is represented as:

$$\frac{dA(t)}{dt} = (1 - \Gamma)I(t) - (\lambda + P\frac{R}{d})A(t)$$

Where:

$A(t)$= cumulative ^{137}Cs activity per unit area (Bq m^{-2});

R = erosion rate (kg m^{-2} yr^{-1});

d = cumulative mass depth representing the average plough depth (kg m^{-2});

λ= decay constant for ^{137}Cs (yr^{-1});

$I(t)$ = annual ^{137}Cs deposition flux (Bq m^{-2} yr^{-1});

Γ = percentage of the freshly deposited ^{137}Cs fallout removed by erosion before being mixed into the plough layer;

P = particle size correction factor.

For uncultivated sites, the Profile Distribution Model (PDM) was used since an exponential reduction was observed in undisturbed soil profiles. The depth distribution of ^{137}Cs in the uncultivated soil profile will be significantly different from that in cultivated soils where the ^{137}Cs is mixed within the plough or cultivation layer. The depth distribution of ^{137}Cs in an

undisturbed stable soil exhibits an exponential decline with depth that may be described by the following function:

$$A'(x) = A_{ref}(1 - e^{-x/h_0})$$

Where:

$A'(x)$ = amount of ^{137}Cs above the depth x (Bq m^{-2});

$A_{ref} = {}^{137}$Cs reference inventory (Bq m^{-2});

x = depth from soil surface (kg m^{-2});

h_0 = coefficient describing profile shape (kg m^{-2})

If it is assumed that the total ^{137}Cs fallout occurred in 1963 and that the depth distribution of the ^{137}Cs in the soil profile is independent of time, the erosion rate Y for an eroding point can be expressed as:

$$Y = \frac{10}{(t - 1963)P} \ln(1 - \frac{X}{100})h_0 \tag{27}$$

where:

Y = annual soil loss (t ha^{-1} yr^{-1});

t = year of sample collection (yr);

X = percentage ^{137}Cs loss in total inventory in respect to the local ^{137}Cs reference value

P = particle size correction factor.

For a depositional location, the deposition rate R' (kg m^{-2} yr^{-1}) can be estimated from the excess ^{137}Cs inventory $A_{ex}(t)$ (Bq m^{-2}) and the ^{137}Cs concentration of deposited sediment $C_d(t')$ (Bq kg^{-1}):

$$R' = \frac{A_{ex}}{\int_{t_0}^{t} C_d(t')e^{-\lambda(t-t')}dt'}$$

3 Results and discussion

3.1 ^{137}Cs depth distribution profile in reference sites

The ^{137}Cs depth distribution profiles show a decreasing exponential shape in the reference sites (Figure 3.3 and Figure 3.4) with a maximum ^{137}Cs retained in the top 8 cm, representing 85% of total ^{137}Cs in reference 1 and 84% in reference2, followed by an exponential decline with depth.

In Reference 1 profile, the ^{137}Cs reach depth of 20 cm, , whereas in Ref 2, ^{137}Cs is observed until 28 cm, this can be explained by the differences in soil texture, altitude and rainfall. In Ref 1, soil is loamy, while in Ref 2 it is sandy loam soil. The altitudes are 1212 and 1438 m respectively for Ref 1 and Ref 2. Rainfall is related to the altitude in the watershed and increases as the altitude increases. It is respectively 479 and 533 mm/year (1968-2015) for Ref 1 and Ref 2. The penetration depth of ^{137}Cs increases with the proportion of sand in the soil and with the increase of rainfall.
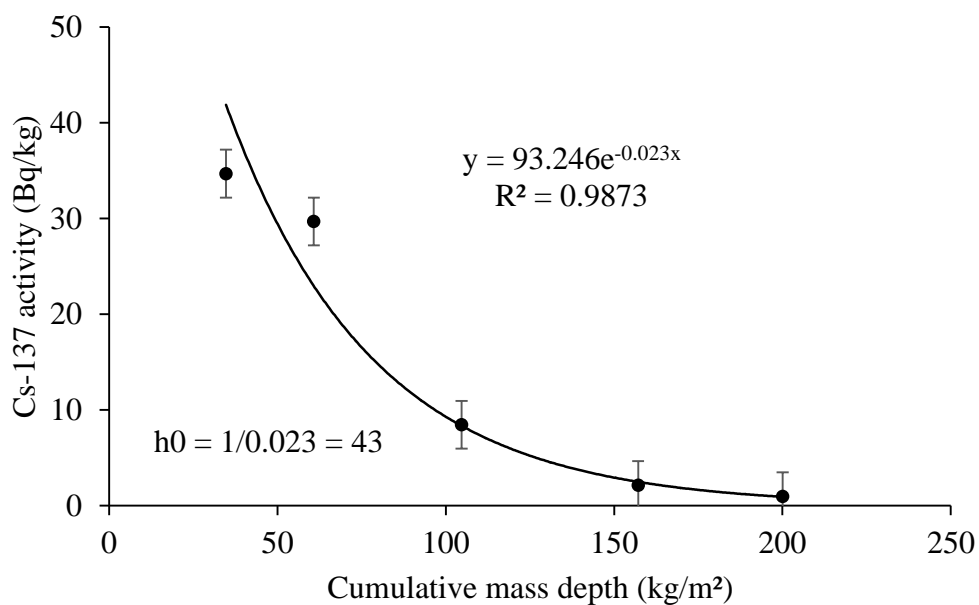
Figure 3.3. ^{137}Cs Depth distribution for reference site 1
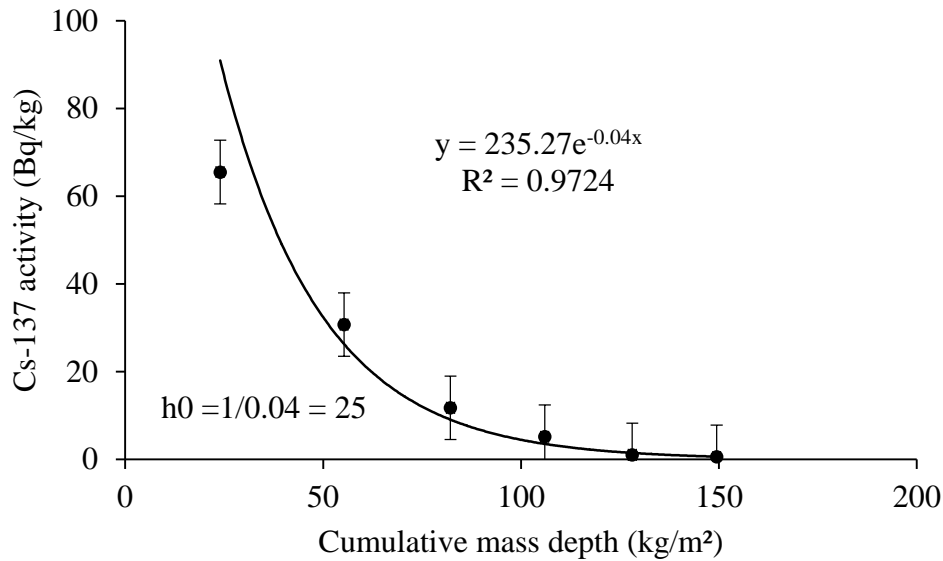
Figure 3.4. ^{137}Cs Depth distribution for reference site 2

The exponential distribution of both ^{137}Cs depth profiles confirms that the reference sites were undisturbed during the last decades. The maximum penetration depth is approximately 20-28 cm for the references sites. ^{137}Cs depth distribution observed are similar to other studies, reporting that a large proportion of the ^{137}Cs total inventory is contained within the top 15 cm of the soil (Mabit et al., 2008) and 10-15 cm reported by Benmansour et al. (2013).

For the reference sites, the mean values of ^{137}Cs inventories are found about 1927 ± 385 Bq.m^{-2} and 2229 ± 608 Bq.m^{-2} (mean ± sdev) for Ref 1 and Ref 2, respectively, with relative standard deviations of 20% and 27%. Previous similar investigations reported relative standard deviations varying from 15 to 30% for reference sites (Sutherland, 1996). The coefficient of variation obtained for our references sites are within this range. Also, reference inventories are within obtained values from earlier Moroccan studies on soil erosion using ^{137}Cs technique, with reference inventories varying from 1021 to 4491 Bq.m^{-2} (Bouhlassa et al., 2000; Nouira et al., 2003; Sadiki et al., 2007; Benmansour et al., 2013; Damnati et al., 2013). The estimated reference inventories using CsModel (Walling et al., 2002; Walling et al., 2014) are 1756 and 2010 Bq.m^{-2} for Ref 1 and Ref 2, respectively. These values are close to obtained values for the reference sites.

3.2   Depth distribution of 1^{37}Cs in the studied sites

Both vertical and spatial distributions of ^{137}Cs were examined from the top of the hillslope to the bottom. The depth distribution profiles along the six transects exhibit dissimilarities that

reflected differences in land use, topographic roughness, soil particle distribution, stoniness. Those factors can cause significant variations in ^{137}Cs content, as widely recognized in Mediterranean environments (Quine et al., 1994; Navas et al., 2007, Gaspar and Navas, 2013).
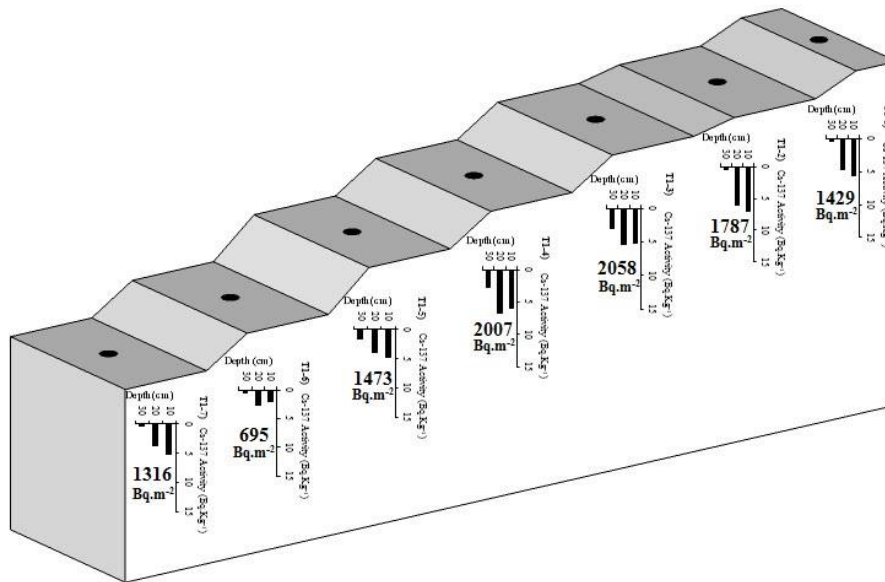
Figure 3.5. ^{137}Cs Depth distribution in sampling points along T1
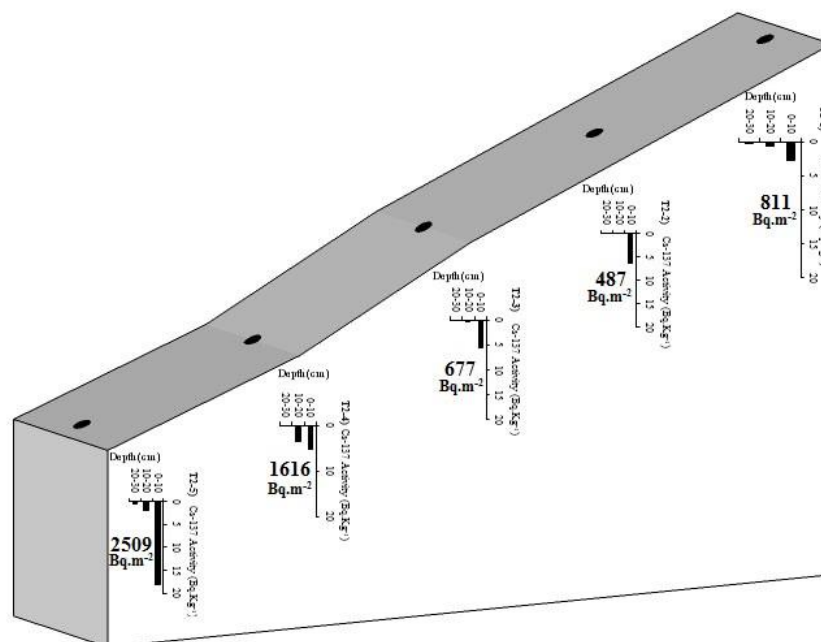
Figure 3.6. ^{137}Cs Depth distribution in sampling points along T2
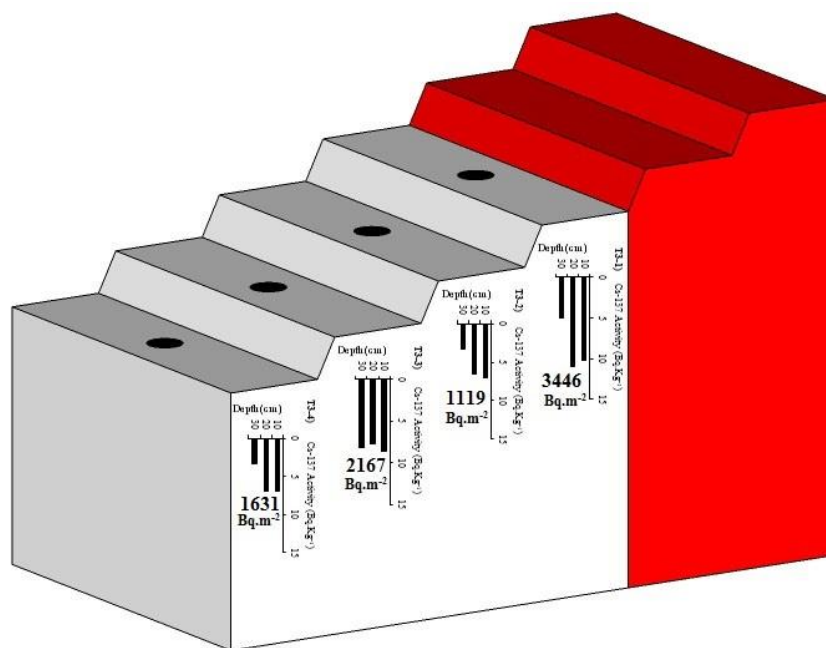
Figure 3.7. ^{137}Cs Depth distribution in sampling points along T3
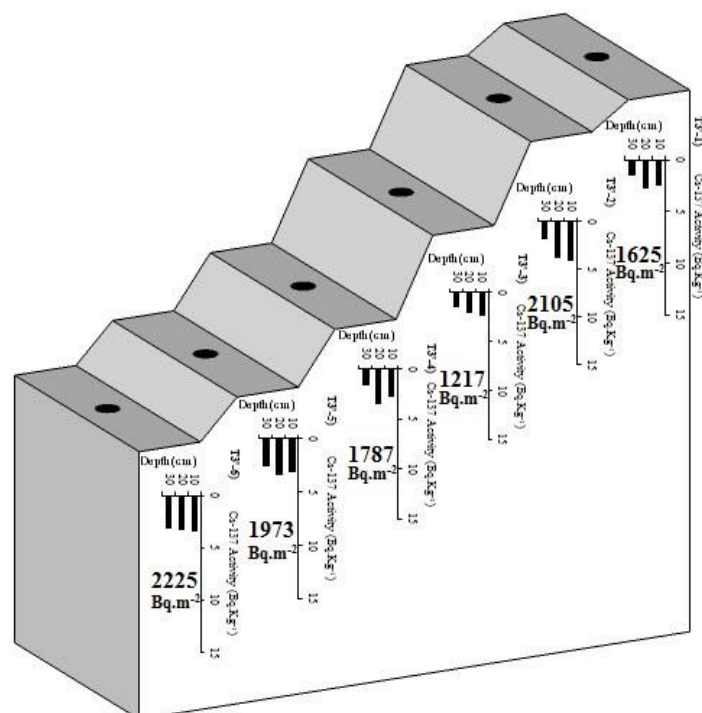
Figure 3.8. ^{137}Cs Depth distribution in sampling points along T3'
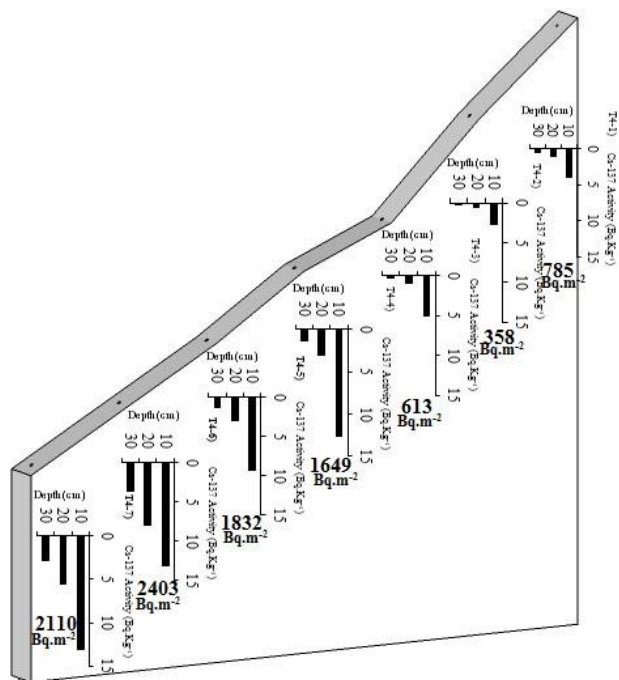
Figure 3.9. ^{137}Cs Depth distribution in sampling points along T4
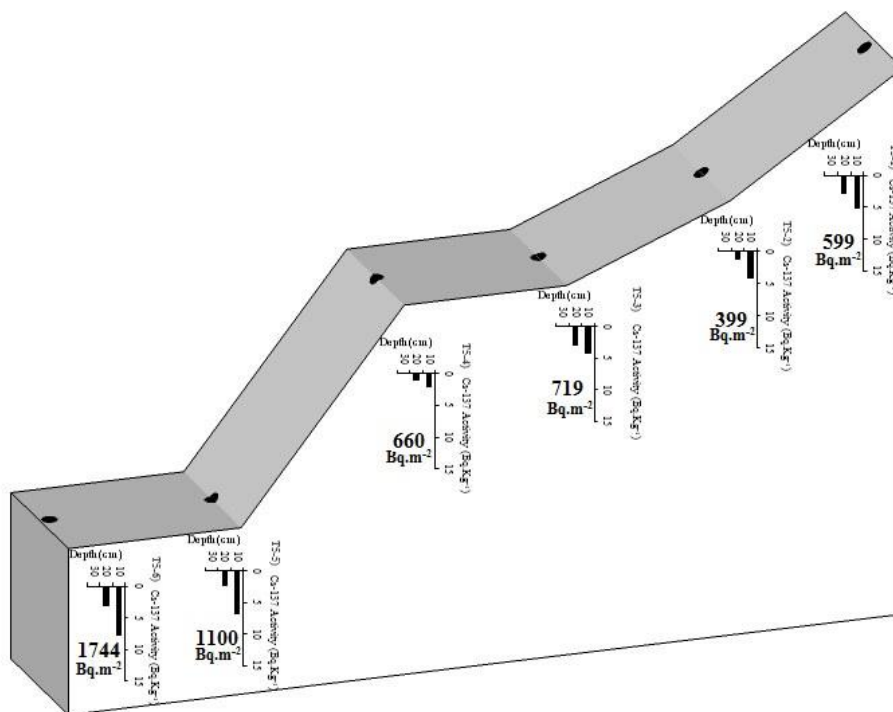
Figure 3.10. ^{137}Cs Depth distribution in sampling points along T5

3.3 ^{137}Cs inventories distribution and some soil parameters

The ^{137}Cs inventories were measured along the six transects. The values range between 358 and 3446 Bq m^{-2}. Most of ^{137}Cs inventory is in the   topsoil of uncultivated sites (T2, T4 and T5) and it is lower than the reference inventory, indicating a soil loss, while it is higher in down slope, showing a soil deposition. On the other hand, the cultivated fields (T1, T3 and T3') illustrate an irregular and oscillating behavior of ^{137}Cs inventory, suggesting a variation of soil loss along the transects which can be due to succession of terraces in each transect. The Figure 3.11 exemplifies the observed ^{137}Cs inventories behavior's along the six transects.
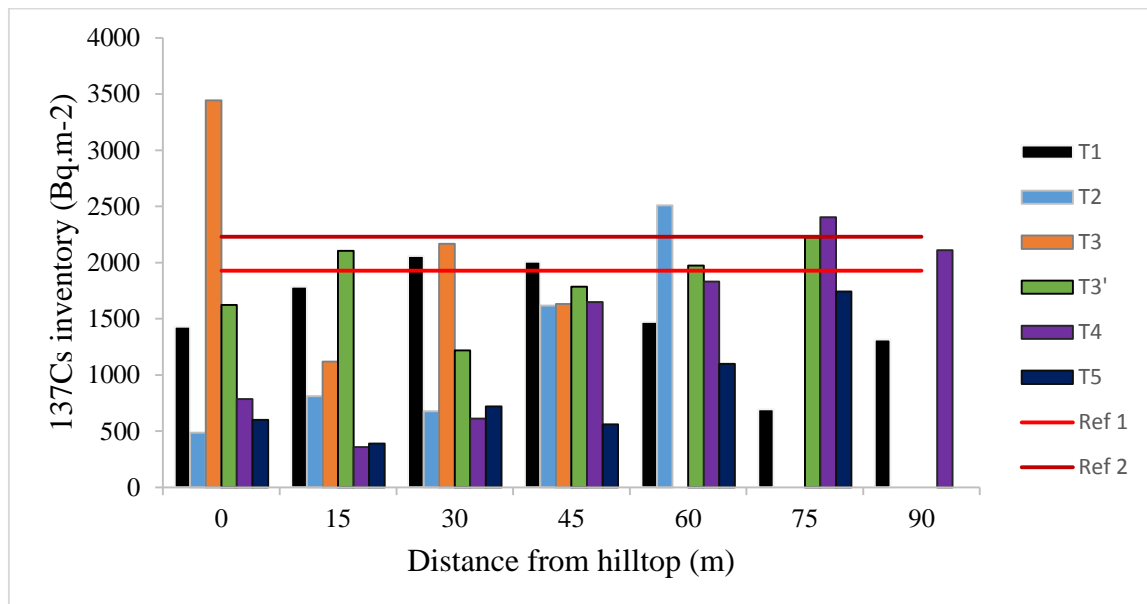
Figure 3.11. Distribution of ^{137}Cs inventories along the six studied transects

In the study areas, slope is very low on terraces from 0 to 2 % but varying between terraces along transects from 25 to 76%. In uncultivated field, it is from 27 to 95%. The relationships between ^{137}Cs inventory (Bq.m^{-2}) and mean slope gradient (%) along each transect is investigated (Figure 3.12). For all slopes, from the top to the bottom of the field, a reduction of ^{137}Cs inventory with increasing slope gradient is observed (Figure 3.12). This implies an increase of soil loss with slope gradient in both cultivated and uncultivated soils. A strong linear relationship (p < 0.05) is found between ^{137}Cs inventory and slope gradient in cultivated terraces (R^2 = 0.65, R^2 = 0.83, R^2 = 0.50 for T1, T3 and T3' respectively) and in uncultivated soils (R^2 = 0.82, R^2 = 0.62 and R^2 = 0.62 for T2, T4 and T5 respectively). This is in line with the results

reported in the literature, according to which topographic factors greatly influence soil redistribution (eg: Tiessen et al., 2009, Xiaojun et al., 2010).
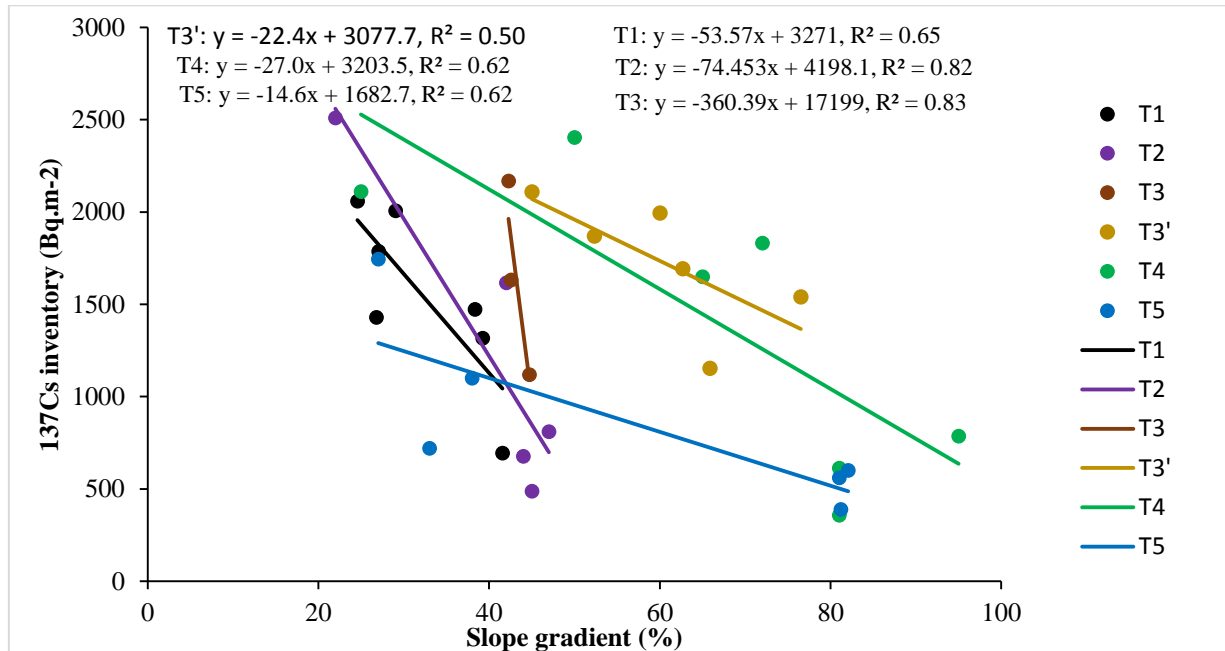
Figure 3.12. Relationship between 137Cs inventories and slope gradient

Table 3.1. Pearson correlation coefficients between 137Cs inventories and soil properties for cultivated and uncultivated soils

	^{137}Cs mass activity (Bq kg^{-1})		Inventory (Bq m^{-2})	
Soil parameters	Cultivated soil	Uncultivated soil	Cultivated soil	Uncultivated soil
Slope (%)	-0.293	-0.452	-0.144	**-0.556***
Sand (%)	-0.199	0.115	0.142	-0.119
Clay (%)	0.341	0.367	0.035	0.467
Silt (%)	0.042	-0.282	-0.188	-0.052
CF (%)	-0.088	-0.010	-0.252	-0.349
C (%)	-0.300	**0.548**	0.006	**0.673***
BD (g/cm^{-3})	-0.224	**-0.563**	-0.212	**-0.620***
SOC (t/ha)	-0.365	**0.598***	-0.095	**0.699***

CF: Coarse fraction, C: soil organic carbon (%), BD: Bulk density, SOC: Soil organic carbon (t/ha). * indicates significant relationship p<0.05.

The correlation between ^{137}Cs and soil properties was studied over the entire 30 cm of soil depth. In the uncultivated sites, the ^{137}Cs inventory is significantly and positively correlated with both C and SOC, while it is negatively correlated with slope gradient and BD (Table 3.1).

Same result is obtained for ^{137}Cs mass activity, but still strong correlations with ^{137}Cs inventory than with ^{137}Cs mass activity (Table 3.1). This result is in line with the previous studies (Zhang et al., 2006; Martinez et al., 2010; Gaspar and Navas, 2013). Soil organic carbon is important for ^{137}Cs adsorption. However, this adsorption is supposed to be non-specific and, thus, is influenced by the cation exchange capacity of organic matter when compared with the specific adsorption of ^{137}Cs on clays (Rigol et al., 2002). These relationships suggest that ^{137}Cs and carbon are probably moving along similar physical pathways, suggesting the same pathway during soil redistribution (Ritchie and McCarty, 2003, Xiaojun et al., 2010). Given this strong correlations between SOC and ^{137}Cs, the ^{137}Cs technique could provide a useful tool for extensive research on the dynamics of soil erosion and SOC stock (Xiaojun et al., 2010) in uncultivated soils of the High Atlas of Morocco (Table 3.1).

Considering the three transects of uncultivated soils separately, ^{137}Cs mass activity and inventory are significantly and positively correlated with clay along T2 (r = 0.80 and r = 0.83 respectively) and T4 (r = 0.92 and r = 0.87 respectively). This implies that fine soil particles were selectively moved mainly by water in the downslope direction (Zhang et al., 2006; Xiaojun et al., 2010). Along T5, the ^{137}Cs mass activity and inventory are negatively correlated with CF (r = -0.58 and r = -0.59 respectively). This was contrary to what was observed elsewhere (Schoorl et al., 2004, Gaspar and Navas, 2013). For these authors, assuming the same amount of ^{137}Cs deposited as in other surfaces, the ^{137}Cs adsorbed per unit mass of soil matrix becomes higher when less soil matrix for adsorption is available. The negative correlation observed between ^{137}Cs and soil stoniness in the non-forest empty area of our study zone, could be explained by the fact that the stoniness of the soil accelerates runoff (reduces water infiltration in the soil matrix), and thus causes the loss of ^{137}Cs freshly deposited through precipitations by runoff.

In cultivated soils (considering all the three transects), the distribution of ^{137}Cs is highly variable with no significant relationships observed between ^{137}Cs mass activity and inventory and the soil properties studied. The homogenous depth distribution of these properties in the cultivated soils and the limited range of their variation may explain the lack of a significant correlation between soil properties and ^{137}Cs. This could be attributed to the tillage effect as stated by another author's works, which were done under similar terracing conditions (Zhang et al., 2006).

[137]Cs inventory loss variations are shown to be significant along the transects. [137]Cs redistribution behavior within the studied field could be explained by the influence of slope shape of each transect of the field. Indeed, the slope angle varied along the transects, which reflected the complexity of the topography of the watershed. The ^{137}Cs inventory loss increased with the slope gradient, and decreased with the gradual increase of slope (Nouira et al., 2003).

3.4   Soil redistribution rates from 137Cs measurements

MBM II and PDM (Walling et al., 2002) are used to convert the measured ^{137}Cs inventories into soil erosion and deposition rates. The parameters of the models are shown in the Table 3.2.

Table 3.2. [137]Cs conversion models parameters used to convert 137Cs inventories into soil erosion and deposition rates

Model parameters	Transects					
	T1	T2	T3	T3'	T4	T5
Tillage year	1954	-	1954	1954	-	-
Tillage depth (kg m^{-2})	312	-	303	287.8	-	-
The relaxation mass depth (kg m^{-2})	4	-	4	4	-	-
Proportion factor	0.67	-	0.67	0.67	-	-
Coefficient describing profile shape (kg m^{-2})	-	43	-	-	25	25
Sampling year	2016	2016	2016	2016	2016	2016
Reference inventory (Bq m^{-2})	1927	1927	2229	2229	2229	2229

In the use of MBM II for the conversion of the ^{137}Cs inventories into soil movement, in the cultivated soils, the selectivity of erosion process is ignored. A default value of 4 kg m^{-2} is taken for the relaxation depth parameter, H, of the model due to the difficulty to determine this value empirically. This is due to the current ^{137}Cs fallout flux being negligible (Benmansour et al., 2013). Taking into account both temporal and local rainfall distribution with respect to the time of tillage, the proportion factor was calculated for the study areas. A value of 0.67 corresponding to the proportion factor is found. Tillage depth was calculated, it is of 312 kg m^{-2} and 303 kg m^{-2} along T1 and T3' respectively. For the uncultivated soil, the profile distribution model (PDM) was used.

Table 3.3. Punctual erosion and deposition rates within the study area

Transects/ Sampling points	Distance (m)	Elevation (m)	Slope (%)	Inventory (Bq/m^2)	Soil redistribution rate (t ha^{-1} yr^{-1})	Soil mouvement
T1-1	0	1132	2	1429.3	-8.94	Erosion
T1-2	15	1130	0	1786.7	-2.23	Erosion
T1-3	30	1129	2	2058.1	1.39	Deposition
T1-4	45	1126	1	2006.8	2.27	Deposition
T1-5	60	1123	1	1472.5	-8.03	Erosion
T1-6	75	1119	1	694.6	-32.23	Erosion
T1-7	90	1116	2	1315.7	-11.48	Erosion
T2-1	0	963	47	810.6	-7.22	Erosion
T2-2	20	955	45	487.0	-11.46	Erosion
T2-3	40	947	44	676.6	-8.72	Erosion
T2-4	60	937	42	1616.4	-1.46	Erosion
T2-5	80	930	42	2509.4	2.52	Deposition
T3-1	0	1458	2	3445.6	-	Deposition
T3-2	10	1456	2	1118.9	-20.97	Erosion
T3-3	20	1454	1	2166.8	-0.83	Erosion
T3-4	30	1452	2	1631.3	-9.25	Erosion
T3'-1	0	1538	1	1624.7	-9.41	Erosion
T3'-2	10	1536	1	2105.3	-1.68	Erosion
T3'-3	20	1530	2	1217.3	-18.36	Erosion
T3'-4	30	1524	1	1787.1	-6.54	Erosion
T3'-5	40	1524	2	1972.9	-3.59	Erosion
T3'-6	50	1517	2	2225.1	-0.06	Erosion
T4-1	0	1402	95	785.0	-4.83	Erosion
T4-2	50	1361	81	358.2	-8.46	Erosion
T4-3	100	1313	81	612.6	-5.98	Erosion
T4-4	150	1293	65	1648.5	-1.4	Erosion
T4-5	200	1261	72	1831.6	-0.91	Erosion
T4-6	250	1234	50	2403.1	0.36	Deposition
T4-7	300	1207	45	2110.2	-0.25	Erosion
T5-1	0	1546	82	599.4	-6.08	Erosion
T5-2	20	1533	81	389.4	-8.08	Erosion
T5-3	40	1525	33	719.4	-5.24	Erosion
T5-4	60	1525	81	559.8	-6.4	Erosion
T5-5	80	1500	38	1099.6	-3.27	Erosion
T5-6	100	1500	27	1743.8	-1.14	Erosion

Table 3.4. Soil redistribution assessment estimated from 137Cs measurement.

Soil redistribution parameters	T1	T2	T3	T3'	T4	T5
Number of eroded points	5	4	3	6	6	6
Number of deposited points	2	1	1	0	1	0
Mean erosion (t ha^{-1} yr^{-1})	-12.6	-7.2	-10.35	-6.6	-3.6	-5.0
Mean deposition (t ha^{-1} yr^{-1})	1.8	2.5	-	0.0	0.4	0.0
Gross erosion (t ha^{-1} yr^{-1})	-9.0	-5.8	-10.4	-6.0	-3.1	-5.0
Gross deposition (t ha^{-1} yr^{-1})	0.5	0.5	-	0.0	0.1	0.0
Net erosion (t ha^{-1} yr^{-1})	-8.5	-5.3	-10.4	-6.0	-3.1	-5.0
Sediment delivery ratio (%)	94	91	100	100	100	100
Eroding area (%)	71	80	75	100	86	100
Depositional area (%)	29	20	25	0	14	0

3.4.1. Cultivated studied sites

^{137}Cs converting models for soil erosion assessment was used only for 5 transects, because in transect T3, the upslope section was not accessible, that explains why the first point was a depositional one, and thus impossible to use the model for erosion rate assessment. T3' was chosen with the same land use and soil type to replace T3. However, benefit was taken from sampling points extracted from T3 by using the second point as the first one in the conversion model.

The soil erosion rate in the study sites varied between 0.06 and 32.23 t ha^{-1} yr^{-1} (T1 and T3') (Table 3.3). The mean and gross erosion rates are about 9.6 and 7.5 t ha^{-1} yr^{-1} while mean and gross deposition rates are about 0.9 and 0.25 t ha^{-1} yr^{-1}, respectively. The net soil loss is about 7.3 t ha^{-1} yr^{-1} with a SDR of 97%, suggesting an efficient sediment transport mechanism. It can be concluded that significant amount of soil particles moved from the upper to the bottom and even the terracing did not stop totally soil movement. This is probably due to the farmer soil management system. Indeed, the net soil erosion rate is higher in cereal crop (8.5 t ha^{-1} yr^{-1}) than in arboriculture (6.0 t ha^{-1} yr^{-1}) (Table 3.4). Transect T1 terraces are cultivated with cereal

crop (barley) whereas Transect T3' terraces with arboriculture (apple trees). Traditional irrigation canal system called "seguia" and vegetation separate T1 terraces as embankment. For T3' terraces, there was no embankment. Embankments establishment at the lower end of the terrace impeded the formation and development of surface water flow, creating a downward soil line leading to soil deposition induced by tillage on the upslope side of the embankment with small size particles sorting (Zhang et al., 2014). According to these authors, embankments at the lower end of the sloped terrace played a crucial role in the pattern of soil redistribution of the toposequence, resulting in the transition from a water-dominated erosion process to a tillage-dominated process and a different pattern of the soil particle size distribution. In the Ourika watershed, arboriculture on terraces is more effective for soil protection against water erosion, and it effectiveness could be improved if embankments are established at the lower end of the terraces. The impact of tillage erosion is more important on cereal crop terraces than on arboriculture terraces because of the frequency of ploughing. Arboriculture is perennial and protects more the soil against erosion than annual cereal crop.

3.4.2 Uncultivated studied sites

Erosion rate varied from 0.25 to 11.42 t ha^{-1} yr^{-1} (T2, T4 and T5) and deposition rate ranged between 1.39 and 2.27 t ha^{-1} yr^{-1} (Table 3.3). Erosion rates decrease downslope, indicating downslope movement of eroded soil, transport and deposition of eroded materials. Eroded soils are deposited at the lowest section of the slope at a rate ranging between 0.36 and 2.52 t ha^{-1} yr^{-1}. Mean and gross erosion rates are estimated 5.3 and 4.6 t ha-1 yr-1 while soil deposition is lying from 1.0 to 0.2 t ha^{-1} yr^{-1}. The net soil erosion is about 4.5 t ha^{-1} yr^{-1} (Table 3.4).

 Net erosion rates of 5.3, 3.1 and 5.0 t ha^{-1} yr^{-1} are related to T2, T4 and T5 respectively (Table 3.4). The low values obtained in uncultivated loamy soil (5.3 t ha^{-1} yr^{-1}) and uncultivated sandy soil (3.1 t ha^{-1} yr^{-1}) can be explain by the forest cover which protects the soil against soil erosion. Previous studies have suggested the effects of land use on soil erosion (Valentin et al. 2005; Alejandro and Kenji 2007, Albergel et al. 2010). Forest vegetation is known to favor water infiltration and to protect soil from erosion. The low erosion rate obtained along T5 can be explained by its higher stoniness (> 60 %), which causes the loss of ^{137}Cs freshly deposited, through precipitations, by runoff. In other words, the net erosion rate is low because there is very little soil fine particle in the matrix the soil because of its high stoniness.

The difference between average net soil erosion in cultivated and uncultivated soils (7.3 t ha^{-1} yr^{-1} and 4.5, respectively) illustrates that despite the important role of terraces in reducing soil erosion in sloping landscape, uncultivated forest land remains best suited in reducing soil erosion in the High Atlas region of Morocco (Table 3.4). Nevertheless, arboriculture reduces more soil erosion than cereal crop in the study area. The extension of arboriculture on sloping terraces plays an important role in the reduction of soil erosion. In addition to its environmental role of soil protection against erosion, arboriculture plays an important socio-economic role in the watershed and contributes to the fixing of the population in rural areas. The agricultural terraces studied constitute an interesting social and economic solution except that it would be better to manage them in an intelligent and sustainable way through arboriculture.

Water and tillage erosion are two processes that contribute to soil erosion in hilly areas (Zhang et al., 2006, Zhang et al., 2009, Zhang et al., 2012) such as Moroccan High Atlas. In these landscapes, an intensive erosion due to ploughing occurs on upper slopes, while soil movement by water erosion is greater on downslope boundaries (Govers et al., 1996).Tillage moved soil downslope on the top terrace and delivered soil to the middle section where severe water erosion occurred, thereby intensified soil loss from the toposequence (Zhang et al., 2012).

The erosion rate obtained in cultivated soils is relatively low compared to other Moroccan regions. Despite its steep slopes, the High Atlas region of Morocco experiences an average erosion rate relatively low compared to the northern region of Morocco, 30-50 t ha^{-1} yr^{-1} (Nouira et al., 2003 ; Damnati et al., 2013) and 11.9 t ha^{-1} yr^{-1} (Benmansour et al., 2013). The reduced erosion rate observed with the ^{137}Cs method reveals the positive impact of the traditional agricultural practices (terraces) of the farmers in the study area. This solution can be an example for other mountainous regions of Morocco that suffer from significant soil erosion. Soil erosion depends not only on physical and climate parameters, but also on land use and farming practices. To limit water erosion, most of the hillslopes have been dissected into terraces to reduce slope gradients. The net erosion rate in the field (7.3 t ha^{-1} yr^{-1}) is not significant compared to the acceptable threshold for soil loss set for Morocco (< 7 t ha^{-1} yr^{-1}). However, point erosion rates in the field of more than 32.23 t ha^{-1} yr^{-1} indicate that soil erosion is a serious threat in the watershed and effective control measures need to be adopted.   (Rabesiranana et al., 2016). As the effectiveness of forests and arboriculture in reducing soil erosion has been proven, more efforts need to be made to preserve forests in the upslope sections of the region and encourage arboriculture agrosystems.

4 Conclusion

In Moroccan mountain agroecosystems, ^{137}Cs distribution is influenced by land use. The results of this study highlight the differences associated with both vertical and lateral distribution of^{137}Cs in cultivated and non-cultivated landscapes. The depth distribution profiles and hillslope transects demonstrate the differences associated with the land use and soil characteristics within the study watershed. The relationship between ^{137}Cs and SOC and slope gradient at the hillslope scale is affected by land use. There was no correlation between ^{137}Cs and either SOC or slope gradient under cultivated terraces. Stronger relationships, however, were found in uncultivated areas. The difference between net soil erosion under cultivated and uncultivated soils (7.3 and 4.5 t ha^{-1} yr^{-1} respectively) shows that despite the important role of terraces in reducing soil erosion in sloping landscape, forests (4.2 t ha^{-1} yr^{-1}) remain best suited in regards to reducing soil erosion in the High Atlas region of Morocco. However, arboriculture, in addition to its important socio-economic role, contributes to significantly reducing soil erosion. The income from terraced arboriculture represents an important means of survival of the population. This study was carried out as part of a study on the development of the Ourika area to give some elements of answer based on which the area will have a socio-economic development with more entrances while preserving the soil from erosion.

The net erosion rate observed on agricultural terraces (6.0 t ha^{-1} yr^{-1}) reveals that they are more effective in reducing soil erosion than other agricultural practices in Morocco. This area of research requires further work, which would be vital for the improvement of tillage techniques. This would help to limit the downward soil redistribution in the cultivated terraces. The ^{137}Cs technique has led to interesting and fast results on terracing studies and its relation with soil organic carbon is interesting particularly in the forest.

Chapter 4

Assessment of the effect of vegetation cover on potential soil erosion risk in a mountainous watershed of Morocco

Assessment of the effect of vegetation cover on potential soil erosion risk in a mountainous watershed of Morocco.

Abstract

Water erosion is a serious environmental problem, which affects particularly developing countries. Morocco is vulnerable to soil erosion due to many specific factors such as high rainfall intensity, steep slopes and sparse vegetation. The main objective of this work is to analyze and spatialize different factors involved in soil erosion phenomenon, leading to the establishment of an erosion risk map of the Ourika watershed and to highlight the impact of vegetation cover on potential soil erosion risks, using quantitative erosion model with remote sensing data and GIS. Moreover, the impact of vegetation on water erosion is also studied using multi-temporal satellite images, NDVI and TSAVI index. The results show that a large area of the Ourika watershed is seriously affected by erosion. This potential high risk is especially due to severe slopes, poor vegetation cover, high soil erodibility and high rainfall erosivity in this watershed. The watershed was subject to strong climatic aggressiveness ranging from 55 to 101 MJ.mm/ha.h. Topographic factor, LS, values ranged from 0.01 to 94.5 and C values were higher than 0.5 for approximately 80% of the watershed's area. The highest potential soil loss occurs in 2000 when a wide area of the watershed was bare. However, the soil loss was diminished in 2015 with the presence of vegetation due to afforestation and the expansion of arboriculture in the watershed. The average potential soil loss was 143.99, 174.51 and 122.46 t/ha/year, respectively, for 1984, 2000 and 2015. Furthermore, the use of multi-temporal satellite images and vegetation index show that the effect of vegetation is a significant factor to protect the soil against erosion. Erosion model, combined with a GIS and remote sensing, is an adequate method to evaluate the water erosion risk. Decision makers can use the findings as a guideline to develop measures of soil conservation and water resources management.

Keywords: Water erosion risk, remote sensing, Erosion model, GIS, TSAVI, Morocco.

1 Introduction

Soil erosion has been recognized as the major cause of land degradation worldwide. Soil erosion is an inevitable natural phenomenon, which becomes a serious environmental and economic problem when accentuated by human activities (Lal 1998; Del Mar López et al. 1998). Water erosion has increased all over the world (De Graaf 1996). Population pressure and the expansion of agriculture by various human activities, agricultural practices, forest exploitation, grazing, construction of roads and buildings; associated with the amplifying effects of climate change, have led to the exposure of land to runoff, and thus to soil degradation by water erosion (Vezena & Bonn 2006 ; Wachal 2007). As such, water erosion affects soil quality by inducing land degradation by loss of top soil rich in organic matter. This eventually leads to loss of soil productivity.

The High Atlas is the highest mountain range in Morocco, and includes Mount Toubkal with its peak at 4167 m. This mountain range is divided into a multitude of watersheds that is a real water tower for the neighboring arid plains (Boudhar et al.2007). However, the different mountainous areas of the High Atlas are subject to high stress that negatively affects their hydrology and make the High Atlas particularly vulnerable to human activities (Meliho et al. 2016). These constraints include dramatic topography, land subject to heavy erosion, a harsh and brutal climate, plant cover that is for the most part sparse and an increasing human presence. Similar to other areas of the High Atlas, the Ourika watershed perfectly illustrates the problem of degradation of natural resources and raises many questions about the rationality of the management of its resources in the both the current and future states. This watershed, characterized by dramatic topography, friable substrates, a harsh climate, sparse vegetation and a growing human presence, is particularly vulnerable to water erosion (Meliho et al. 2016).

Quantification of water erosion was performed using several models depending on the purpose. Researchers in many countries are continuously improving the mathematical models used by adapting them to local conditions (Arnalds et al. 2001). Several models are being developed and used in several countries and in different regions. The erosion prediction models help decision-makers in planning the management of natural and agricultural environments (Angima et al. 2003). Although it is difficult to find a model that covers all forms of erosion, some models have been developed to help water and soil resources managers identify the most vulnerable areas to erosion, where conservation measures are indispensable. The RUSLE model (Renard et al. 1997) is widely used in the Mediterranean region. This is an empirical model based on the USLE model (Wischmeier & Smith 1978). The use of remote sensing and geographic

information system has made possible the estimation and spatial distribution of soil erosion at a reasonable cost and efficiency on large scales (Boggs et al. 2001; Wilson & Lorang 2000; Wang et al. 2003; Jasrotia & Singh 2006). The idea is to integrate the factors in the empirical RUSLE model into a geographic information system. Remote sensing tools using satellite images or vegetation indices can detect vegetation cover. Landsat images are commonly used for land use classification and vegetation types mapping (Vrieling 2006). In addition, multi-temporal satellite images is used to assess vegetation cover in different years (Cyr et al. 1995). The objective of this work is to analyze and spatialize different factors involved in the phenomenon of erosion, leading to the establishment of erosion risk map of the Ourika watershed and to highlight the impact of vegetation cover on potential soil erosion risks using vegetation index. The mapping of erosion factors and identifying areas of vulnerability to soil erosion would help assess the risks of erosion and develop measures of soil conservation and water resources management.

2 Materials and methods

2.1 Study zone

The Ourika watershed is located in the High Atlas in the Marrakech region and is a sub-watershed of the larger Tensift watershed (Figure 4.1).It covers an area of 576 km² and is located between latitudes 31° and 31°21'North and longitudes 7°30' and 7°60'West. It is limited to the south by the upper basin of the Oued Souss, to the north by the Haouz plain, to the east by the Zat watershed and to the west by the Rheraya watershed. Three main physiographic units characterize the area: foothills with an average altitude of 600 m; valleys of Oued Ourika and its tributaries; and high mountain plateaus. Topographically, the average altitude is 2500 m with a predominance of land between 1600 and 3200 m (75%). The slopes of the watershed are generally steep, amplifying runoff and erosion.
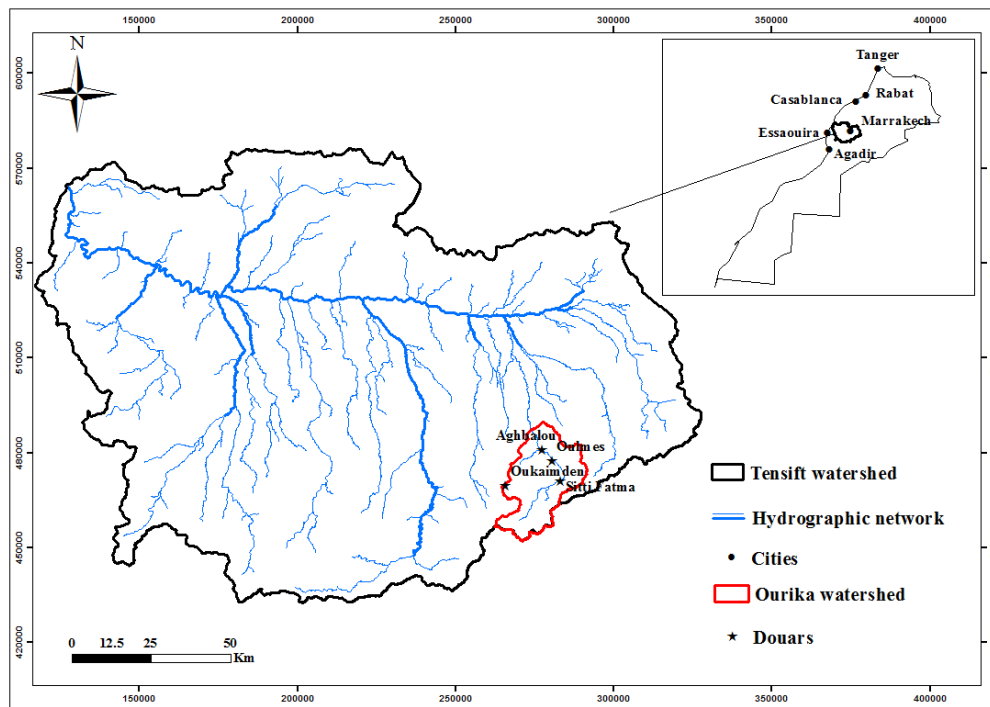
Figure 4.1. Location of the watershed Ourika

Geologically, the watershed presents two types of facies (Biron 1982): i) a hard bedrock (igneous or metamorphic rock) located upstream, representing approximately 61% of the watershed with presence of pink granite, Toubkal andesite and migmatite; ii) a soft to moderately soft substrate located at lower elevations, composed of Permo-Triassic and Quaternary deposits, representing approximately 39% of the watershed. These include friable sandstone and red marl, conglomerates and massive red sandstones, shale and sandstone flysch. Sandstone and red marl account for 31% of the watershed while shale and sandstone flysch represent only 8%.

The climate of the watershed is characterized by high spatial and temporal variability. Annual precipitation averages 500 mm. This increases with altitude and is of the order of 400 mm in the foothills while exceeding 700 mm on the high peaks of the watershed. Average temperatures range from 21.5 to 32°C and 4 to 5.7 ° C for maxima and minima respectively. July and August are the hottest months of the year, while December and January are the coldest. The temperature varies between 48.2°C and -7.2°C, with an average of 27.8 ° C. The vegetation cover in the area is largely in the Oromediterranean stage and largely dominated by thorny xeric shrubland and hemicryptophytes (Ouhammou 1986). The same composition dominates at the montane stage, which is also marked by the presence of juniper. Tree cover in the watershed is represented by the Mediterranean and Mesomediterranean and Thermomediterranean stages. For the most part,

it is under holm oak, juniper and cedar forests (Ouhammou 1986).The main crops systems are arboriculture and cereal cultivation

2.2   Methodology

The most widely used models for evaluating soil loss are the USLE and the revised RUSLE models due to their ease of implementation and compatibility with geographic information systems (Millward & Mersey 1999; Lu et al. 2004; Dabral et al. 2008; Pandey et al. 2009; Bonilla et al. 2010). The RUSLE model has been widely used in both agricultural and forest environments for the prediction and spatial distribution of mean annual soil loss by integrating the various erosion factors (Wischmeier & Smith 1978; Renard et al. 1997).

The equation is expressed by the equation:

$$A=R*K*LS*C*P$$

Where:

A = potential soil erosion rate (t/ha/year)

R = rainfall erosivity (MJ.mm/ ha.h.an)

K = soil erodibility (t.h/ha. MJ.mm)

LS = topographic factor (L in m, S in %),

C = plant cover factor

P = agricultural practices factor

2.2.1 Rainfall erosivity factor (R)

Erosivity is the rain's potential capacity to induce erosion (Hudson 1981). It is the product of rainfall's kinetic energy and maximum rainfall intensity over a period of 30 minutes (Wischmeier & Smith 1978). It can also be considered as an annual average index of erosion by rain. Given that the kinetic energy and rainfall intensity data are difficult to obtain, alternative formulas requiring only monthly and annual data for determining the R-factor were developed (Arnoldus 1980; Rango & Arnoldus 1987).

The Rango & Arnoldus formula (1987) was applied to 5 stations in the Ourika watershed over a period of 20 years (1995-2015).

$$\text{Log } R = 1.74 * \log \Sigma \ (Pi^2 \ / \ P) + 1.29$$

Where:

Pi monthly rainfall

P: annual rainfall in mm.

A period of 20 to 25 years is recommended to calculate the average value of R at a given station (Millward & Mersey1999). The spatial interpolation factor, R, was determined by kriging using ArcGIS geo-spatial tool.

2.2.2 Soil erodibility factor (K)

Soil erodibility is function of grain size, drainage potential, structural integrity, organic content, and cohesiveness. Erodibility of soil is its resistance to both detachment and transport. Because of the absence of soil data for the watershed, a Food and Agriculture Organization (FAO) soil map was used to derive K factor. The Soil erodibility map was obtained by attributing to the different soil types the corresponding K values. The corresponding K values for the soil types were identified based on texture and organic matter content using a table proposed by Roose (1996).

2.2.3 Topographic factor (LS)

The length and gradient of a slope affect the production and transport of sediment within an area and are included in the RUSLE model. In addition to the steepness and length of slope, other factors such as compaction and soil disturbance are also considered in the determination of LS factor (Prasannakumar et al. 2012). Erosion increases with slope gradient but, unlike the L factor which expresses the effect of the length of the slope, the RUSLE model does not differentiate between sheet erosion and linear in the S factor, which represents the effect of slope gradient on soil erosion (Renard et al. 1997; Lu et al. 2004; Krishna Bahadur 2009).

The LS factor was calculated using LS-TOOL developed by Zhang et al. (2013). The methodology for calculating the LS factor is applied to each pixel of the digital elevation model. Calculating L is based on the equation developed by Desmet and Govers (1996). The calculation of S is based on the equation developed by Wischmeier & Smith (1978) which was amended in the RUSLE model for better representation of the degree of slope inclination (McCool et al. 1987).

The DEM's resolution plays an important role with regard to the accuracy of the result obtained for the LS factor (Molnar & Julien 1998; Panagos et al. 2015). Although DEMs of high resolution are quite expensive, in the interests of accuracy, a 10 m resolution DEM provided with Harris Corporation/Space and Intelligence Systems was used to calculate LS factor.

2.2.4 Vegetation cover factor (C)

Soil that well protected by vegetation cover greatly reduces the effects of climatic aggressiveness, soil erodibility and slope gradient, regardless of their importance in the sense that appropriate cover facilitates infiltration thus reducing runoff and preventing the onset of erosion.

The C factor compares the soil loss related to both land covered by dense natural vegetation, bare land without vegetation cover and land subject to specific management (Wischmeier & Smith 1978). It varies from 0,001 under dense forests to 1 under bare soil.

In recent years, because of large spatial and temporal variability of vegetation cover, remote sensing data are used to calculate the factor C (Karydas et al. 2009; Tian et al. 2009). The NDVI (normalized vegetation index) is an indicator of the vegetation and its health was used (Jensen 2000). The formula used for determining the factor C (Zhou et al. 2008; Kouli et al. 2009) is:

$$C = \exp [- (\alpha NDVI / (\beta\text{-}NDVI))]$$

Where α and β are parameters without units that determine the shape of the curve connecting NDVI to C.

This equation has been proven to be more accurate than a linear relation (Van der Knijff et al. 2000). These authors attributed values 2 and 1 to α and β respectively. This equation has been successfully used in the areas of similar soil and climatic conditions (Markhi et al. 2015). Downloaded Landsat images from USGS were used. In this research, multi-temporal imagery is used taking into account the seasonal variability. Images of 1984 (22/06/1984), 2000 (12/06/2000) and 2015 (22/06/2015) that correspond to spring were used.

Transformed soil adjusted vegetation index (TSAVI) was also used to estimate the vegetation coverage. The application of the TSAVI leads to a significant reduction of soil effects in areas with sparse vegetation cover or bare soil (Purevdorj et al. 1998). The TSAVI is based on soil line slope, intercept, and can be written as:

$$TSAVI = \frac{a(NIR - aR - b)}{aNIR + R - ab}$$

where a is the slope of the soil line, b the intercept of the soil line, NIR the near infrared band and R the red band.

The soil line is a linear relationship between the bare soil reflectance observed in two different wavebands (Baret et al. 1993). It can be built by establishing a relationship between the reflectance of the NIR band and red band and can be written as follows:

$NIRsoil = aREDsoil + b$

where NIRsoil is the soil reflectance in the near-infrared band, REDsoil is the soil reflectance in the red band and a and b represent the parameters of the soil line.

2.2.5 Anti-erosive practice factor, P

Agricultural practices along contours, in alternating strips or terraces, ridging etc., are effective soil conservation practices. P values were estimated based on slope (Shin 1999), according to Table 4.1.

Table 4.1. Value factor related to erosion control practices based on the slope

Slope (%)	P
0.0 – 7.0	0.55
7.0 – 11.3	0.60
11.3 – 17.6	0.80
17.6– 26.8	0.90
> 26.8	1.00

3   Results and discussion

To estimate potential soil erosion rate in the Ourika watershed, the RUSLE model was used. The various factors in the model were estimated and spatialized in a GIS environment and the combination of these factors resulted in the watershed's erosion risk map.

3.1   Rain erosivity factor (R)

The rainfall erosivity in the Ourika watershed ranged from 55 to 101 MJ.mm/ha.h.year (Figure 4.2). Rainfall aggressiveness showed an increasing gradient from the northeast to the southwest of the watershed. These R-values exceeding 50 MJ.mm/ha.h.an indicate that the entire Ourika watershed is subject to a high climatic aggressiveness.

It can therefore be deduced that the erosive power of rainfall was important in the Ourika watershed. The values obtained were higher than those obtained in the N'fis watershed (41.40 to 57.28 MJ.Mm/ha.h.year), which is a neighboring basin (Markhi et al. 2015). It was also higher than those obtained from the Boussouab watershed (31.2 to 60 MJ.mm/ha.h.year) in oriental Rif (Sadiki et al. 2004) and those obtained in the central Rif with values ranging from 43 to 87.56 MJ.mm/ha.h.year (Rahhou 1999). Conversely, they were lower than those obtained in the Oum Er-Rbia basin between ranging from 70 to 119 MJ.mm/ha.h.year (Yjjou et al. 2014)

and those obtained in the Tlata basin comprised between 215 and 228 MJ.mm/ha.h.year (Merzouk & Dahman 1998).

3.2   Soil erodibility factor (K)

In the Ourika watershed, it ranged from 0.20 to 0.34 t.ha.h/ha.MJ.mm (Figure 4.3). The soils are of high sensitivity to erosion in the low part of the watershed and less erodible in the upper part.

3.3   Topographic factor (LS)

LS values ranged from 0.01 to 94.5 and were grouped into four classes (Figure 4.4). Slope length and gradient were determinants in the process of erosion. In the Ourika watershed, LS values were very high in areas of intrusive tributaries. The LS index considered low (between 0 and 5) represented only 25% of the basin area. This corresponded to low-lying areas of the watershed, plains and streambeds. As such, the watershed is subjected to a high risk of erosion from upstream. These results were similar to those obtained by several authors in other watersheds (Yjjou et al. 2012; Yjjou et al. 2014; Markhi et al. 2015). It has been shown that erosion increases exponentially depending on the degree of slope with an average exponent of 1.4 (Elbouqdaou et al. 2005). Similarly, it has been reported that when the degree of inclination of the slope increases, the kinetic energy of rainfall is constant while the carriage is accelerated downward due to an increase of runoff's kinetic energy (Ibrahimi 2005).

3.4   Vegetation cover factor (C)

The factor C represents both cover and the level of plant production. The spatial distribution map of the hedged index showed that the areas most sensitive to erosion were those of low vegetation cover mainly located upstream (Figure 4.5-4.7).

In order to estimate the vegetation cover, vegetation index TSAVI was produced. TSAVI comes out from the soil line. Different parameters for soil lines for each Landsat scene are indicated in Table 4.3. TSAVI was correlated with C factor estimated using NDVI to evaluate vegetation cover. A linear regression was applied to estimate the percentage of vegetation cover from the TSAVI. This relationship can be written as follows (Kefi et al. 2010) :

Vegetation cover (%) = α.TSAVI+β
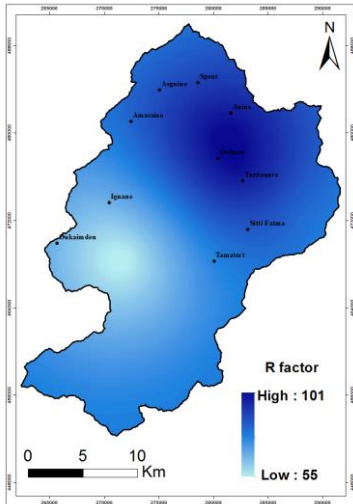
Figure 4.2. R factor map
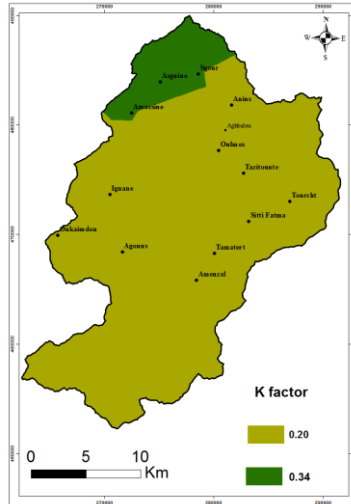
Figure 4.3. K factor map
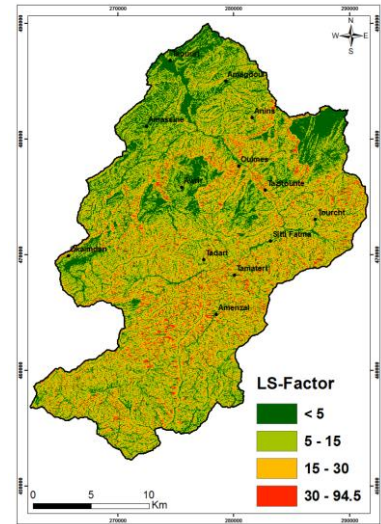
Figure 4.4. LS factor map
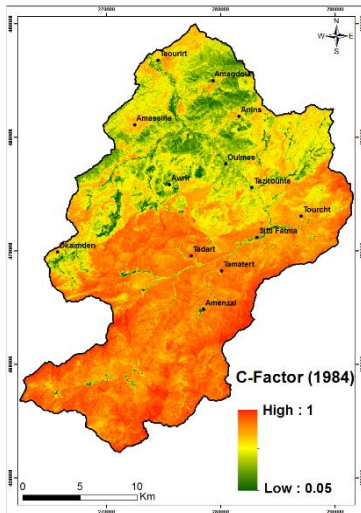
Figure 4.5. C factor map (1994)
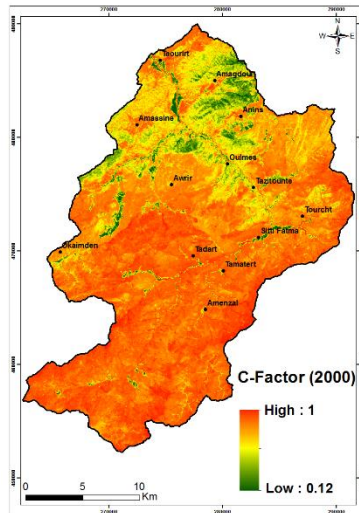
Figure 4.6. C factor map (2000)
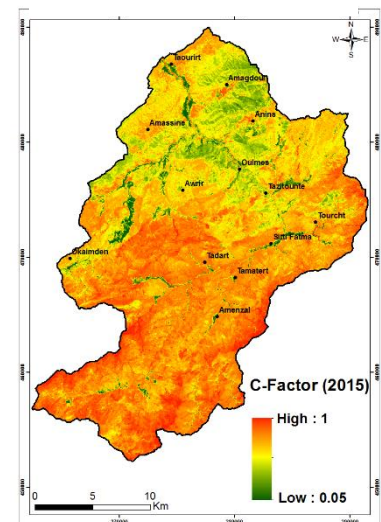
Figure 4.7. C factor map (2015)
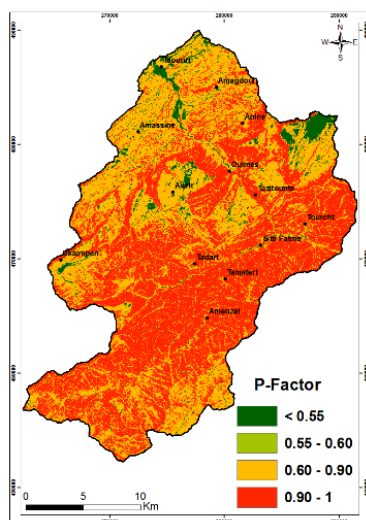
Figure 4.8. P factor map

The parameters of this relationship are shown in Table 4.4. Vegetation cover classes are presented in Table 4.5. C factor depends on vegetation cover. C factor which is close to 0 means a high density of vegetation whereas close to 1 shows a low density of vegetation (Kefi et al. 2010). Furthermore, in our study, the findings show that areas with C factor<0.4 were 3.49, 0.10 and 5.22%, respectively, for 1984, 2000 and 2015 (Table 4.2). It indicated that C factor rose between 2000 and 2015 due to the increase of vegetation cover (Table 4.5).

The areas with C factor ranging from 0.6 to 1 were 82.16, 99.29 and 75.42%, respectively, in 1984, 2000 and 2015. This signifies scarce vegetation. Furthermore, vegetation cover more than 75% represented 5.04, 1.34 and 3.09% in 1984, 2000 and 2015, respectively. Vegetation cover less than 25% represented 69.96, 85.29 and 78.52% in 1984, 2000 and 2015, respectively. There was vegetation cover reduction in 2000 and vegetation cover improvement in 2015. The improvement of vegetation cover between 2000 and 2015 is due to *Pinus halepensis* afforestation programs and the expansion of arboriculture in the watershed.

Table 4.2. C factor distribution

Class	C factor value	1984		2000		2015	
		Area (ha)	%	Area (ha)	%	Area (ha)	%
1	0 - 0.20	102.21	0.18	0.81	0.00	467.50	0.81
2	0.20 - 0.40	1909.03	3.31	57.40	0.10	2542.44	4.41
3	0.40 - 0.60	8263.60	14.35	350.89	0.61	11152.43	19.36
4	0.60 - 0.80	14176.76	24.61	1265.01	2.20	30318.24	52.64
5	0.80 - 1	33148.41	57.55	55925.89	97.09	13119.40	22.78
	Total	57600.00	100.00	57600.00	100.00	57600.00	100.00

Table 4.3. Soil line characteristics

No.	Scene date	Slope (a)	Intercept (b)	R^2
1	1984	0.964	12.692	0.970
2	2000	0.604	4.948	0.997
3	2015	1.287	813.220	0.979

Table 4.4. Parameters of linear regression

No.	Scene date	α	β	R^2
1	1984	1.334	0.382	0.87
2	2000	1.265	0.491	0.84
3	2015	1.21	0.361	0.97

Table 4.5. Distribution of vegetation cover classes per scene

Class	Vegetation cover classes	1984		2000		2015	
		Area (ha)	%	Area (ha)	%	Area (ha)	%
1	<25%	40297.60	69.96	49129.47	85.29	45229.08	78.52
2	25–50%	9168.20	15.92	5591.67	9.71	7191.29	12.48
3	50–75%	5233.35	9.09	2109.17	3.66	3396.96	5.90
4	> 75%	2900.85	5.04	769.69	1.34	1782.67	3.09
	Total	57600.00	100.00	57600.00	100.00	57600.00	100.00

3.5   Erosion control practices factor P

Agricultural techniques such as cultivation along contours, alternating strips or terraces, mounding and ridging are effective soil conservation practices. P values were mostly lower than or equal to 1. A value of 1 corresponded to land without erosion control practices. P varied according to both agricultural and erosion control practices, and with slope.

In this study the factor P values were determined with respect to slope. Low and average values corresponded to low to moderate slope areas. The P factor values ranged between 0.55 and 0.6 for low-slope areas and 0.8 to 1 for areas with steep slopes. P equal to 1 represented 50% of the watershed area (Figure 4.8).

3.6   Evaluation of soil loss

Soil losses result from a combination of the RUSLE model's factors including climate aggressiveness (R), soil erodibility (K), topographic factor (LS), vegetation cover (C) and erosion control practices (P). The combination of these in a GIS environment resulted in the soil loss map of the watershed.

According to the soil loss value, the spatial distribution of annual soil loss can be classified into five classes ranging from lower than 20 to more than 200 t/ha. These results confirm that the risk of soil erosion is serious in this watershed. In order to evaluate the effect of vegetation cover on the soil erosion risk using the RUSLE model, of the five factors only the C factor will be altered. The C factor map was derived using images of 1984, 2000 and 2015. The soil loss values calculated with the RUSLE model are shown in Table 4.6.

About 26.70, 34.79 and 19.35% of the area, respectively, in 1984, 2000 and 2015 has a soil loss value of more than 200 t/ha. Soil loss potential value increased in 2000 but, in 2015, it diminished. The highest soil loss occurs in 2000 when a wide area of the watershed remained

bare. However, the soil loss was diminished in 2015 with the presence of vegetation. Furthermore, the average of potential soil loss is 143.99, 174.51 and 122.46, respectively, for 1984, 2000 and 2015. These results were close to those obtained in similar conditions in the Oum Er-Rbia watershed where 50-400 t/ha/year soil loss class represented 54% of the watershed area (Yjjou et al. 2012; Yjjou et al. 2014).

The spatial distribution of the soil erosion risk is illustrated in Figure 4.9-4.11. Therefore, the vegetation cover provides protection for the soil against the erosion process (Vrieling 2006). In addition, it was possible to predict and delimitate vegetation cover areas using the relationship between the vegetation factor and the TSAVI.

Table 4.6. Distribution of soil loss in the Ourika watershed

Potential soil loss (t/ha/year)	Erosion risk classes	1984		2000		2015	
		Area (ha)	%	Area (ha)	%	Area (ha)	%
< 20	Very low	6486	11.26	4479	7.78	7281	12.64
20 - 50	Low	8603	14.94	7082	12.29	9790	17.00
50 - 100	Moderate	11680	20.28	10421	18.09	12821	22.26
100 - 200	High	15450	26.82	15578	27.05	16215	28.15
> 200	Very high	15382	26.70	20041	34.79	11493	19.95
Total		57600	100.0	57600	100.0	57600	100.0

Serious risk of erosion is shown especially in the mountainous areas. This increased soil erosion risk from 1984 to 2000 is due to conversion of rangeland and forest to bare land and the high slope gradient. A large area of the Ourika watershed is in very serious risk due to slope and land use changes. Furthermore, the watershed has a wide area with steep slopes which can increase the runoff velocity and, consequently, the soil erosion risk. Besides the slope, the effect of land use on soil erosion has been assessed. The vegetation cover is effective in preventing erosion to some extent. It absorbs the kinetic energy of raindrops, covers a large proportion of the soil during periods of the year when rainfall is most aggressive, slows down runoff, and keeps the soil surface porous (Roose 1996). Therefore, the soil erosion risk increases when soils remain bare and decreases with the presence of vegetation.

The results are different from those obtained in the neighboring N'fis watershed (Markhi et al. 2015). The average potential value of soil loss was 115 t/ha/year in the N'fis watershed while it was 122.46 t/ha/year in the Ourika watershed in 2015. This could be explained by the fact that the rainfall erosivity and topographic factors are more significant in Ourika than in N'fis.
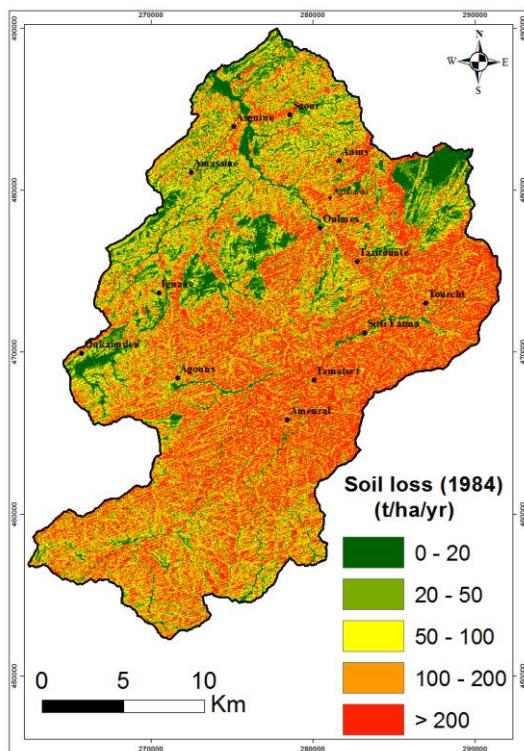
Figure 4.9. Potential soil loss map (1984)
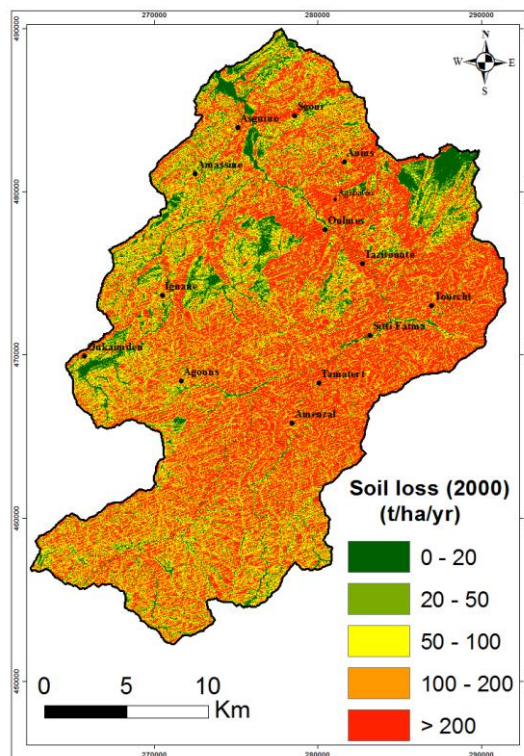
Figure 4.10. Potential soil loss map (2000)
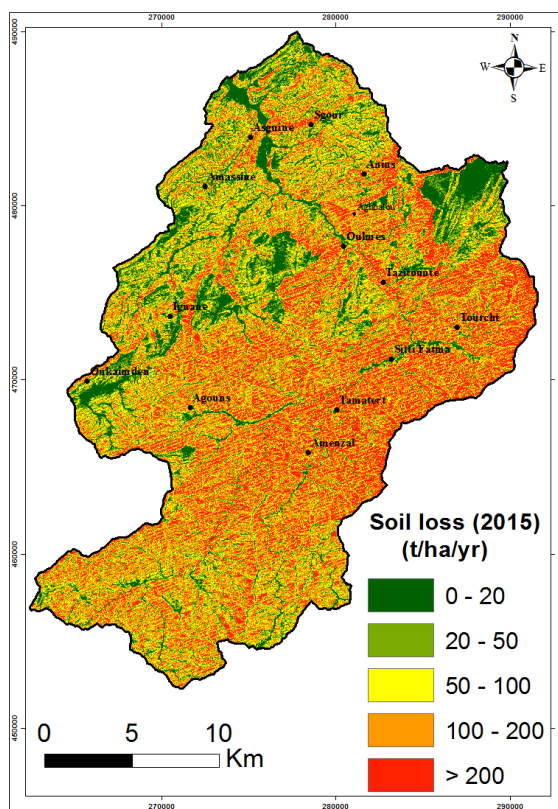
Figure 4.11. Potential soil loss map (2015)

The rainfall erosivity reached 100 MJ.mm/ha.h.year in the Ourika watershed while the maximum value is 57 MJ.mm/ha.h.year in the N'fis watershed. Similarly, the topographic factor was more important in the Ourika watershed than in N'fis. As such, even though the two watersheds are in the same geographic region (separated by Rheraya watershed), climatic and topographic conditions are slightly different, which may explain the observed differences in the vulnerability of both watersheds to water erosion.

The results are different from those obtained in the neighboring N'fis watershed (Markhi et al. 2015). The average potential value of soil loss was 115 t/ha/year in the N'fis watershed while it was 122.46 t/ha/year in the Ourika watershed in 2015. This could be explained by the fact that the rainfall erosivity and topographic factors are more significant in Ourika than in N'fis. The rainfall erosivity reached 100 MJ.mm/ha.h.year in the Ourika watershed while the maximum value is 57 MJ.mm/ha.h.year in the N'fis watershed. Similarly, the topographic factor was more important in the Ourika watershed than in N'fis. As such, even though the two watersheds are in the same geographic region (separated by Rheraya watershed), climatic and topographic conditions are slightly different, which may explain the observed differences in the vulnerability of both watersheds to water erosion.

The applicability of the empirical universal soil loss equation under different conditions from those in which it was developed exposes it widespread criticism over the fact that it applies only to sheet erosion. In addition, the model assumes that all surfaces are subject to erosion if all factors are non-zero and does not reveal deposits. Nevertheless, uncertainty remains tolerable if both field measurements and laboratory analysis are performed rigorously.

Furthermore, the integration of the model into a GIS has many benefits. It allows the effective maintenance of large quantities of data on various water erosion related factors and the establishment of synthetic soil loss maps, erosion potential maps or spatial distribution maps on vulnerability to erosion of the different areas of the watershed resulting from the combination of different factors in the erosion process. Thus, despite the fact that the validity of the results is subject to discussion, the method allows policy makers and managers to plan the fight against the erosion by interventions in areas where the risk of erosion is high. It also allows for a proper land use by adopting management practices oriented toward fighting against erosion.

4 Conclusion

Soil erosion by water is an environmental problem which can cause soil damage and, consequently, affect agriculture, particularly in developing countries. Therefore, a suitable

assessment of this phenomenon can be useful and helpful for decision makers in order to establish strategies and programs for erosion control management. The study of risks of erosion in the Ourika watershed was done using the Revised Universal Soil Loss Equation (RUSLE) integrated into a GIS. The various factors involved in the processes of erosion were identified and their combination in a GIS environment resulted in potential soil loss results of the watershed. The impact of vegetation on water erosion is also studied using multi-temporal satellite images, normalized vegetation index and the transformed soil adjusted vegetation index.

Mapping soil erosion using RUSLE model helped to identify areas of high risk of water erosion. Furthermore, the detection of land use changes using several satellite images shows the importance of vegetation in protecting the soil against soil erosion by water. In addition, the use of remote sensing data such as satellite images and vegetation index was significant to get the vegetation factor of the model. The results show that the watershed is exposed to high potential soil erosion risk. Regarding its positive impact, vegetation coverage should be preserved and increased

The universal soil loss equation only estimates the average losses caused by sheet erosion. This model is based on data from plots or watersheds of limited area, and as such poses problems with respect to precision when used on a larger scale and in conditions other than those in which it was adopted. Nevertheless, the results are of great interest for land managers leading to actions against erosion. Using a GIS and remote sensing tools can be suitable for planning measures and strategies for soil and water conservation.

Chapter 5

A GIS-based approach for gully erosion susceptibility modelling using bivariate statistics methods in the Ourika watershed, Morocco[3]

[3] Meliho M., Khattabi A., Mhammdi N. (2018) A GIS-based approach for gully erosion susceptibility modelling using bivariate statistics methods in the Ourika watershed, Morocco. *Environ Earth Sci* (2018) 77: 655.

A GIS-based approach for gully erosion susceptibility modelling using bivariate statistics methods in the Ourika watershed, Morocco

Abstract

Gully erosion is an important environmental issue with severe impacts. This study aimed to characterize gully erosion susceptibility and assess the capability of information value (InfVal) and frequency ratio (FR) models for its spatial prediction in Ourika watershed of the High Atlas region of Morocco. These two bivariate statistical methods have been used for gully erosion susceptibility mapping by comparing each data layer of causative factor to the existing gully distribution. Weights to the gully causative factors are assigned based on gully density. Gullies have been mapped through field surveys and google earth high-resolution images. Lithofacies, land use, slope gradient, length-slope, aspect, stream power index, topographical wetness index and plan curvature were considered predisposing factors to gullying. The digitized gullies were randomly split into two parts. Sixty-five percent (65%) of the mapped gullies were randomly selected as training set to build gully susceptibility models, while the remaining 35 % cases were used as validation set for the models' validation.

The results showed that barren and sparse vegetation lands and slope gradient above 50% were very susceptible to gully erosion. The ROC curve was used for testing the accuracy of the mentioned models. The analysis confirms that the FR model (AUC = 80.61 %) shows a better accuracy than InfVal model (AUC = 52.07 %). The performance of the gully erosion susceptibility map constructed by FR model is greater than that of the map produced by InfVal model.

The findings proved that GIS-based bivariate statistical methods such as frequency ratio model could be successfully applied in gully susceptibility mapping in Morocco mountainous regions and in other similar environments. The produced susceptibility map represents a useful tool for sustainable planning, conservation and protection of land from gully processes.

Keywords: Gully erosion, information value, frequency ratio, Ourika watershed, Morocco.

Chapter 5 – A GIS-based approach for gully erosion susceptibility modelling using bivariate statistics methods in the Ourika watershed, Morocco

1 Introduction

Soil erosion is a serious problem, especially in semi-arid areas (Lal 2001). Soil erosion by water is the principal factor of land degradation in Morocco, destroying agricultural lands and forest ecosystems. Water erosion is a major problem because of its impacts on agricultural productivity and on soil properties (Morgan 1995; Poesen et al. 1996). Gully erosion, which is a highly intense form of soil erosion, is a major contributor to land degradation (Vanwalleghem et al. 2005; Bou Kheir et al. 2007). It is a process where surface water is concentrated in narrow flow paths and eliminates soil, resulting in incised canals that are too large to be destroyed by normal plowing operations. The expansion of individual gullies into a network of active gullies contributes significantly to soil loss in a watershed (e.g. Martinez-Casasnovas et al. 2003; Erskine 2005). For a sustainable management of the affected areas, it is necessary to establish the spatial extent of the problem and the factors that cause it (Tamene et al. 2006).

Several models have been developed for gully erosion but only a few authors focused on gully erosion susceptibility mapping (e.g Bou Kheir et al. 2007; Conoscenti et al. 2008; Gómez Gutiérrez et al. 2009 ; Krishna Bahadur 2009 ; Pike et al. 2009 ; Conforti et al. 2010 ; Conoscenti et al. 2014). Statistical methods are appropriate for detecting quantitative estimates of the location of future events, since the susceptibility assessment should be as objective as possible. The estimation of the contribution of each predisposing factor makes it possible to divide the area into zones characterized by different susceptibilities. All these statistical techniques, little used in gully erosion research, can be grouped into bivariate and multivariate methods (Gómez Gutiérrez et al 2009; Lucà et al. 2011).

Bivariate statistical approaches are based on the calculation of weighting values based on the gully density for each causal factor class (Yalcin 2008). Bivariate-statistics-based approaches are easier to use than multivariate statistics methods. Differently from these latter, the bivariate-statistics based methods present the disadvantage of not taking into account the mutual interrelationships among the different causal factors. Among the existing bivariate statistics methods for quantitative susceptibility assessment, the information value method and frequency ratio are the most commonly applied statistical methods (Pardeshi et al. 2013).

The mountainous areas of Morocco and, in particular, the high Atlas region is vulnerable to soil erosion (Meliho et al., 2017) and gully development, due to its edaphic and climatic conditions, and its unsustainable land management. Concentrated runoff causes a consistent soil loss and mainly results in gully erosion. In the last decades, a number of studies have been carried out in Morocco, with the aim of developing and applying models for the assessment of soil loss rates and water erosion risk. Most of the erosion models focus on the quantification of soil eroded by sheet and rill erosion using USLE and RUSLE models and at test plot scale through rainfall simulations (Meliho et al. 2007). However, the literature reveals that gully erosion studies are rare and particularly non-existent in Morocco. For that reason, it is necessary to establish useful models for gully erosion susceptibility assessment in different environmental conditions. In this work, we investigate susceptibility conditions to gully erosion in a watershed of the High Atlas Mountains of Morocco, by following a statistical approach aimed to define spatial relationships between gully occurrence and variability of the gully erosion predisposing factors. The goal of the research is to characterize the driving factors of gully erosion, to map the susceptibility of the study area to gully erosion and compare the information value and frequency ratio models based on their predictive accuracy. The possibility of adopting these statistical bivariate methods could be appreciated in a medium-scale gully erosion prediction assessment.

2 Materials and methods

2.1 Presentation of the study area

The Ourika watershed is a well-individualized hydro system of the High Atlas of Marrakech, between 31° and 31°20' North and between 7°30' and 7°60' West (Figure 5.1). The main wadi has its sources in the high foothills of the High Atlas Mountains. The climate of the Ourika watershed is characterized by its great spatial and temporal variability. Annual rainfall is on average 500 mm/year with a coefficient of variation of 34%. The monthly and seasonal variability is even more marked, with respective coefficients of variation of 55% and 50%. This rainfall increases with altitude. It can exceed 700 mm/year on the high peaks of the watershed. The region of Ourika is famous for its high and complex reliefs. Seventy-five percent of the watershed's area is between 3200 and 1600 m of altitude with the average of 2500 m. The slopes are generally steep. A slope greater than 50% characterizes more than 50% of the watershed

area. The slopes are low downstream and very high upstream of the watershed. The Ourika watershed is made up of magmatic and metamorphic rocks in the upper zone, and Permo-Triassic and Quaternary Age deposits are located at lower altitudes. The soils are mainly skeletal and rocky. Forest and pre-forest ecosystems in the watershed are generally degraded and sparse. The populations live mainly from terraced farming and extensive livestock farming depending on the forest rangelands.
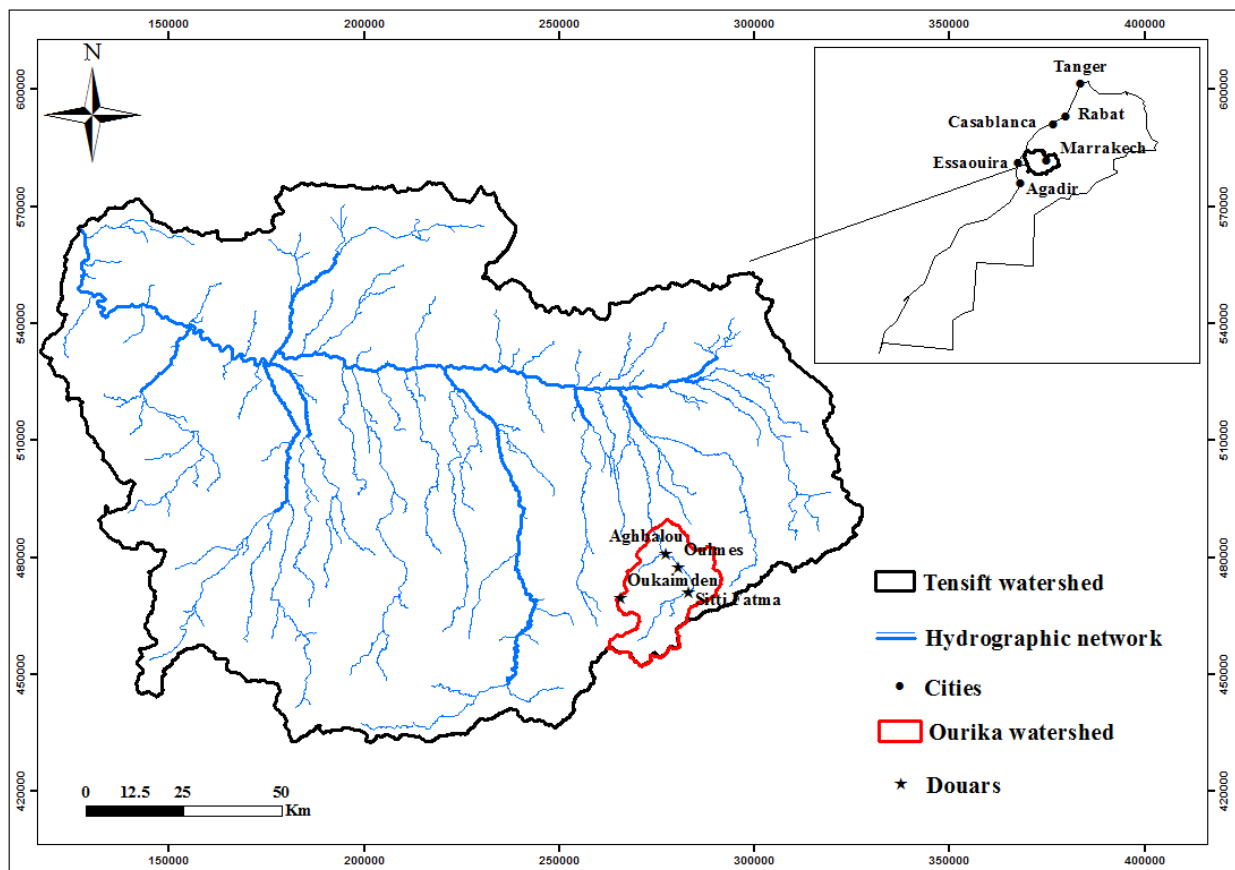
Figure 5.1. Location of the watershed Ourika

2.2 Gully inventory and predisposing factors analysis

High-resolution imagery from Google Earth and multiple field surveys made it possible to assess the spatial distribution of gully erosion processes in the watershed (Figures 5.2 & 5.3). Factors recognized in the literature as predisposing to gully erosion were considered. The contributing factors used in this work are lithofacies, land use, slope, length-slope factor, aspect, plan curvature, stream power index and topographical wetness index. All the morphometric parameters were derived from the DEM with a resolution of 10 x 10 m pixel size, using the

management features offered by GIS. Harris Corporation/Space and Intelligence Systems provided the DEM.

Gully erosion depends on the hardness of the substrate. Lithofacies map identifies the different types of rock or sediment/soil surface based on chemical and physical resistance of different formations to weathering process (ICONA 1997). By analyzing the geological map, geological formations were classified into four groups (Table 5.1 and Figure 5.4), according to their resistance to weathering in order to prepare the lithofacies layer. The lithofacies class of high resistance to gully erosion represented 55% of the watershed while the low resistance class represented 27%.

Land use change, ecosystem destruction by road construction and vegetation clearance are mentioned to be the main causes of gully erosion in the world (Wemple et al. 1996; Bork et al. 2001; Nachtergaele 2001; Alejandro and Kenji 2007). The land use map of the study area (Meliho et al., 2016) have been classified in six classes (Figure 5.5). In particular, 50% of the study area represents empty non-forested lands and woodland represents 25%.
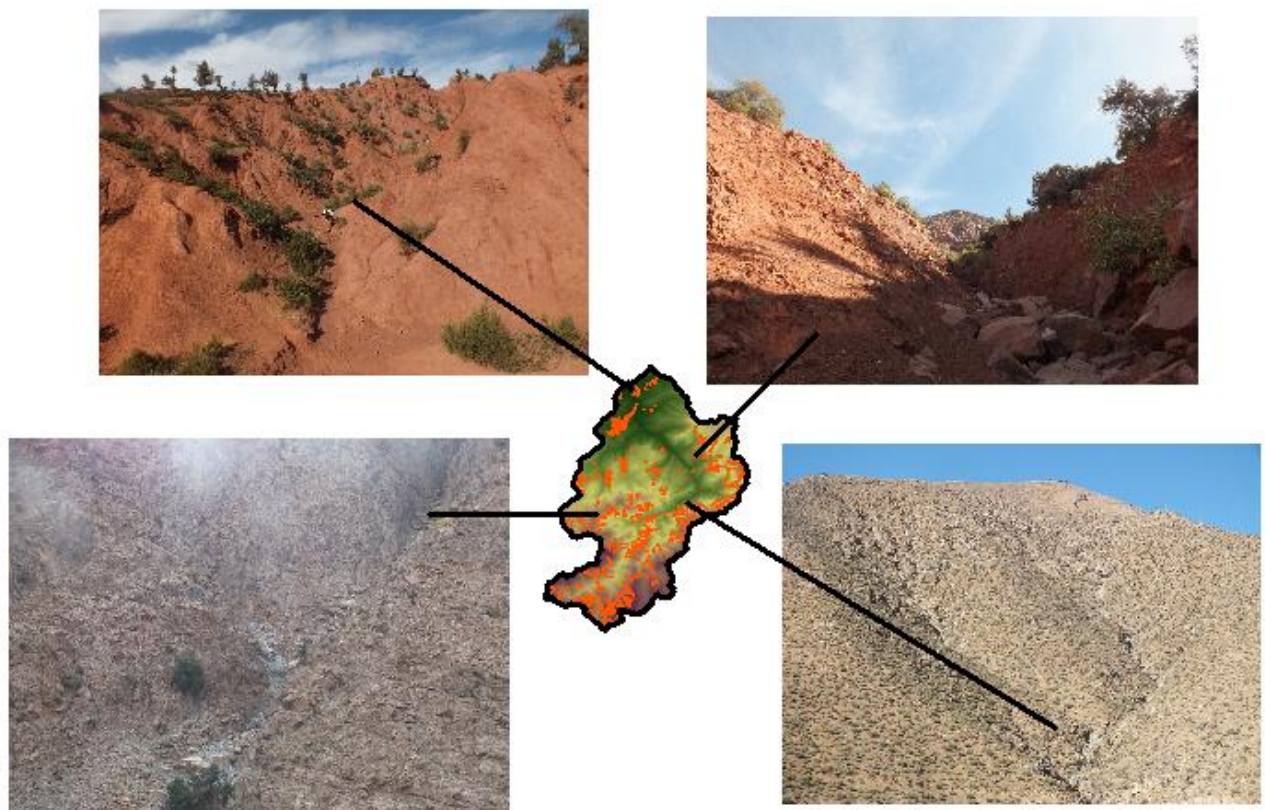
Figure 5.2. Map of the observed gullies and pictures of some of the mapped gullies

Slope gradient is an important factor in gully erosion dynamics. By affecting surface runoff, drainage density and soil erosion, it plays a crucial role in gully erosion process. The slope gradient was derived from the DEM and was divided in five classes (Figure 5.6). More than 50% of the study area have a slope of more than 50%.

Table 5.1. Lithofacies classes description

Lithofacies (resistance classes)	Description
Very high	Non-weathered compact rock, strongly cemented conglomerates or soils, crusts, hard pans (massif, limestone, highly stony soils, igneous or eruptive rocks)
High	Fractured and/or medium weathered cohesive rocks or soils
Low	Slightly to medium compacted sedimentary rocks (slate, schists, compacted marls etc.) and soils
Very low	Soft, low-resistant or strongly/deeply weathered rock (marl, gypsum, clayey slates, etc.) or soils. Loose, non-cohesive sediment/soils and detritic material

Slope gradient is an important factor in gully erosion dynamics. By affecting surface runoff, drainage density and soil erosion, it plays a crucial role in gully erosion process. The slope gradient was derived from the DEM and was divided in five classes (Figure 5.6). More than 50% of the study area have a slope of more than 50%.

The LS-factor considers the effect of topography on soil erosion (Renard et al. 1997). It can be assessed using the upslope contributing area and slope steepness of each cell according to the equation described by Moore and Burch (1986):

$$LS = (fa \times cellsize / 22.13)^{0.4} \times (\sin \beta / 0.0896)^{1.3}$$

Where: fa is flow accumulation and β, slope gradient (°)

LS factor has been classified in five classes and it spatial pattern is shown in the map of Figure 5.7. The aspect, expressed in degrees from the north and clockwise, ranges from 0 to 360°. It can indirectly influence the erosion processes, because it controls the exposition to several climatic conditions such as the intensity of precipitation, duration of exposition to light, etc. and the vegetation cover (Dai et al. 2001). The aspect map of the study area was classified into eight classes: N, NE, E, SE, S, SW, W and NW; flat class was negligible (Figure 5.8).

The plan curvature can be determinant in terrain instability by controlling the surface and subsurface hydrological regimes of the slope (Lucà et al. 2011). Positive plan curvature values define convexity, negative values indicate concavity and zero values indicate a flat surface. Values of plan curvatures around zero indicate that the surface is flat. Plan curvature in the Ourika watershed is shown in Figure 5.9.

The stream power index (SPI) is a secondary topographic attribute derived from slope and the contributing area of flow accumulation. It provides a correlation between water flow paths, flow accumulations and slope that together define the energy potential surface water has for erosion (Figure 5.10). SPI implies that discharge is proportional to the specific catchment area (Moore et al. 1991).

$$SPI = As \times \tan \beta$$

Where: As is specific catchment area (m) and β, slope gradient (°)

Topographic wetness index (TWI), which combines local upslope contributing area and slope, is used to quantify topographic control on hydrological processes (Figure 5.11). It is an important parameter frequently employed to describe the effect of topography on soil moisture in watersheds. TWI is generally extracted from Digital Elevation Models (DEMs) and is a function of both the slope and the upstream area per unit width orthogonal to the flow direction. TWI can be calculated as follows:

$$TWI = \ln (As / \tan \beta)$$

Where: As is specific catchment area (m) and β, slope gradient (°)

2.3   Susceptibility analysis

The bivariate statistical analysis is generally considered the simplest and the easiest statistical method in the assessment of the quite complex phenomenon that is gully erosion. This approach involves the adoption of a strategy focusing on the relationships between the predisposing factors and the distribution of gullies. The two bivariate methods used in this study were Information Value and Frequency Ratio Method. They were chosen based on their successful use in the literature. The Information Value Method (eg: Zezere 2002; Wang and Sassa 2005; Sarkar et al. 2006; Sharma et al. 2009; Pereira et al. 2012) and the Frequency Ratio Method (eg: Lee 2005; Goswami et al. 2011; Lee and Pradhan 2006; Balteanu et al. 2010) have been widely used in landslide susceptibility assessment. However, few researchers have used these

methods in gully erosion susceptibility assessment (Conforti et al. 2010; Lucà et al. 2011; Rahmati et al. 2016).
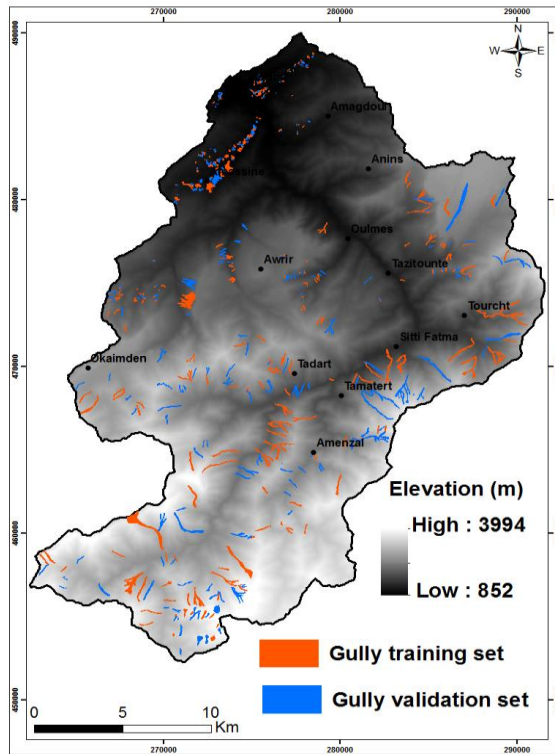
Figure 5.3. Gully inventory map with training and validation set
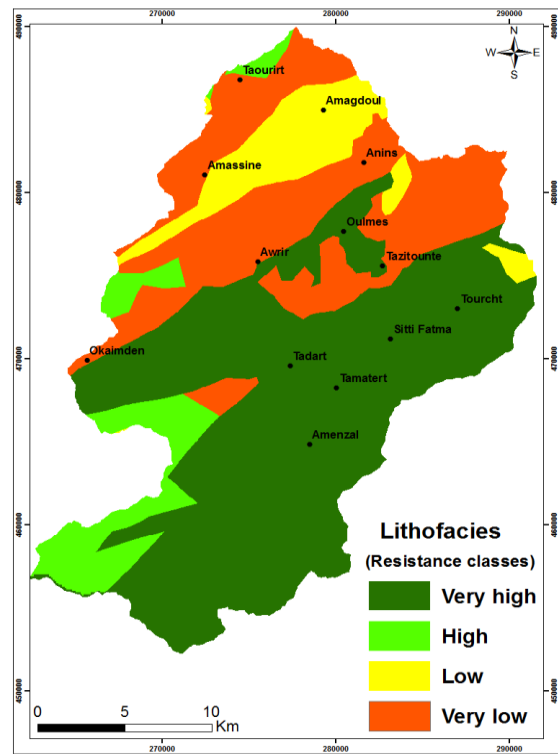
Figure 5.4. Lithofacies map
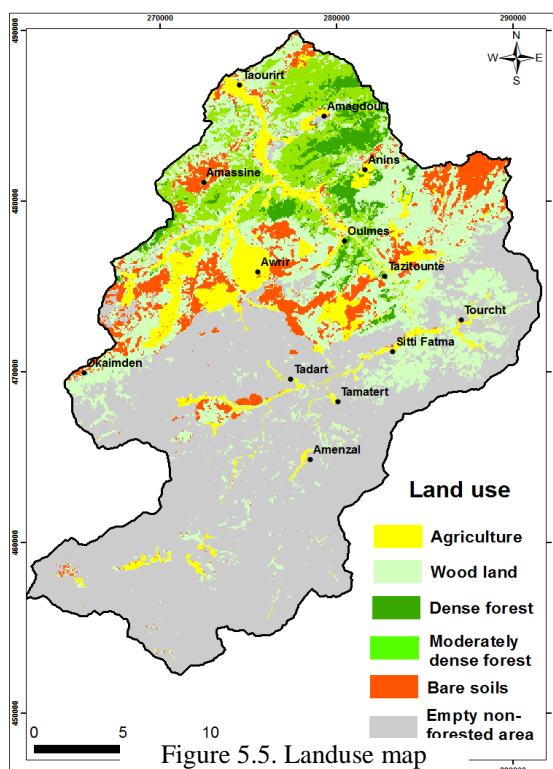
Figure 5.5. Landuse map
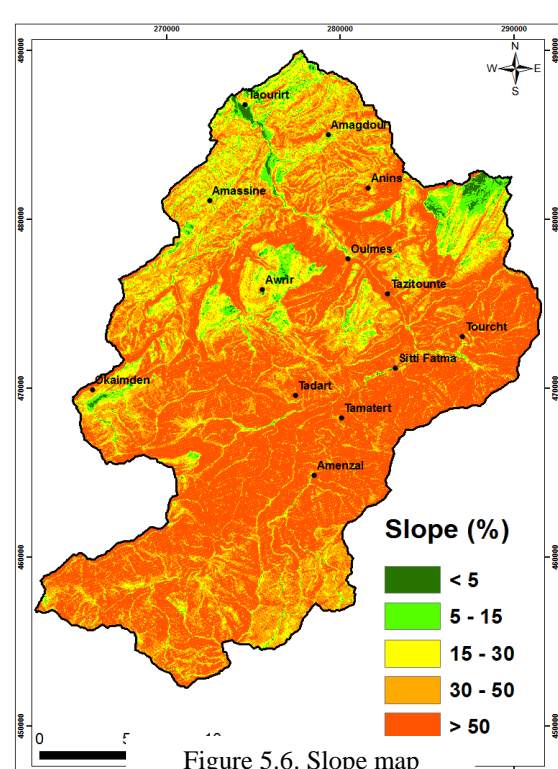
Figure 5.6. Slope map
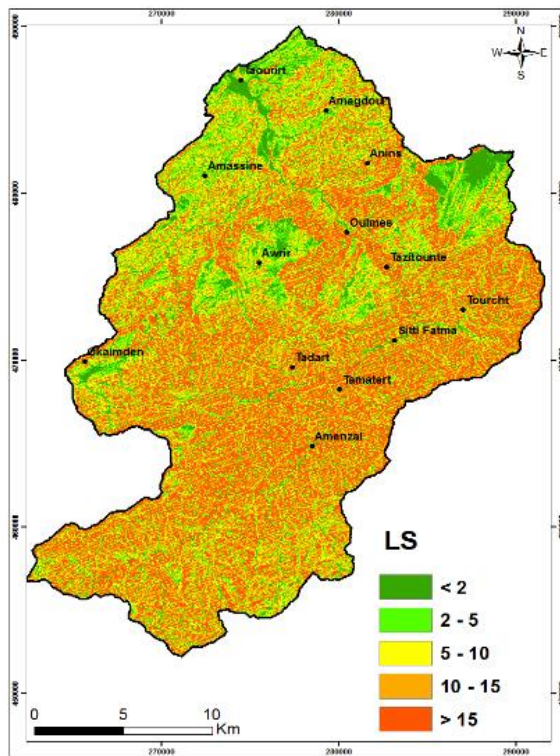
Figure 5.7. LS map
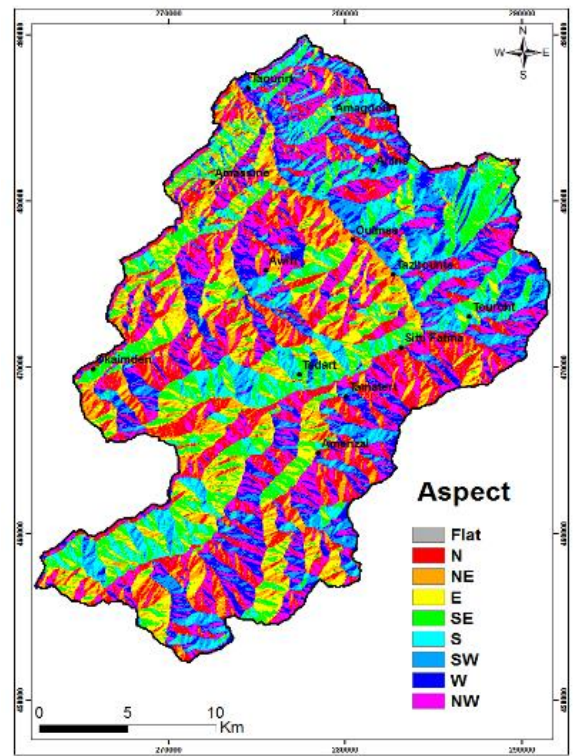
Figure 5.8. Aspect map
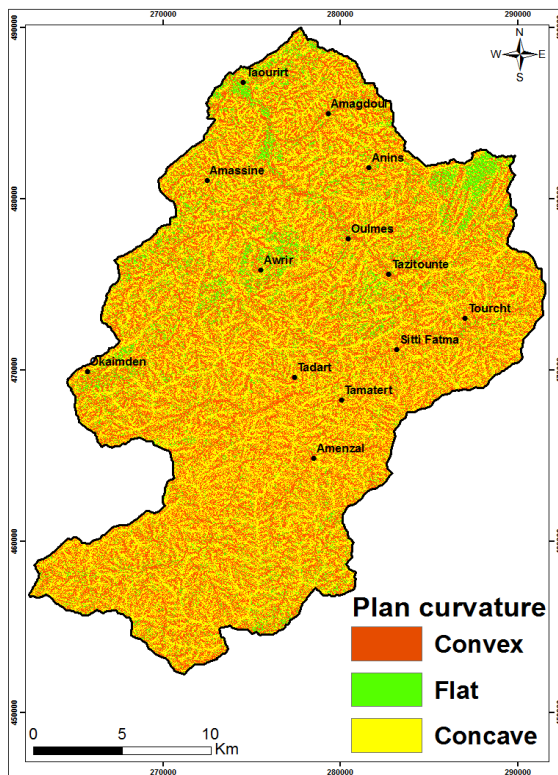
Figure 5.9. Plan curvature map
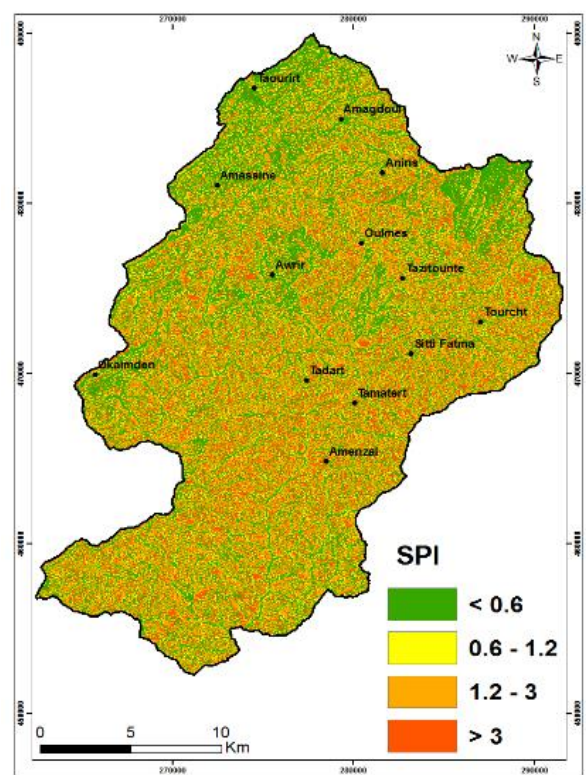
Figure 5.10. SPI map
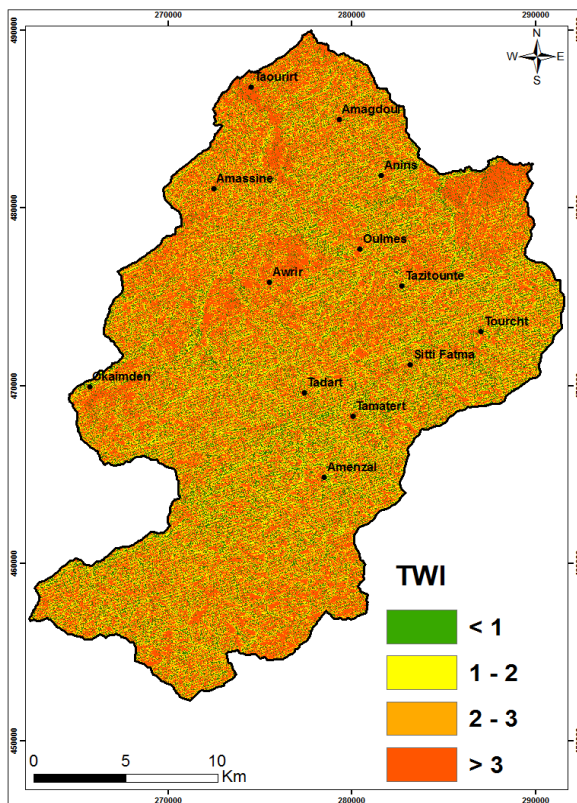
Figure 5.11. TWI map

2.3.1 Information Value method

Information Value Model (InfVal) is a bivariate statistical method for spatial prediction of hazard based on relationships between hazard occurrence and related parameters (Sarkar et al. 2006). The information values are determined for each hazard-related parameter subclass based on the presence of the hazard in a given map unit. Several studies have applied this method for landslides and it has proved to be a useful method for determining the degree of influence of the individual causal factor responsible for the occurrence of landslides (Pardeshi et al. 2013). Many works consider the information value method as the simplest and quantitatively suitable method in gully susceptibility mapping (eg. Conforti et al. 2010, Lucà et al. 2011, Conoscenti et al. 2014). This approach is based on the relationships observed between each predisposing factor and the distribution of the gully zones (Conforti et al. 2010). The density of the gullies of the training set in each class was evaluated for each predisposing factor. The weighting values for each class were computed through the formula of Van Westen (1993):

$$W_i = ln \frac{DC}{DM} = ln \frac{a/b}{c/d}$$

Where:

Wi = weighting value of class i; DC = gully density in class i; DM = gully density in the whole study area; a = number of pixels containing gullies in class i; b = number of pixels in class i; c = total number of pixels containing gullies throughout the study area; d = total number in the entire study area.

2.3.2 Frequency Ratio Method

The frequency ratio method, as a means for susceptibility analysis, has been widely adopted in the assessment of land degrading phenomena such as erosion, landslides and flood (Balteanu et al. 2010; Goswami et al. 2011; Rahmati et al. 2015). It is based on the relationships observed between the distribution of the resulting features such as gullies and the corresponding predisposing factors. Statistical approaches are based on the relationships between each corresponding predisposing factor and the distribution of past gullies, and this correlation can be quantitatively assessed using the frequency ratio method.

The number of gully pixels in each class has been evaluated and the frequency ratio for each factor class is found by dividing the gully ratio by the area ratio, denoted as:

$$FR_{i,j} = \frac{N_{pix}(S_{i,j}) \, / \, \Sigma_j N_{pix}(S_{i,j})}{N_{pix}(N_{i,j}) \, / \, \Sigma_j N_{pix}(N_{i,j})}$$

Where:

FRi,j is the frequency ratio of class j in factor i;

Npix (Si,j) is the number of pixels of gully occurrence within class j in factor i;

Npix (Ni,j) is the number of pixels of class j in factor i.

In relation analyses, a value greater than 1.0 indicates a strong correlation between landslide occurrence and the factor's class, and a value lower than 1.0 means a weak correlation (Pradhan and Lee 2010).

The predictor rate was calculated for each predisposing factor using the following equation (Althuwaynee et al. 2014):

PR = (SAmax - SAmin)/(SAmax - SAmin)min

where SA is the index of the spatial association (FR) of spatial factors and gullies. The calculated absolute difference between the maximum and minimum SA values was divided by the lowest absolute difference of all factors. PR is the predictor rate.

2.3.3 Susceptibility map validation

The occurrence of gullies with respect to predisposing factors was analyzed using the training set and the resulting model was applied to the entire study area. The validation set was used to evaluate the prediction performance of the model. Spatial random partition method was used to split the gully areas dataset into two subsets. In order to consider the prediction model as the result of ''future'' gully erosion processes, the partitioning strategy selected 65% of gully areas as training set and the remnant 35% as validation set (Chung and Fabbri 2003; Conoscenti et al. 2008).

The validation curves represent the cumulative percentage of gullies in the validation set compared to the percentage of the area classified as unstable for the increasing values of the selected susceptibility index (Lucà et al., 2011). The area under the curve (AUC) characterizes the quality of the model by predicting the occurrence or non-occurrence of a gully. The best model shows a curve that has the largest AUC. The gully areas training set was used for the success rate curve which indicates the goodness fit of the gully erosion susceptibility map (Chung and Fabbri 2003; Conforti et al. 2010).

For a better comparison of the models, we weighted the susceptibility classes' zones with respect to the corresponding gully densities in the validation set, using the modified Seed Cell Area Index (SCAI) introduced by Suzen and Doyuran (2004):

SCAI = Areal extent of susceptibility classes (%) / Gully of the validation set in each susceptibility class (%)

The best model detects gully without considering large areas of the map as unstable to reflect the generally low density of the event. In addition, it should have the highest percentage of gullies in areas classified as high and very high susceptibility (Lucà et al., 2011).

3 Results and discussion

3.1 Susceptibility Assessment

3.1.1 Information Value

The obtained weighting values of each predisposing factor are reported in Table 5.2. Contrary to what could be expected, the highest density of gullies for lithofacies (Wi = 0.10) occurs in areas of very high resistance to soil erosion. This could be explained by the effect of land use, with almost non-existence of vegetation cover in the upstream area of the watershed with lithofacies of very high resistance to soil erosion, and more or less important in the downstream area with lithofacies of low to very low resistance to water erosion.

The highest Wi occur in bare soils and empty non-forested area with values of 0.15 and 0.13, respectively. The lowest Wi value (Wi = - 1.54) was obtained in the dense forest area. The spatial relationship between gully erosion processes and land use with low vegetation cover was very strong. The influence of lithofacies on gully erosion seems to be inverted by land use effect in the watershed.

The highest density of gullies for slope steepness factor occurs in areas of slope gradient more than 50 %. Gully occurrence increases by the increase in slope angle. Gully erosion areas were strongly related to areas with the high value of LS, SPI and low value of TWI. On the contrary, gullies density is low where slope gradient is less than 5% (Wi = -0.47), on which the LS is low (Wi = -0.20) and SPI is low (Wi = -0.07) and TWI is high (Wi = -0.06). The same relationships have been reported in the literature (Conforti et al. 2010; Lucà et al. 2011).

In the case of slope aspect, Wi is positive for the areas facing the west, southwest, east and northeast. The same value (Wi = 0.00) was obtained for concave plan curvature and convex plan curvature whereas flat areas have a low Wi value (Wi = -0.19).

The calculated weighting values were used to produce the susceptibility map for the Ourika watershed (Figure 5.12). The weighting values obtained have an average value of -0.21. The susceptibility map was classified into five groups (Table 5.4): 6.33% very low, 10.42% low, 17.20% moderate, 29.89% high and 36.16% very high. The upstream area of the Ourika watershed is subject to high to very high gully erosion susceptibility.

Table 5.2. Distribution of weighting values for each class of predisposing factors to gully erosion

Factors	Classes	Class area (%)	Gully area (%)	Wi
Lithofacies	Very high	55.08	68.28	0.10
	High	8.67	8.78	0.01
	Low	9.04	5.03	-0.25
	Very low	27.21	17.92	-0.17
Land use	Agriculture	7.19	1.99	-0.55
	Wood land	24.67	20.71	-0.07
	Dense forest	3.41	0.10	-1.54
	Moderately dense forest	7.56	0.77	-0.98
	Bare soils	7.44	10.25	0.15
	Empty non-forested area	49.74	66.19	0.13
Slope (%)	< 5	0.98	0.34	-0.47
	5 - 15	5.60	3.04	-0.28
	15 - 30	15.15	9.72	-0.21
	30 - 50	27.33	21.73	-0.12
	> 50	50.95	65.17	0.09
LS	< 2	8.09	4.99	-0.20
	2 - 5	17.07	14.61	-0.06
	5 - 10	23.86	21.77	-0.03
	10 - 15	18.19	18.09	0.01
	> 15	32.80	40.54	0.10
Aspect	N	15.80	12.61	-0.11
	NE	10.34	11.31	0.02
	E	11.02	11.93	0.02
	SE	13.38	12.23	-0.06
	S	10.20	10.58	0.00

	SW	9.64	11.19	0.05
	W	12.09	15.58	0.09
	NW	17.54	14.58	-0.10
	Convex	42.03	43.54	0.00
Curvature	Flat	9.93	6.66	-0.19
	Concave	48.03	49.80	0.00
	< 0.6	38.10	34.04	-0.07
SPI	0.6 - 1.2	13.81	12.78	-0.05
	1.2 - 3	34.42	37.31	0.02
	> 3	13.67	15.87	0.05
	< 1	19.16	21.28	0.03
TWI	1 - 2	17.23	18.67	0.02
	2 - 3	25.81	25.81	-0.02
	> 3	37.79	34.24	-0.06

3.1.2 Frequency Ratio model

The result of the gully erosion susceptibility mapping based on the frequency ratio model are shown in the Table 5.3. The highest frequency ratio values were observed in the empty non-forested area (1.33) and bare soils (1.25), slope gradient more than 50% (1.29) and lithofacies of very high resistance (1.28). Furthermore high frequency ratio values were obtained for slope aspect facing west (1.27), southwest (1.11), east (1.06) and northeast (1.06), LS more than 15 (1.25), SPI more than 3 (1.17), TWI less than 1(1.09), convex (1.04) and concave (1.03) plan curvature.

Previous studies have suggested the effects of land use on gully erosion. Vegetation is known to favor water infiltration and to protect soil from erosion (Valentin et al 2005).

Slope aspect can influence gully erosion processes by controlling the exposition to several climate conditions such as precipitation intensity, duration of sunlight exposition, moisture retention, etc. and the vegetation cover (Ayalew and Yamagishi 2005). Both the length and the steepness of the slope substantially affect the rate of soil erosion by water. The combined LS-factor represents the effect of topography on soil erosion. High values of LS indicate high

susceptibility of gully erosion. The relation between plan curvature and gully probability shows that concave and convex areas have a higher frequency ratio value, whereas flat areas have a low frequency ratio. Gully erosion was strongly related to areas with the high value of SPI. The impact of the SPI factor on gully erosion is confirmed by frequency ratio more than 1 for SPI values more than 1.2.

Predictor rate values for each predisposing factor are shown in Table 5.3. The highest PR values were obtained for land use (6.46) and slope gradient (5.18). Land use and slope are the main predisposing factors to gully erosion in Ourika watershed. Susceptibility map has been produced for the Ourika watershed (Figure 5.13) using the predictor rate for each predisposing factor. The susceptibility map was classified into five classes using the natural-breaks technique as follows (Table 5.4): 10.36% very low, 18.11% low, 16.12% moderate, 25.74% high and 29.67% very high. The upstream area of the watershed is highly susceptible to gully erosion.

Table 5.3. Frequency ratio values distribution for each class of the selected gully erosion predisposing factors

Factors	Classes	Class area (%)	Gully area (%)	FR	PR
Lithofacies	Very high	55.08	70.62	1.28	4.42
	High	8.67	8.04	0.93	
	Low	9.04	4.77	0.53	
	Very low	27.21	16.56	0.61	
Land use	Agriculture	7.19	2.47	0.29	6.46
	Wood land	24.67	21.17	0.84	
	Dense forest	3.41	0.14	0.04	
	Moderately dense forest	7.56	0.70	0.09	
	Bare soils	7.44	9.29	1.25	
	Empty non-forested area	49.74	66.24	1.33	
Slope (%)	< 5	0.98	0.34	0.35	5.18
	5 - 15	5.60	2.98	0.53	
	15 - 30	15.15	9.39	0.62	
	30 - 50	27.33	21.31	0.78	

	> 50	50.95	65.97	1.29	
LS	< 2	8.09	4.96	0.61	2.7
	2 - 5	17.07	14.42	0.84	
	5 - 10	23.86	21.63	0.91	
	10 - 15	18.19	18.10	1.00	
	> 15	32.80	40.89	1.25	
Aspect	N	15.80	13.21	0.84	1.04
	NE	10.34	10.96	1.06	
	E	11.02	11.69	1.06	
	SE	13.38	12.28	0.92	
	S	10.20	10.72	1.05	
	SW	9.64	10.89	1.13	
	W	12.09	15.37	1.27	
	NW	17.54	14.88	0.85	
Plan curvature	Convex	42.03	43.52	1.04	2.51
	Flat	9.93	6.78	0.68	
	Concave	48.03	49.70	1.03	
SPI	< 0.6	38.10	33.75	0.89	1.38
	0.6 - 1.2	13.81	12.84	0.93	
	1.2 - 3	34.42	37.38	1.09	
	> 3	13.67	16.03	1.17	
TWI	< 1	19.16	21.31	1.11	1.00
	1 - 2	17.23	18.67	1.08	
	2 - 3	25.81	25.91	1.00	
	> 3	37.79	34.11	0.90	

3.2   Validating and comparing the models
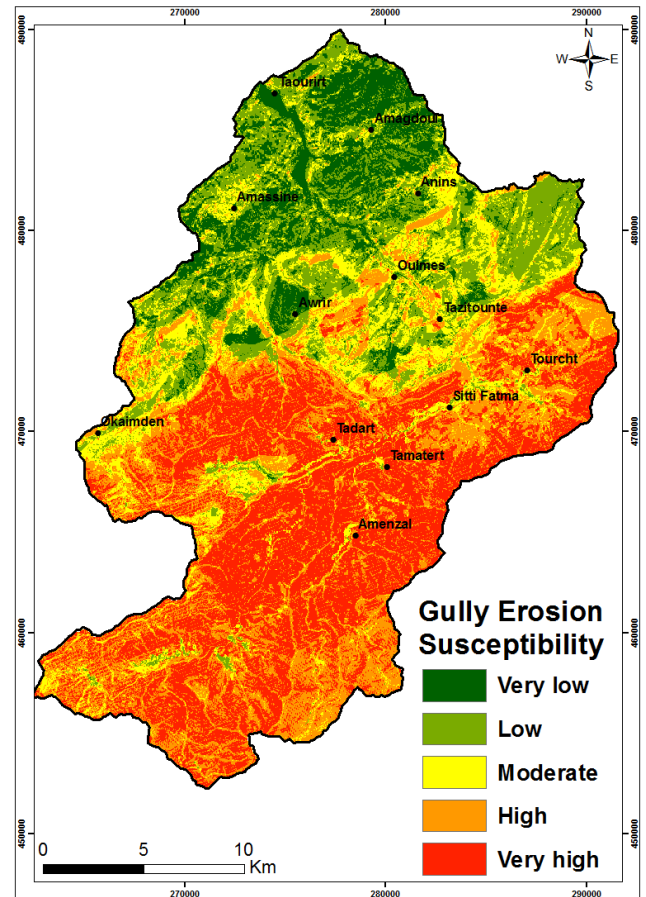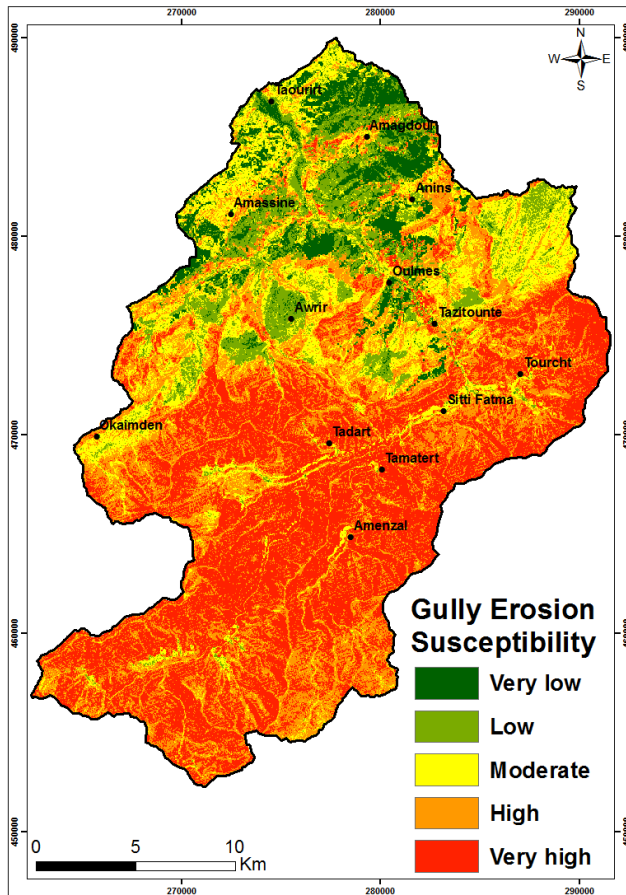
Figure 5.12. Gully erosion susceptibility map (InfVal)

Figure 5.13. Gully erosion susceptibility map (FR model)

The results of the success rate and the prediction rate curves are shown in Figure 5.14. In the InfVal model, the AUC was 50.73 and 52.07 % for success and prediction rates, respectively. In contrast, the success and prediction rates were 78.37 and 80.61 %, respectively in the FR model. The most accurate method for preparing gully susceptibility maps in Ourika Watershed was the FR method because it had the highest area under the curve and the highest degree of accuracy (80.61 %). The relationship between AUC value and prediction accuracy can be classified as follows: poor (0.5-0.6), average (0.6-0.7), good (0.7-0.8), very good (0.8-0.9) and excellent (0.9-1) (Yesilnacar 2005).

Table 5.4. Susceptibility classes for InfVal and FR models

Susceptibility class	Area (%)		Gully-validation set (%)		SCAI	
	InfVal	FR	InfVal	FR	InfVal	FR
Very low	6.33	10.36	0.38	1.22	16.75	8.46
Low	10.42	18.11	3.76	15.78	2.77	1.15
Moderate	17.20	16.12	15.74	12.87	1.09	1.25
High	29.89	25.74	26.12	25.67	1.14	1.00
Very high	36.16	29.67	54.01	44.46	0.67	0.67
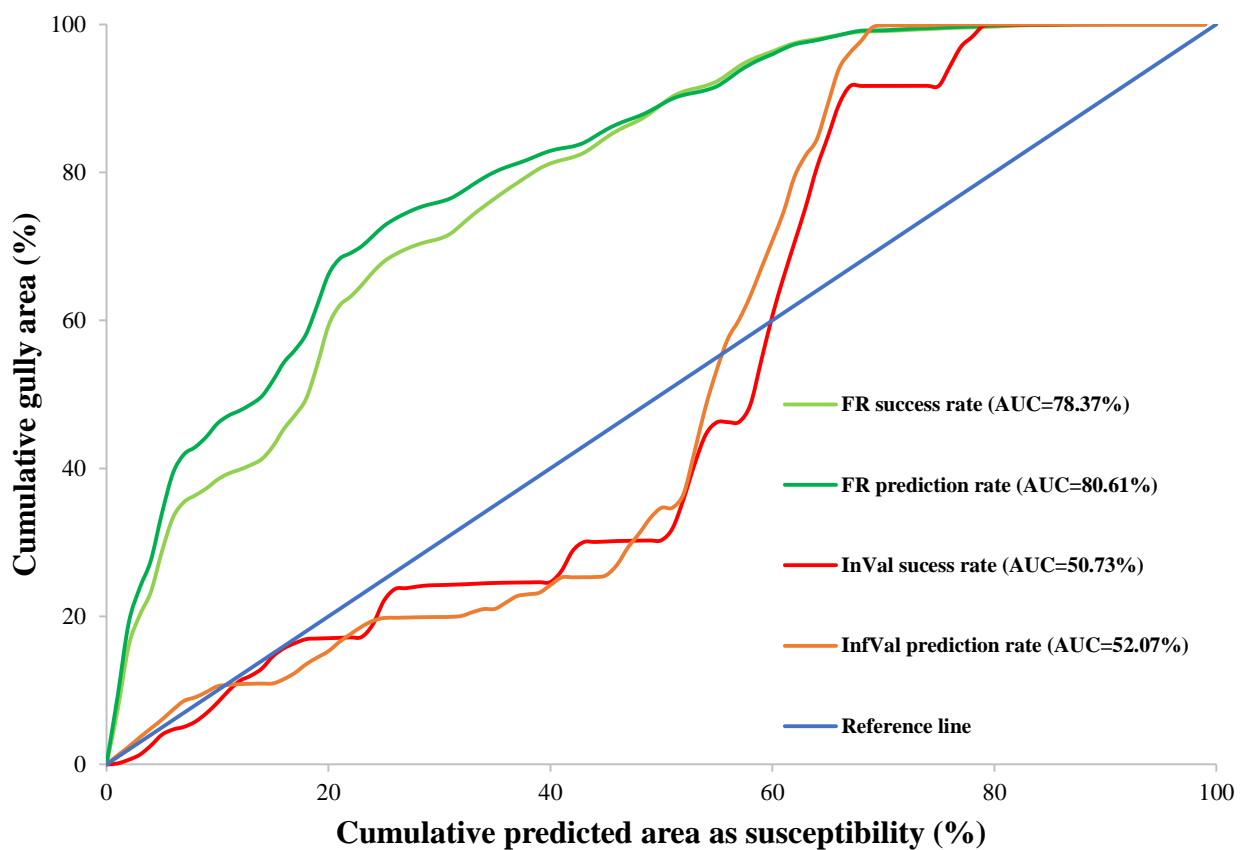
Figure 5.14. Representation of the accuracy of the susceptibility model used by prediction and success rates curves

ROC curve results and AUCs values (Figure 6.14) indicated that InfVal model was of poor prediction accuracy (AUC = 52.07%) and FR model was of very good prediction accuracy (AUC = 80.61%) for gully susceptibility mapping in the Ourika watershed. Therefore, it is observed that the gully susceptibility map produced by FR model exhibited better performance than the InfVal model in the study area (Figure 6.14).

The reliability of the gully susceptibility maps produced by the InfVal and FR methods was tested using SCAI. Results of SCAI values for the used the two methods are shown in Table 5.4. The results show that SCAI is high for very low and low classes and small for high and very high classes. In other words, SCAI is descending from very low class to very high class.

Table 5.5. Kappa statistics corresponding to the gully erosion susceptibility maps

	Susceptibility classes				
	Very low	Low	Moderate	High	Very high
Kappa	1.00	0.56	0.25	0.25	0.70
KLoc	1.00	0.76	0.37	0.26	0.97
KHisto	1.00	0.74	0.69	0.94	0.72

The results of the two models were compared using the kappa statistic of the Map Comparison Kit (Visser and Nijs 2006). The kappa statistic results from similarity of location (KLoc) and similarity of quantity (KHisto) (Hagen 2002): Kappa = KHisto * KLoc, where KHisto only depends on the total number of cells taken in by each category, and KLoc strictly depends on the spatial distribution of the categories on the map.

The results of the map comparison are presented in the Table 5.5. The results of the similarity between the two susceptibility maps revealed that Very low susceptibility class shows an excellent similarity (kappa = 1), Low and Very high classes show good similarity (Kappa = 0.56 and 0.70 respectively) whereas Moderate and High susceptibility classes show low similarity (Kappa = 0.25). In the Moderate and High gully erosion susceptibility classes, the similarity of location was low (0.37 and 0.26 respectively) whereas the similarity of quantity was high (0.69 and 0.94, respectively). The dissimilarity between the two susceptibility maps essentially depends on the spatial distribution of the susceptibility classes. This highlights differences between the results of the two models in the prediction of gully erosion susceptibility in the study area. These differences can be explained by the difference in the

nature of the models. In this study, the two models were compared based on their predictive accuracy. The area under the ROC curves (AUCs) proved that the frequency ratio model was better than the information value method in the prediction of gully erosion susceptibility in the study area (Figure 6.14).

4   Conclusion

Gully erosion is a serious environmental. In this study, we compare the performances of information value and frequency ratio models in gully susceptibility mapping in a watershed of the High Atlas of Morocco. The relationships between gullies and the predisposing factors (lithology, land use, slope gradient, LS, aspect, plan curvature, SPI, TWI) have been assessed using InfVal and FR models.

In this analysis, the most important predisposing factors in the gully erosion processes have been highlighted. It has been observed that barren and sparse vegetation lands were the most susceptible to gully erosion. The area of slope gradient above 50% is highly susceptible to gully erosion. Slope aspect, LS, SPI, and TWI factors have also a strong control on the susceptibility to gully erosion. The lithofacies effect on gully erosion was biased by its relationship with land use in the watershed. The ROC curve was used for testing the accuracy of the mentioned models. It confirms that the FR model (AUC = 80.61 %) shows a better prediction accuracy than InfVal model (AUC = 52.07 %).

Finally, the findings of the present research proved that GIS-based bivariate statistical methods such as frequency ratio model could be successfully used in gully susceptibility mapping in Morocco. The produced susceptibility map, using a low cost and low time-consuming methodology is a useful tool for sustainable land management. Frequency ratio model can be accurately used to assess gully erosion susceptibility in the Moroccan High Atlas, as well as in other regions of Morocco and in similar environmental conditions elsewhere.

General conclusion

1. Reminder of the thesis objectives

The overall goal of the thesis is to evaluate the risks of water erosion at the Moroccan scale using the RUSLE model, and particularly in the Ourika watershed area by means of rainfall simulations. Additionally, it includes the quantification and comparison of soil losses using both the RUSLE model and the ^{137}Cs radioactive marker.

The specific objectives assigned to this thesis include mapping of the risk of water erosion in Morocco using the RUSLE empirical model, GIS and remote sensing, the search for and identification of potential indicators of runoff and erosion risks in the Ourika watershed, and highlighting the relationship between these indicators. Thus, it involves quantifying the risk of water erosion by using ^{137}Cs and the RUSLE model, as well as mapping the susceptibility to gully erosion using GIS and bivariate statistical methods in the Ourika watershed. A comparison of the findings from these methods is subsequently performed. Finally, the effect of land use on water erosion was discussed.

2. RUSLE Model integrated with GIS and remote sensing

The application of the RUSLE model at the Moroccan scale shows that the average rate of soil loss in Morocco is 22.24 t/ha/year, with a standard deviation of 78.70 t/ha/year. At this scale, in the Moroccan context, 79.14% of the territory presents a low risk of erosion, 10.27% a moderate risk, 7.55% a high risk and 3.04% a very high risk. Similar results are obtained in the eastern and western Mediterranean, in regions with similar environmental and landscape conditions (Irvem et al. 2007; Efe et al. 2008; Panagopoulos and Ferreira 2010; Demirci and Karaburun 2012; Alexakis et al. 2013; Saygin et al. 2014; Farhan and Nawaiseh 2015). The average annual rate of soil loss obtained in Morocco is lower than that reported by other authors in various regions and watersheds in the country (Poesen and Lavee 1994; Merzouk et al. 1996; Ait Brahim et al. 2003; Al Karkouri 2003; Sadiki 2004; Moukhchane et al. 2005; Zouagui et al. 2012; Tribak et al. 2012; Khali Issa et al. 2014; Tahiri et al. 2014 ; Yjjou et al. 2014 ; Markhi et al. 2015 ; Khali Issa et al. 2016 ; Meliho et al. 2016).

The relationship between soil loss and the biogeographic regions of Morocco revealed that the highest average soil losses were obtained in the High Atlas, Rif, Middle Atlas and Anti-Atlas,

with average losses of 147.90, 100.23, 96.15 and 56.50 t/ha/year respectively. The higher average soil loss values obtained in these biogeographic regions are due to the strong correlation between soil loss and LS ($R^2 = 0.92$). The Saharan region of the country, the plains and plateaus of eastern Morocco and the Middle Atlantic region appear to be less vulnerable to water erosion as illustrated by their low LS values. The topographic factor has been the determining factor in the vulnerability of Morocco's biogeographical regions to water erosion. When taking into account the Tensift watershed, the average soil loss is 55.72 t/ha/year, with a standard deviation of 134.36 t/ha/year. In the Ourika watershed, the average soil loss is 171.60 t/ha/year, with a standard deviation of 189.83 t/ha/year.

In order to study the sensitivity of the RUSLE empirical model to the accuracy of the data, the model was applied to both the Tensift and Ourika watersheds with more precise data. In the Tesift basin, the erosivity factor of the rains was determined from the 17 stations (climatic and pluviometric). Land use mapping was done by remote sensing while the P factor was determined from the analysis of land occupations and slopes. The R and P factors are low in comparison with those obtained by taking into account national data. Thus, the average soil loss increased from 55.72 ± 134.36 t/ha/year to 44.03 ± 87.96 t/ha/year, due to variations in the R and P factors determined with more accurate data. In the Ourika watershed area, the R factor was determined from the rainfall data of 5 rainfall stations. Due to the absence of a soil map, the geological and land use maps were superimposed to identify homogeneous units. Soil samples were taken from these units (17 samples) and analyzed in the laboratory for the determination of the soil erodibility factor, K. The digital elevation model (DEM) resolution plays an important role in the accuracy of the result obtained for LS factor (Molnar and Julien 1998, Panagos et al., 2015). Although high-resolution DEMs are expensive, a 10m resolution DEM was used to determine the LS factor. The results show that the average soil loss increased from 171.60 ± 189.83 t/ha/year to 352.40 ± 342.60 t/ha/year, due to variations in the R, K and LS factors determined with more accurate data. This can be explained by the spatial resolution of the data that increased from 30 m at the national scale to 10 m at the Ourika watershed scale. DEMs are very practical in representing the variable topographic surface of the Earth. Advances in GIS allow calculation of the LS topographic factor at the watershed scale from DEMs (Hickey et al. 1994). The accuracy of the LS factor plays an important role in the accurate quantification of soil losses. Moreover, the accuracy of the DEM is very sensitive to the horizontal, vertical resolution and density of the sampling points as well as the altitude data source. The accuracy of LS is dependent on the accuracy of the DEM (Quinn et al. 1991; Zhang

and Montgomery 1994; Wang and Yin 1998; Thieken et al. 1999). The precise determination of K-factor by fieldwork and physico-chemical analyses in the laboratory yielded K = 0.56 ± 0.13 while a lower value of K was obtained from the global FAO soil map (K = 0.21 ± 0.04). This also affected the result of the model.

The most commonly cited limitation of the USLE / RUSLE models is their applicability to regions outside the United States. The USLE model was originally formulated based on soil erosion studies in the United States and, when applied to different climatic regimes and land-use conditions, may result in overestimation or an underestimate of the actual average annual loss (Kinnell 2010). For instance, the initial equation for soil erodibility is less accurate for soils with high clay content, sandy-loam soils and soils with high organic matter content (Stewart et al. 1975). Because model parameters were derived from agricultural field studies, there are uncertainties associated with the use of the model at the watershed or regional scale (Nagle et al. 1999; Naipal et al. 2015). Improvements and modifications to the model, particularly the LS factor, have made it applicable on larger scales, including coarse resolution on a global scale (Naipal et al. 2015). Uncertainties related to soil erosion modeling also arise from the low availability of reliable long-term data for modeling, a problem that is not unique to the application of the RUSLE model but especially more complex models requiring more data (de Vente & Poesen 2005; Hernandez et al. 2012). Its application in regions with scarce data leads to uncertainty regarding the actual amounts of soil loss and these applications have reported a vulnerability to erosion as a category (low to extreme) rather than actual annual averages (Adornado et al. al. 2009; Schmitt 2009). Another frequently cited limitation is that the RUSLE model is limited to estimating groundwater erosion without taking into account other forms of erosion such as gully erosion, landslides, etc. (Nagle et al. 1999; Wischmeier and Smith 1978). Additionally, the model does not consider sediment overestimation deposits (Desmet and Govers 1996; Wischmeier and Smith 1978). These limitations are related to the model's representation of more topographically complex terrain, and previous studies have attempted to address this by improving the LS factor through integrating the upstream contributory zone (Desmet and Govers 1996; Moore et al. 1991). Despite these drawbacks, the RUSLE model is still widely used because of its relative simplicity and low data requirements compared to more complex physical-based models (Aksoy and Kavvas 2005). Studies around the world continue to improve the parameterization and application of the model in different environments and at different scales.

3. Identification of risk indicators for runoff and erosion by rainfall simulations

The results of rainfall simulations in the Ourika watershed reveal that vegetation enhances the physical and surface properties of the soil by creating cavities. Indeed, it improves soil structure through the incorporation of organic matter, thus reducing bulk density, penetration resistance and shear strength. It also increases the porosity and roughness of the surface. On the other hand, tillage results in a rapid loss of organic matter, through either mineralization, erosion or aggregate destruction (Sabir et al. 2007). By improving the physical properties and surface condition of the soil, vegetation cover facilitates the infiltration of water into the soil, reducing the risk of runoff and erosion. Several authors have highlighted that vegetation cover is the most important factor in improving water infiltration into the soil and, consequently, to mitigate the risks of runoff (Roose 1996; Al Karkouri and al. 2000; Sabir et al. 2007; She et al. 2014, Liu et al. 2014).

In the Ourika watershed, total infiltration was negatively correlated with both the runoff coefficient (r = -0.99) and the resistance to penetration (r = -0.81). On the other hand, there was a positive correlation with the covered and open soil surfaces (r = 0, 84 and r = 0.83 respectively), thus confirming the importance of the vegetation cover in the mitigation the runoff and consequently the water erosion. Infiltration in the Ourika watershed is a function of the soil surface condition. Some authors (Sabir et al. 2007; Sabir et al. 2004; Al Karkouri et al. 2000) have observed similar results in different regions of Morocco. They found final infiltration being closely related to soil surface conditions. The runoff coefficient observed in this study ranges from 0 (dense forest) to 50.16% (open forest). These results are similar to the values obtained in the regions of the western Mediterranean (4.7 to 47.4%) (Martínez-Murillo et al. 2013). High runoff coefficients ranging from 25.35 (straw-covered soil) to 65.15% (bare soil) have been observed by other authors in Mediterranean vineyards (Prosdocimi et al., 2016).

Detachability is negatively correlated with soil cover (r = -0.81), with bare soils being the most sensitive to runoff and erosion. These findings confirm those obtained by Cheggour (2008) who reported an exponential relationship between turbidity and bare soil in the Rheraya basin.

Total infiltration is not correlated with the physical parameters of the soil. This could be explained by the small variations of these parameters in the study area. These results are in line with those obtained by other authors (Sabir et al. 2007; Sabir et al. 2004; Al Karkouri et al.

2000) who carried out similar infiltration tests, but on more developed soils of the central Rif region in Morocco. Their results showed that the total infiltration was not correlated with the physical parameters of the soil but rather with the surface condition of the soil.

The use of rain simulators offers several advantages including (Hudson 1993):

- Fastens the ability to take multiple measurements without waiting for natural rain.
- Ability to work with constant controlled rain, eliminating the erratic and unpredictable variability of natural rain.
- Simplicity and speed in simulator configuration compared to runoff plots.

The disadvantages are all related to the scale and include:

- It is simple and inexpensive to use a small simulator on a test plot of only a few square meters, but the simulators covering a plot of about 100 m² are bulky and expensive.
- Runoff and erosion measurements from simulator trials on small parcels cannot be extrapolated to field conditions. It is preferable to limit them to comparisons, such as the one of the three crop treatments that undergo the least erosion under the specific conditions of the simulator test, or the comparison of the relative erodibility values of different soil types.
- Simulators may be affected by wind, but mounting a windshield compromises the advantage of simplicity.

4. Quantification of water erosion using 137Cs

In the Ourika watershed, the Cs-137 study results reveal that on non-cultivated soils, ^{137}Cs inventory is significantly positively correlated with both soil organic carbon and soil organic carbon (SOC) stock, and negatively correlated with slope gradient and bulk density.

The net rate of soil erosion was higher under cereal croplands (8.5 t/ha/year) than in arboriculture (6.0 t/ha/year). In the Ourika watershed, arboriculture on terraces is more effective for soil protection against water erosion. Soil erosion is more marked on cereal terraces than on tree terraces due to the frequency of plowing. Indeed, trees protect the soil against erosion better than the annual cereal crops.

On uncultivated sites, net erosion rates along the transects were 5.3, 3.1 and 5.0 t/ha/year respectively. The low values obtained in uncultivated loam soils (5.3 t/ha/year) and uncultivated sandy soils (3.1 t/ha/year) can be explained by the presence of forest cover that protects soil against soil erosion. Previous studies have pointed out the effects of land use on soil erosion (Valentin et al 2005; Alejandro and Kenji 2007; Albergel et al. 2010). Forest vegetation is known to promote water infiltration and protect the soil from erosion. The low value obtained in the empty non-forest land can be explained by the high rate of pebbles in the soil (> 60%), which results in the loss of freshly deposited ^{137}Cs with precipitation by runoff. In other words, the net erosion rate is low due to the relatively low content fine soil particles in the soil matrix resulting from strong stoniness.

The difference between net soil erosion on cultivated and uncultivated sites (7.3 and 4.5 t/ha/year respectively) shows that despite the important role of terraces in reducing soil erosion in the mountain areas, untouched forest lands remain the best adapted in mitigating soil erosion in the Moroccan High Atlas region. Nevertheless, arboriculture reduces soil erosion better than cereal crops in the study area. The erosion rate observed on cultivated sites was relatively low compared to values obtained in other regions of Morocco. Despite its steep slopes, the Moroccan High Atlas is characterized by relatively low rate of erosion as opposed to the northern region of Morocco, with values ranging between 30 to 50 t/ha/year (Nouira et al. 2003). Damnati et al. 2013) and 11.9 t/ha/year (Benmansour et al. 2013). The low erosion rate observed with the ^{137}Cs method reveals the positive impact of traditional agricultural practices (terraces) practiced by farmers in the study area.

5. Mapping of susceptibility to gully erosion using GIS and bivariate statistics methods

The results of the application of bivariate statistical models in the Ourika watershed reveal that land use and slope are the main predisposing factors to gully erosion in the Ourika watershed. The sensitivity map was classified into five groups. For the information value model, the values corresponding to the watershed area obtained were 6.33%, 10.42%, 17.20%, 29.89% and 36.16% very low, low, moderate, high, and very high respectively for susceptibility to gully erosion. The upstream area of the Ourika watershed is subject to high to very high susceptibility to gully erosion. On the other hand, the values corresponding to the watershed area were

10.36%, 18.11%, 16.12%, 25.74%, and 29.67% for very low, low, moderate, high, and very high susceptibilities respectively using the frequency ratio model. For both models used, the area upstream of the watershed was highly vulnerable to gully erosion.

For the information value model, the area under the curve is 50.73 and 52.07% for success and prediction rates respectively. In contrast, success and prediction rates were 78.37 and 80.61%, respectively, for the frequency ratio model. The most accurate method for producing susceptibility to gully erosion maps in the Ourika watershed is the frequency ratio method because it presents both the largest area under the curve and the highest degree of accuracy (80.61 %).

The results of the similarity between the two susceptibility maps revealed that the very low susceptibility class shows excellent similarity (kappa = 1), the low and very high classes show good similarity (Kappa = 0.56 and 0.70 respectively), while moderate and high sensitivity classes show low similarity (Kappa = 0.25). In moderate and high erosion susceptibility classes, site similarity was low (0.37 and 0.26 respectively), while quantity similarity was high (0.69 and 0.94, respectively). The dissimilarity between the two susceptibility maps depends essentially on the spatial distribution of susceptibility classes. This highlights the differences between the results of the two models in predicting susceptibility to gully erosion in the study area. These differences can be explained by the different nature of the models. In this study, both models were compared according to their predictive accuracy.

6. RUSLE model and Cs-137 technique

The comparison between the RUSLE model and Cs-137 reveals that the values of the erosion rates estimated by the RUSLE model are very much higher than the rates estimated by the Cs-137. These results are in line with those obtained by other authors (Busacca et al. 1993; Alonso et al. 2012). The RUSLE model estimates potential erosion. Several authors have chosen to present their soil loss results categorically in order to produce maps indicating areas of low, medium or high vulnerability instead of indicating annual average quantities (Adornado et al. 2009; Schmitt 2009).). It is therefore recommended to interpret the results of the RUSLE model qualitatively more than quantitatively in the mountainous areas of Morocco, such as the High Atlas. Cs-137 makes for a better estimator compared with the RUSLE model. However, its use

is far too expensive to use on a large scale. By contrast, the RUSLE model makes it possible to identify areas most vulnerable to erosion on a large scale.

7. Land use and soil erosion: effect of terracing on erosion

The results of soil erosion show that despite the important role of agricultural terraces in reducing soil erosion, forests remain best suited in regards to reducing soil erosion in the High Atlas region of Morocco. However, arboriculture, in addition to its important socio-economic role, contributes to significantly reducing soil erosion.

The density of vegetation cover also plays an important role in reducing soil erosion. Thus, dense and moderately dense forests protect better the soil against erosion than clear forests or woodlands.

The extension of arboriculture on sloping terraces in the Ourika watershed plays an important role in the reduction of soil erosion. In addition to its environmental role of soil protection against erosion, arboriculture plays an important socio-economic role in the watershed and contributes to the fixing of the population in rural areas. The agricultural terraces studied constitute an interesting social and economic solution except that it would be better to manage them in an intelligent and sustainable way through arboriculture.

It may be concluded that terraces could considerably reduce soil loss due to water erosion if they are well planned, correctly constructed and properly maintained (FAO, 2000). There are many examples showing that terraces have to be maintained to prevent processes leading to land degradation such as excessive soil erosion, gully formation and landsliding. The most important aspect of terracing is that it has to be combined with additional soil conservation practices, of which the most important one is the maintenance of a permanent soil cover. This latter is especially needed on the foot slope of the terrace, because terraces themselves could be easily eroded and they generally require a lot of maintenance and repair. A very important point regarding terraces or any soil and water conservation practice is that most farmers are more concerned with production than with conservation. Therefore, the challenge is to develop conservation practices that are also productive. The ancient farming techniques such as terracing may provide a good basis for that, because far too often attempts have been made to modernize or improve farming practices without looking at existing well established practices first (Mountjoy and Gliessman, 1988). It has been shown by many researchers that terraces

could provide a basis for good farming that aims to keep fertile soil resources in place and in a good productive state.

8. Recommandations

The results of this study confirm the positive effects of vegetation cover, especially forested areas, on the protection and conservation of soils against water erosion. Based on them as well as the conclusions, the following approaches can be recommended for the Ourika watershed area:

- The results of the RUSLE model should be interpreted qualitatively and not quantitatively in the mountainous areas of Morocco, such as the High Atlas;
- Continuing the study of water erosion using ^{137}Cs by increasing the number of transects and samples in the watershed;
- Use of ^{7}Be on terraces to study short-term erosion and compare different water erosion control techniques used in the watershed;
- Reinforcing the role of plant cover, particularly woody vegetation, by rehabilitating existing forests in the basin, planting new stands in degraded areas and encouraging farmers to plant trees on their farms;
- Improving farming techniques by adopting more appropriate tillage practices and encouraging arboriculture on agricultural terraces.

Unique bibliographic list

Achhal A. (1986) Etude phytosociologique et dendrométrique des écosystèmes forestiers du bassin versant du N'fis (Haut Atlas central). Thèse Doct. és-Sc, Fac. St. Jérôme, Marseille, 204p + annexes.

Aderdar M. (2000) Espaces forestiers et aménagement des zones de montagne : le cas du Haut Atlas de Marrakech. Thèse, Institut de géographie alpine, université Joseph Fournier, Grenoble, 463p.

Adornado HA & Yoshida M (2010) Assessing the Adverse Impacts of Climate Change: A Case Study in the Philippines, J. Dev. Sus. Agr. 5, 141–146, 2010.

Ait Brahim L., Sossey Alaoui F., Siteri H. (2003) Quantification of soil loss in the Nakhla watershed (northern Rif). Sécheresse - Science et changements planétaires, Vol. 14 (2), 101-106.

Aksoy H. & Kavvas ML (2005) A review of hillslope and watershed scale erosion and sediment transport models, Catena, 64, 247– 271.

Al Karkouri J (2003) Dégradation du milieu naturel dans le bassin de Beni Boufrah (Rif Central -Maroc) : analyse des facteurs et des processus, essai de quantification et modélisation spatiale. Thèse doctorat d'Etat, Université Mohamed V, Rabat, faculté des lettres, Rabat.

Al Karkouri J, Laouina A, Roose E, Sabir M (2000) Capacité d'infiltration et risques d'érosion des sols dans la vallée des Beni boufrah- Rif central (Maroc). Bull Réseau Erosion. Montpellier : IRD, 20: 342-356.

Alifriqui M., Michalet R., Peltier J.P. & Peyre C (1993) Hétérogénéité des courants perturbés et répartition de la végétation sur les versants du Haut Atlas occidental marocain. Publication de l'Association Internationale de Climatologie, 5 : 203-211.

Albergel J, Collinet J, Zante P, Hamrouni H (2010) Le rôle de la forêt méditerranéenne dans la conservation de l'eau et du sol. What Science Can Tell Us, 1.5., 12p.

Alejandro M. and Kenji O (2007) Estimation of vegetation parameter for modeling soil erosion using linear Spectral Mixture Analysis of Landsat ETM data. Graduate School of Agricultural and Life Sciences, The University of Tokyo, Yayoi 1-1-1, Bunkyo-ku, Tokyo, 113-8657, Japan, 16p.

Alexakis D, Hadjimitsis D, Agapiou A (2013) Integrated use of remote sensing, GIS and precipitation data for the assessment of soil erosion rate in the catchment area of Yialias in Cyprus. Atmos Res 131:108-124.

Alonso J, Audicio P, Martinez L, Scavone M, Rezzano E (2012) Comparison of measured 137cs data and usle/ rusle simulated long-term erosion rates. Agrociencia Uruguay, Special Issue, 261-267.

Althuwaynee OF, Pradhan B, Park HJ, Lee JH (2014) A novel ensemble bivariate statistical evidential belief function with knowledge-based analytical hierarchy process and multivariate statistical logistic regression for landslide susceptibility mapping. Catena 114:21-36.

Angima SD, Stott DE, O'Neill MK, Ong CK, Weesies GA (2003) Soil erosion prediction using RUSLE for central Kenyan highland conditions. Agriculture, Ecosystems and Environment, 97 (1–3), pp. 295–308

Arnalds O, Þorarinsdottir EF, Metusalemsson S, Jonsson A, Gretarsson E, Arnason A (2001) Soil Erosion in Iceland. Soil Conservation Services and Agricultural Research Institute. Iceland.

Arnoldus H MJ (1980) Methodologie used to determine the maximum potentiel average soil loss due to sheet and rill erosion in Morrocco, Bulletin F.A.O., 34p.

Ayalew L, Yamagishi H (2005) The application of GIS-based logistic regression for landslide susceptibility mapping in the Kakuda- Yahiko Mountains, Central Japan. Geomorphology 65(1-2): 15-31.

Bai ZG, Dent DL, Olsson L, Schaepman ME (2008) Global assessment of land degradation and improvement. 1. Identification by remote sensing. Report 2008/01, ISRIC–World Soil Information, Wageningen. LADA technical Report no. 12.

Balaghi R, Jlibene M, Tychon B, Eerens H (2013) Agrometeorological Cereal Yield Forecasting in Morocco. INRA, Morocco. 157p. ISBN: 978 - 9954 - 0 - 6683 - 6.

Balteanu D, Chendes V, Sima M, Enciu P (2010) A countrywide spatial assessment of landslide susceptibility in Romania. Geophys J Roy Astron Soc 124:102-112.

Baskaran M., Coleman C.H., Santschi P.H. (1993). Atmospheric depositional fluxes of 7Be and 210Pb at Galveston and College Station, Texas, Journal of Geophysical Research, 98, 20555–20571.

Beasley DB, Huggins LF, Monke EJ (1980) A model for watershed planning. Tran ASAE 23:938–944

Bedhri M. (2000) Le réchauffement du climat Quels impacts sur le Maroc ?. Faculté des sciences juridiques et économiques Oujda, Maroc, 170p.

Benabid A, Fennane M (1994) Connaissances sur la végétation du Maroc : Phytogéographie, phytosociologie et séries de végétation. Lazaroa 14 : 21-97 (1994. 37.

Benabid A, Fennane M (1999) Principales formations forestières au Maroc in « Le Grand Livre de le Forêt Marocaine ». Mardaga éditeur. 26-144.

Benmansour M, Mabit L, Nouira A, Moussadek R, Bouksirate H, Duchemin M, Benkdad A (2013) Assessment of soil erosion and deposition rates in a Moroccan agricultural field using fallout 137Cs and 210Pbex. J. Environ. Radioact. 115, 97-106.

Benmansour M, Nouira A, Bouksirat H, Duchemin M, El Oumri M, Mossadek R, Benkdad A, Ibn Majah M (2011) Estimates of long and short-term rates of soil erosion using 137Cs, 210Pbex and 7Be measurements: case study of one agricultural field in semi-arid West Morocco. In: Impact of Soil Conservation Measures on Erosion Control and Soil Quality. IAEA-TECDOC-1665, pp. 159-174.

Benzer N (2010) Using the geographical information system and remote sensing techniques for soil erosion assessment. Pol J of Environ Stud 19(5):881-886.

Bini C, Gemignani S, Zilocchi L (2006) Effect of different land use on soil erosion in the pre-alpine fringe (North–East Italy): ion budget and sediment yield. Sci Total Environ 369:433-446.

Biron PE (1982) Le Permo-Trias de la région de l'Ourika (Haut- Atlas de Marrakech, Maroc). Thèse de 3ème Cycle, Université de Grenoble, 170 p.

Boggs G, Devonport C, Evans K, Puig P (2001) GIS-based rapid assessment of erosion risk in a small catchment in the wet/dry tropics of Australia. Land Degradation & Development 12: 417–434.

Boiffin J (1984) La dégradation structurale des couches superficielles du sol sous l'action des pluies. Thèse doct. Ing., Paris INA- PG : 320 p.

Boiffin J (1976) Histoire hydrique et stabilité structurale de la terre, Ann Agron. 274 : pp. 447-463.

Bonilla CA, Reyes JL, Magri A (2010) Water erosion prediction using the Revised Universal Soil Loss Equation (RUSLE) in a GIS framework, central Chile. Chilean Journal of Agricultural Research 70 (1), 159-169.

Bonn F (1998). La spatialisation des modèles d'érosion des sols à l'aide de la télédétection et des SIG: possibilités, erreurs et limites. Sécheresse, 9: 185-92.

Bontemps S, Defourny P, Bogaert EV, Arino O, Kalogirou V, Perez JR (2011) GLOBCOVER. Product s Description and Validation Report.

Bork HR, Li Y, Zhao Y, Zhang J and Shiquan Y (2001) Land Use Changes and Gully Development in the Upper Yangtze River Basin, SW-China. Journal of Mountain Science 19(2), 97-103.

Bou Kheir R, Wilson J, Deng Y (2007) Use of terrain variables for mapping gully erosion susceptibility in Lebanon. Earth Surf. Process. Landforms 32, 1770-1782.

Bou Kheir R, Abdallah C, Khawlie M (2008) Assessing soil erosion in Mediterranean karst landscapes of Lebanon using remote sensing and GIS. Eng. Geol. 99, 239-254.

Boudhar A, Duchemin B, Hanich L, Chaponnière A, Maisongrande P, Boulet G, Stitou J and Chehbouni A (2007) Analyse de la dynamique des surfaces enneigées du Haut Atlas Marocain à partir des données SPOT-VEGETATION. Sécheresse 18 (4): 278-88.

Bouhlassa S, Moukhchane M, Aiachi A (2000) Estimates of soil erosionand deposition of cultivated soil of Nakhla watershead, Morocco, using137Cs technique and calibration models. Acta Geol. Hisp. 35, 239–249.

Busacca AJ, Cook CA & Mulla D J (1993) Comparing landscape-scale estimation of soil erosion in the Palouse using Cs-137 and RUSLE. Journal of Soil & Water Conservation, 48(4), 361-367.

Cheggour A (2008) Mesures de l'érosion hydrique à différentes échelles spatiales dans un bassin versant montagneux semi-aride et spatialisation par des S.I.G. : Application au bassin versant de la Rhéraya, Haut Atlas, Maroc. Thèse de doctorat, Université Cadi Ayyad faculté des sciences Semlalia – Marrakech, 209p.

Chung CF, Fabbri AG (2003) Validation of spatial prediction models for landslide hazard mapping. Nat Hazards 30:451-472.

Comité national MAB (1990) Rapport national marocain. Séminaire méditerranéen sur l'aménagement intégré des bassins-versants, 67 p.

Conforti M, Aucelli PPC, Robustelli G, Scarciglia F (2010) Geomorphology and GIS analysis for mapping gully erosion susceptibility in the Turbolo stream catchment (Northern Calabria, Italy). Nat. Hazard. 56, 881-898.

Conoscenti C, Angileri S, Cappadonia C, Rotigliano E , Agnesi V, Märker M (2014) Gully erosion susceptibility assessment by means of GIS-based logistic regression: A case of Sicily (Italy). Geomorphology 204 (2014) 399-411.

Conoscenti C, Di Maggio C, Rotigliano E (2008) Soil erosion susceptibility assessment and validation using a geostatistical multivariate approach: a test in Southern Sicily. Nat Hazards 46:287-305.

Dabral PP, Baithuri N, Pandey A (2008) Soil erosion assessment in a hilly catchment of North Eastern India using USLE, GIS and remote sensing. Water Resources Management 22, 1783-1798.

Damnati B, Sanaa I, Radakovitch O (2013) Quantifying erosion using 137Cs and 210Pb in cultivated soils in three Mediterranean watershed: synthesis study from El Hachef, Raouz and Nakhla (North West Morocco). J. Afr. Earth Sci. 79, 50-57.

De Graaf J (1996) Price of soil erosion: an economic evaluation of soil conservation and watershed development, Landbouwuniversiteit Wageningen (LUW), Wageningen, 300 pp.

de Vente J & Poesen J (2005) Predicting soil erosion and sediment yield at the basin scale: Scale issues and semi-quantitative models, Earth Sci. Rev., 71, 95–125.

Del Mar López T, Mitchel Aide T, Scatena FN (1998) The effect of land use on soil erosion in the Guadiana watershed in Puerto Rico. Caribbean Journal of Science, 34: 298–307.

Demirci A, Karaburun A (2012) Estimation of soil erosion using RUSLE in a GIS framework: a case study in the Buyukcekmece lake watershed, northwest Turkey. Environ Earth Sci 66:903-913.

Dercon G, Mabit L, Hancock G, Nguyen ML, Dornhofer P, Bacchi OOS, Benmansour M, Bernard C, Froehlich W, Golosov VN, Haciyakupoglu S, Hai PS, Klik A, Li Y, Lobb DA, Onda Y, Popa N, Rafiq M, Ritchie JC, Schuller P, Shakhashiro A, Wallbrink P, Walling DE, Zapata F, Zhang X (2012) Fallout radionuclide-based techniques for assessing the impact of soil conservation measures on erosion control and soil quality: an overview of the main lessons learnt under an FAO/IAEA Coordinated Research Project. J. Environ. Radioactiv. 107:78-85.

Desmet P JJ, Govers G (1996) A GIS-procedure for automatically calculating the USLE LS-factor on topographically complex landscape units. Journal of Soil and Water Conservation, v. 51, n. 5, p. 427-433.

Efe R, Ekinci D, Curebal I (2008) Erosion analysis of Sahin Creek watershed (NW of Turkey) using GIS based on Rusle (3d) method. J Appl Sci 8:49-58.

El Qayedy J. (2008) Apport de la télédétection et du système d'information géographique dans la caractérisation et l'identification des zones de susceptibilité à l'érosion hydrique dans le Haut Atlas de Marrakech, 145p.

Elbouqdaou K, Ezzine H, Badrahou M, Rouchdi M, Zahraoui M. and Ozer A (2005) Approche méthodologique par télédétection et SIG de l'évaluation du risque potentiel d'érosion hydrique dans le bassin versant de l'Oued Srou (Moyen Atlas, Maroc), Geo-Eco-Trop, 29, 25-36.

Elirehema YS (2001) Soil water erosion modeling in selected watersheds in Southern Spain. IFA, ITC, Enschede.

Ellison W D (1944) Studies of raindrop erosion. Agricultural Engineering, 25:131-136, 181-182.

Elwell HA (1978) Soil loss estimation: compiled works of the Rhodesian multi-disciplinary team on soil loss estimation. Institute of Agricultural Engineers, Salisbury, Zimbabwe.

Erskine W (2005) Gully erosion. In: Lehr, J., Keeley, J. (Eds.), Water Encyclopaedia: Surface and Agricultural Water. Wiley-Interscience, Hoboken, pp. 183-188.

FAO (2000) Manual on integrated soil management and conservation practices. FAO Land and Water Bulletin 8, Rome, Italy: 230 pp.

FAO (1990) Conservation des sols et des eaux dans les zones semi-arides. Bulletin pédologique 57: 182 p.

FAO, UNEP & UNESCO (1979) A provisional methodology for soil degradation assessment, Rome

Farhan Y and Nawaiseh S (2015) Spatial Assessment of Soil Erosion Risk Using RUSLE and GIS Techniques. Environmental Earth Sciences, 74, 4649-4669.

Fernandez LM, Nunez MM (2011) An empirical approach to estimate soil erosion risk in Spain. Sci Total Environ. 409:3114–3123.

Flanagan D (2002) Erosion Encyclopedia of Soil Science, 1st ed.; Marcel Dekker: New York, NY, USA; pp. 395–398.

Foster GR, Yoder DC, Weesies GA, McCool DK, McGregor KC, Binger RL (2002) RUSLE2 User's guide, USDA-Agricultural Research Service, Washington, pp 1–76.

Gaspar L & Navas A (2013) Vertical and lateral distributions of 137 Cs in cultivated and uncultivated soils on Mediterranean hillslopes. Geoderma, 207, 131-143.

Gerits JJP, De Lima JLMP, Van Den Broek TMW (1990) Overland flow and erosion, in Process Studies in Hillslope Hydrology, édité par M.G. Anderson et T.P. Burt, 173-214, John Wiley & Sons Ltd, Angleterre. in Lajili, 1999.

Ghanam M (2003) La désertification au Maroc- Quelle stratégie de lutte ? Second FIG Regional Conference Marrakech, Morocco, December 2-5, 2003.

Gimenez R & Govers G (2002) Flow detachment by concentrated flow on smooth and irregular beds. Soil Science Society of America Journal, 66:1475–1483.

Goldman SJ, Jackson K, Bursztynsky TA (1986) Erosion and Sediment Control Handbook. McGraw-Hill, New York, NY.

Gómez Gutiérrez A, Schnabel S, Felicísimo AM (2009) Modelling the occurrence of gullies in rangelands of southwest Spain. Earth Surf. Process. Landforms 34, 1894-1902.

Goswami R, Mitchell N, Brocklehurst S (2011) Distribution and causes of landslides in the eastern Peloritani of NE Sicily and western Aspromonte of SW Calabria, Italy. Geophys J Roy Astron Soc 132:111-122.

Gourfi A., Daoudi L. & Shi Z. (2018) The assessment of soil erosion risk, sediment yield and their controlling factors on a large scale: Example of Morocco. Journal of African Earth Sciences, 147, 281–299.

Govers G, Quine TA, Desmet PJJ & Walling DE (1996) The relative contribution of soil tillage and overland flow erosion to soil redistribution on agricultural land. Earth Surface Processes & Landforms, 21, 929–946.

Hammi S., Simonneaux V., Alifriqui M., Auclair L., Montes N. (2007) Évolution des recouvrements forestiers et de l'occupation des sols entre 1964 et 2002 dans la haute vallée des Ait Bouguemez (Haut Atlas central, Maroc) Impact des modes de gestion. Sécheresse vol. 18, n° 4.

Hernandez EC, Henderson A, Oliver DP (2012) Effects of changing land use in the Pagsanjan-Lumban catchment on suspended sediment loads to Laguna de Bay, Philippines, Agric. Water Manag., 106, 8–16.

Hickey, R., A. Smith and P. Jankowski (1994) Slope Length Calculations from a DEM within Arc/Info GRID, Computing, Environment and Urban Systems, Vol. 18, No. 5, pp. 365-380.

Hjulström F (1935) Studies of the morphological activity of rivers as illlustrated by the river Fyris. Bulletin of the Geological Institute, University of Uppsala, 25: 221-527.

Hoyos N (2005) Spatial modeling of soil erosion potential in a tropical watershed of the Colombian Andes. CATENA 63 (1), 85-108.

Hudson N (1981) Soil Conservation. Second Edition. Comell University Press, Ithaca, New York.

Hagen A (2002) Multi-method assessment of map similarity. Paper presented at the 5th AGILE Conference on Geographic Information Science, Palma, Spain.

Haut-Commissariat aux Eaux et Forêt et à la Lutte contre la Désertification (2012). Désertification. www.eauxetforets.gov.ma.

Hoyos N (2005) Spatial modeling of soil erosion potential in a tropical watershed of the Colombian Andes. CATENA 63 (1), 85-108.

Hudson NW (1993) Field Measurement of Soil Erosion and Runoff. FAO Soils Bulletin No. 68. FAO, Rome, pp. 139.

Ibrahimi S (2005) Application du 210Pbexe comme une alternative à l'utilisation du 137Cs pour l'étude de la redistribution du sol sur des transects cultivés et non cultivés, Bassins versants El Hachef et Raouz, nord du Maroc, Thèse de doctorat en Sciences, Université Abdelmalek Essaadi, Tanger, Maroc.

IAEA (International Atomic Energy Agency) (2014) Guidelines for Using Fallout Radionuclides to Assess Erosion and Effectiveness of Soil Conservation Strategies. IAEA-TECDOC-1741. IAEA publication, Vienna, Austria, p. 213.

ICONA (1997) Guidelines for mapping and measurement of rainfall-induced erosion processes in the Mediterranean coastal areas. Priority Action Programme Regional Activity Centre, Split, Croatia.

Irvem A, Topaloglu F, Uyagur V (2007) Estimating spatial distribution of soil loss over Seyhan river basin in Turkey. J Hydrol 336:30-37.

Jasrotia AS & Singh R (2006) Modeling runoff and soil erosion in a watershed , using the GIS, in the Himalayan region, India. Environmental Geology 51, 29-37.

Jensen JR (2000) Remote sensing of the environment: An earth resource perspective, published as 1st ed. Upper Saddel River, New Jersey: Prentice Hall, Inc.

Johnson YW (1943) Distribution graphs of suspended-matter concentration. Tran ASCE 108:941–964.

Kalman R. (1967) Le facteur climatique de l'érosion dans le bassin de Sebou. Projet Sebou, Rapp. Ronéo, 40p.

Karydas CG, Sekuloska T, Silleos GN (2009) Quantification and site-specification of the support practice factor when mapping soil erosion risk associated with olive plantations in the Mediterranean island of Crete. Environmental Monitoring and Assessment 149, 19-28.

Kefi M, Yoshino K, Setiawan Y, Zayani K, Boufaroua M (2010) Assessment of the effects of vegetation on soil erosion risk by water: a case of study of the Batta watershed in Tunisia. Environ Earth Sci (2011) 64:707–719.

Khali Issa L., Ben Hamman Lech-Hab K., Raissouni A. (2016) Cartographie Quantitative du Risque d'Erosion des Sols par Approche SIG/USLE au Niveau du Bassin Versant Kalaya (Maroc Nord Occidental), J. Mater. Environ. Sci. 7 (8): 2778-2795.

Khali Issa L., Raïssouni A., El Arrim A. (2014) Mapping and Assessment of Water Erosion in the Khmiss Watershed (North Western Rif, Morocco), CAES, 24 (2014) 119-130.

Kinnell PI A 2010) Event soil loss, runoff and the Universal Soil Loss Equation family of models: A review, J. Hydrol., 385, 384–397.

Kirkby MJ, Jones RJA, Irvine B, Gobin A, Govers G, Cerdan O, Van Rompaey AJJ, Le Bissonnais Y, Daroussin J, King D, Montanarella L, Grimm M, Vieillefont V, Puigdefabregas J, Boer M, Kosmas C, Yassoglou N, Tsara M, Mantel S, Van Lynden GJ, Huting J (2004) Pan-European soil erosion risk assessment: the PESERA map, Publication Ispra 2004 No. 73 (S.P.I.04.73).

Knisel WG (1980) CREAMS: a field scale model for chemicals, runoff and erosion from agricultural management systems. Conservation Research Rep. No. 26, U.S. Dept. of Agriculture.

Kocyigit R and Demirci S (2012) Long-term changes of aggregate associated and labile soil organic carbon and nitrogen after conversion from forest to grassland and cropland in northern Turkey, Land Degrad. Dev., 23, 475–482.

Kouli M, Soupios P, Vallianatos F (2009) Soil erosion prediction using the Revised Universal Soil Loss Equation (RUSLE) in a GIS framework, Chania, Northwestern Crete, Greece. Environ. Geol. 57, 483-497.

Krishna Bahadur KC (2009) Mapping soil erosion susceptibility using remote sensing and GIS: A case of the Upper Nam Wa Watershed,Nan Province Thailand. Environmental Geology, 57, 695-705.

Lajili L (1999) L'érosion hydrique en zone semi-aride tunisienne : modélisation, estimation des paramètres et application à l'aménagement anti-érosif. Thèse de doctorat, universteit GENT, 215p.

Lal, R (Ed.) (2006) Encyclopedia of Soil Science, second ed. CRC Press, p. 2060.

Lal R (2001) Soil degradation by erosion. Land Degrad Dev 12:519-539.

LAL R (2000) Soil management in the developing countries. Soil Science (165), 57–72.

Lal R (1988) Soil degradation and the future of agriculture in sub-Saharan Africa, J. Soil Water Conserv., 43, 444–451.

Lal R (1998) Soil erosion impact on agronomic productivity and environment quality: critical reviews. Plant Sci 17:319–464.

Laouina A (2010) Conservation des eaux et des sols au Maroc, la prise en compte de la diversité géographique. Norois (214) : 85-99.

Le Bissonnais Y, Cerdan O, Lecomte V, Benkhadra H, Souchère V, Martin P (2005) Variability of soil surface characteristics influencing runoff and interrill erosion. Catena 62, 111–124.

Le Bissonnais Y, Le Souder C (1995) Mesurer la stabilité structurale des sols pour évaluer leur sensibilité à la battance et à 1'érosion. Etude et gestion de sols, 2, 1. pp: 43-56.

Lee S, Pradhan B (2006) Probabilistic landslide hazard and risk mapping on Penang Island, Malaysia. J Earth Syst Sci 115:661-672.

Lee S (2004) Soil erosion assessment and its verification using the universal soil loss equation and geographic information system: a case study at Boun, Korea. Environ Geol 45:457-465.

Lee S (2005) Application of logistic regression model and its validation for landslide susceptibility mapping using GIS and remote sensing data.Int J Remote Sens 7:1477-1491.

Legesse D, Vallet-Coulomb D, Gasse F (2003) Hydrological Response of a Catchment to Climate and Land use Changes in Tropical Africa: Case Study South Central Ethiopia, J. Hydrol., 275, 67–85.

Leguedois S, Planchon O, Legout C, Le Bissonnais Y (2005) Splash projection distance for aggregated soils: theory and experiment, Soil Science Society of America Journal, 69, 30–37.

Leguedois S (2003) Mécanismes de l'érosion diffuse des sols : modélisation du transfert et de l'évolution granulométrique des fragments de terre érodés. Thèse Université Orléans. INRA. 167p.

Lin C, Zhou SL, Wu SH, Liao FQ (2012) Relationships between intensity gradation and evolution of soil erosion: a case study of Changting in Fujian Province, China. Pedosphere 22:243–253.

Liu, R., Wang, J., Shi, J., Chen, Y., Sun, C., Zhang, P., & Shen, Z. (2014) Runoff characteristics and nutrient loss mechanism from plain farmland under simulated rainfall conditions. Science of the total environment, 468, 1069-1077.

Laflen JM & Roose E (1997) Methodologies for assessment of soil degradation due water erosion. CRC Press LLC, USA, p 85.

Laouina A, Coelho C, Ritsema C, Chaker M, Nafaa R, Fenjiro I (2004) Dynamique de l'eau et gestion des terres dans le contexte du changement global, dans le bassin du Bouregreg (Maroc). Sécheresse 15 (1): 65-77.

Loch RJ, Silburn DM (1996) Constraints to sustainability - soil erosion. In: Clarke, L., Wylie, P.B. (Eds.), Sustainable Crop Production in the Sub-tropics: an Australian Perspective. QDPI.

Lu D, Li G, Valladares GS, Batistella, M (2004) Mapping soil erosion risk in Rondonia, Brazilian Amazonia: using RUSLE, remote sensing and GIS. Land Degradation and Development 15, 499-512.

Lucà F, Conforti M, Robustelli G (2011) Comparison of GIS-based gullying susceptibility mapping using bivariate and multivariate statistics: Northern Calabria, South Italy. Geomorphology 134, 297-308.

Mabit L, Benmansour M, Walling DE (2008) Comparative advantages and limitations of fallout radionuclides (137Cs, 210Pb and 7Be) to assess soil erosion and sedimentation. Journal of Environmental Radioactivity 99 (12), 1799-1807.

Mabit L, Laverdière MR, Bernard C (2002) L'érosion hydrique : méthodes et études de cas dans le Nord de la France. Cahiers d'études et de recherches francophones / Agricultures. Volume 11, Numéro 3, 195-206.

Markhi A, Laftouhi N, Soulaimani A, Fniguire F (2015) Quantification et évaluation de l'érosion hydrique en utilisant le modèle RUSLE et déposition intégrés dans un SIG. Application dans le bassin versant n'fis dans le haut atlas de Marrakech (Maroc). European Scientific Journal October 2015 edition vol.11, No.29.

Martinez C, Hancock GR, Kalma JD (2010) Relationships between 137Cs and soil organic carbon (SOC) in cultivated and never-cultivated soils, an Australian example. Geoderma 158, 137–147.

Martinez-Casasnovas JA, Anton-Fernandez C, Ramos MC (2003) Sediment production in large gullies of the Mediterranean area (NE Spain) from high resolution digital elevation models and geographical information systems analysis. Earth Surface Processes and Landforms 28 (5), 443- 456.

Martínez-Murillo JF, Nadal-Romero E, Regüés D, Cerdà A & Poesen J (2013) Soil erosion and hydrology of the western Mediterranean badlands throughout rainfall simulation experiments: a review. Catena, 106, 101-112.

Maselli D (1993) Contribution à l'étude de la pluviométrie du Haut Atlas occidental au Maroc : répercussions sur l'environnement et l'exploitation agricole. Publication de l'Assoc. Internationale de Climatologie, 6 :315-323.

Mateh (1998) Déclaration du ministre de l'aménagement du territoire de l'environnement et de l'habitat. Le matin du Sahara et du Maghreb, 19 Novembre 1998.

McCool DK, Brown LC, Foster GR (1987) Revised slope steepness factor for the Universal Soil Loss Equation. Transactions of the ASAE, v. 30, n. 5, p. 1387-1396.

Meliho M, Khattabi A, Mhammdi N, Sabir Mohamed (2017) Effects of land use and cover type on the risks of runoff and water erosion: infiltration tests in the Ourika watershed (High Atlas, Morocco). Euro-Mediterranean Journal for Environmental Integration, 3(1), 8.

Meliho M, Khattabi A, Mhammdi N, Hongming Z (2016) Impact of Land Use and Vegetation Cover on Risks of Erosion in the Ourika Watershed (Morocco). American Journal of Engineering Research, pp-75-82.

Meliho M, Khattabi A, Mhammdi N, Hongming Z (2016) Cartographie Des Risques De L'erosion Hydrique Par L'equation Universelle Revisee Des Pertes En Sols, La Teledetection Et Les Sig Dans Le Bassin Versant De L'ourika (Haut Atlas, Morocco). European Scientific Journal November 2016 edition vol.12, pp: 227-297.

Meliho M, Khattabi A, Zine El Abidine A (2016) Etude de la sensibilité à l'érosion hydrique dans le bassin versant d'Ourika (Haut Atlas, Maroc). 1st AMRS Congress and 23rd APDR Congress 'Sustainability of Territories in the Context of Global Changes', pp: 189-196.

Meliho M (2015) Formations forestières et préforestières du bassin versant de Tensift : Potentialités écologiques, état actuel, facteurs de changement et vulnérabilité aux changements climatiques. Mémoire 3ème cycle, ENFI, 177p.

Meriaux S (1954) Contribution à l'étude de la granulométrie. Thèse d'État, Paris, 118 p.

Merritt WS, Letcher RA, Jakeman AJ (2003) A review of erosion and sediment transport models, Environ. Model Softw., 18, 761–799.

Merzouk A and Dahman H (1998) Shilling land use and impact on sediment yield in the Rif Mountains. In advanced in geoecologique, 31, by CATENA VERLAG, 350447, Reiskirche, 1998.

Millward AA, Mersey JE (1999) Adapting the RUSLE to model soil erosion potential in a mountainous tropical watershed. CATENA 38 (2), 109-129.

Molnar D, Julien P (1998) Estimation of upland erosion using GIS. Comput. Geosci. 1998, 24, 183–192.

Montes N (1999) Potentialités, dynamique et gestion d'une formation arborée à genévrier thurifère (Juniperus thurifera L.) des atlas marocains : le cas de la vallée de l'Azzaden. Thèse de doctorat, Université Paul Sabatier de Toulouse, 213p.

Moore ID, Grayson RB, and Ladson AR (1991) Digital terrain modelling: A review of hydrological, geomorphological and biological applications. Hydrological Processes, 5, 3-30.

Moore ID, Burch GJ (1986) Physical basis of the length-slope factor in the universal soil loss equation. Soil Sci Soc Am J 50:1294 -1298.

Morgan RPC, Quinton JN, Smith RE, Govers G, Poesen JWA, Auerswald K, Chisci G, Torri D, Styczen ME (1998) The European Soil Erosion Model (EUROSEM): a process-based approach for predicting sediment transport from fields and small catchments. Earth Surf Process Landf 23:527–544.

Morgan RPC (1995) Soil Erosion and Consewation. Essex, United Kingdom: Longman.

Moukhchane M., Bouhlassa S., Ahmed Chalouan A. (2005) Détermination des zones vulnérables à l'érosion par la méthode magnétique. Application au bassin versant d'El Hachef (région de Tanger, Maroc). Revista de la Sociedad Geologica de Espana, 18 (3-4), 225-233.

Musgrave GW (1947) The quantitative evaluation of factors in water erosion: a first approximation. J Soil Water Conserv 2:133–138.

Nafaa R (1997) Dynamique du Milieu Naturel de la Mamora et ses bordures, Paléoenvironnements et Dynamique Actuelle. Thèse du Doctorat d'Etat ès Lettres, FLSH., Rabat. 275p.

Nachtergaele J (2001) A Spatial and Temporal Analysis of the Characteristics, Importance and Prediction of Ephemeral Gully Erosion. Unpubl. PhD thesis, Department of Geography-Geology, K.U. Leuven, 255 pp.

Nagle GN, Fahey TJ, Lassoie JP (1999) Management of sedimentation in tropical watersheds, Environ. Manage. 23, 441– 452.

Naipal V, Reick C, Pongratz J, Van Oost K (2015) Improving the global applicability of the RUSLE model – adjustment of the topographical and rainfall erosivity factors, Geosci. Model Dev., 8, 2893–2913.

Nanna, S (1996) A geo-information theoretical approach to inductive erosion modelling based on terrain mapping units. PhD, Wageningen Agricultural University, Wageningen.

Navas A, Walling DE, Quine T, Machin J, Soto J, Domenech S and Lopez-Vicente M (2007) Variability in Cs-137 inventories and potential climatic and lithological controls in the

central Ebro valley, Spain. Journal of Radioanalytical and Nuclear Chemistry, Vol. 274, No.2, pp. 331–339.

Navas A & Walling DE (1992) Using caesium-137 to assess sediment movement on slopes in a semi-arid upland environment in Spain. In: Erosion, Debris Flows and Environnment in Mountain Regions, IAHS Publ. nº. 209, 129-138.

Nearing MA, Foster GR, Lane LJ, Finkner SC (1989) A process based soil erosion model for USDA-water erosion prediction project technology. Tran ASAE 32:1587–1593.

Nouira A, Sayouty EH, Benmansour M (2003) Use of 137Cs technique for soil erosion study in the agricultural region of Casablanca in Morocco. J. Environ. Radioact. 68, 11-26.

Ouhammou A (1986) Recherche sur l'étagement de la végétation dans le versant de l'oued Ourika (Haut Atlas Central, Maroc). Th. 3e cycle. Univ. Cadi Ayyad, Fac. Sci. Marrakech: 181p.

Owens, P.N., Walling, D.E., 1996. Spatial variability of caesium-137 inventories at reference sites: an example from two contrasting sites in England and Zimbabwe. Applied Radiation and Isotopes 47, 699-707.

Panagopoulos T, Ferreira V (2010) Erosion risk map of a Foupana River Watershed in Algarve, Portugal. Trans Environ Dev 6:635-644.

Panagos P, Borrelli P, Meusburger K (2015) A new European slope length and steepness factor (LS-Factor) for modeling soil erosion by water. Geosciences 5, 117–126.

Pandey A, Mathur A, Mishra SK, Mal BC (2009) Soil erosion modeling of a Himalayan watershed using RS and GIS. Environmental Earth Sciences 59 (2), 399-410.

Pandey A, Chowdary VM, Mal BC (2007) Identification of critical erosion prone areas in the small agricultural watershed using USLE, GIS and remote sensing. Water Resour Manag 21:729-746.

Pardeshi SD, Autade SE and Pardeshi SS (2013) Landslide hazard assessment: recent trends and techniques. SpringerPlus, 2(1), 523.

Pereira S, Zezere J, Bateira C (2012) Assessing predictive capacity and conditional independence of landslide predisposing factors for shallow landslide susceptibility models. Nat Hazards Earth Syst Sci 12:979-988.

Pike R, Evans I and Hengl T (2009) Geomorphometry: a brief guide, Geomorphometry: concepts, software, applications, 33, 3-30.

Pimentel D, Harvey C, Resosudarmo P, Sinclair K, Kurz D, McNair M., Crist S, Shpritz L, Fitton L, Saffouri R, Blair R (1995) Environmental and economic costs of soil erosion and conservation benefits. Science 267: 1117– 1123.

Poesen J, Vandaele K, van Wesemael B, (1996) Contribution of gully erosion to sediment production incultivated lands and rangelands. IAHS Publications 236, 251 - 266.

Pradhan B, Lee S (2010) Delineation of landslide hazard areas on Penang Island, Malaysia, by using frequency ratio, logistic regression, and artificial neural network models. Environ Earth Sci 60:1037-1054.

Prasannakumar V, Shiny R, Geetha N, Vijith H (2011) Spatial prediction of soil erosion risk by Remote Sensing, GIS and RUSLE approach: a case study of Siruvani River Watershed in Attapady Valley, Kerala, India. Environ Earth Sci 46:965-972.

Prasannakumar V, Vijith H, Abinod S, Geetha N (2012) Estimation of soil erosion risk within a small mountainous sub-watershed in Kerala, India, using revised universal soil loss equation (RUSLE) and geo-information technology. Geosci Front 3:209-215.

Prosdocimi, M., Jordán, A., Tarolli, P., Keesstra, S., Novara, A., & Cerdà, A. (2016) The immediate effectiveness of barley straw mulch in reducing soil erodibility and surface runoff generation in Mediterranean vineyards. Science of the Total Environment, 547, 323-330.

Prosser IP, Young WJ, Rustomji P, Hughes AO, Moran CJ (2001) A model of river sediment budgets as an element of river health assessment. In: Proceedings of the international congress on modelling and simulation (MODSIM'2001), pp 861–866.

Quine TA, Navas A, Walling DE, & Machin J (1994) Soil erosion and redistribution on cultivated and uncultivated land near Las Bardenas in the central Ebro river basin, Spain. Land Degradation & Development, 5(1), 41-55.

Quinn P, Beven K, Chevallier P, Planchon O (1991) The prediction of hillslope flow paths for distributed hydrological modelling using digital terrain models. Hydrol. Proc. 5, 59–79.

Rabesiranana N, Rasolonirina M, Solonjara AF, Ravoson HN, Andriambololona R & Mabit L (2016) Assessment of soil redistribution rates by 137 Cs and 210 Pb ex in a typical Malagasy agricultural field. Journal of environmental radioactivity, 152, 112-118.

Rahhou M (1999) L'érosion dans le Prérif central, zone interfluviale Leben-Sebou-Ouergha, un prolongement de l'évolution naturelle, une production sociale, Thèse doctorat d'Etat, Université Mohammed V, Rabat, 300p.

Rahmati1 O, Haghizadeh A, Pourghasemi HR, Noormohamadi F (2016) Gully erosion susceptibility mapping: the role of GIS based bivariate statistical models and their comparison. Nat Hazards 82: 1231.

Rahmati O, Pourghasemi HR, Zeinivand H (2015) Flood susceptibility mapping using frequency ratio and weights-of-evidence models in the Golastan Province, Iran. Geocarto Int.

Rango A, Arnoldus HMJ (1987) Aménagement des bassins versants. In : Cahiers techniques de la FAO : 1-11.

Remini W, Remini B (2003) La sédimentation dans les barrages de l'Afrique du nord. Éditeur: Larhyss Journal, Algérie. pp. 45-54.

Renard KG, Foster GR, Weesies GA, McCool DK, Yoder DC (1997) Predicting soil erosion by water: a guide to conservation planning with the Revised Universal Soil Loss Equation (RUSLE). United States Department of Agriculture, Agricultural Research Service (USDA-ARS) Handbook No. 703, pp 404.

Renard KG, Laursen EM (1975) Dynamic behavior model of ephemeral streams. J Hydrol Div 101:511–526.

Rendon-Herrero O (1978) Unit sediment graph. Water Resour Res 14:889–901

Riezebos H T and Loerts A C (1998) Influence of Land use change and tillage practice on soil organic matter in southern Brazil and eastern Paraguay, Soil Till. Res., 49, 271–275.

Rigol, A., Vidal, M., Rauret, G., 2002. Overview of the effect of organic matter on soil-radicaesium interaction, implications in root uptake. Journal of Environmental Radioactivity 58, 191–216.

Rishirumuhirwa T (1997) Rôle du bananier dans le fonctionnement des exploitations agricoles dans les hauts plateaux de l'Afrique orientale (application au cas de la région Kimiro-Burundi). Lausanne : Thèse doctorale, École polytechnique fédérale, 320 p.

Ritchie, J. C., & McCarty, G. W., 2003. 137Cesium and soil carbon in a small agricultural watershed. Soil and Tillage Research, 69(1), 45-51.

Roose E (1996) Méthodes de mesure des états de surface du sol, de la rugosité et des autres caractéristiques qui peuvent aider au diagnostic de terrain des risques de ruissellement et d'érosion, en particulier sur les versants cultivés des montagnes. Bull Réseau Erosion, 16: 87-97.

Roose E (1996) Land Husbandry -Components and strategy. 70 FAO Soils Bulletin, Food & Agriculture Organization of the UN, Rome, Italy.

Roose E (1993) Erosion: a current environmental problem. The GCES, a new strategy for fighting erosion to resolve this dilemnia of a growing society. In: S. Wicherek (Editor),

Farm and land erosion: in temperate plains environment and hills. Elsevier Science Publisher, Amsterdam, 571-585.

Roose E (1994) Introduction à la gestion conservatoire de l'eau, de la biomasse et de la fertilité des sols (GCES). Bulletin Pédologique FAO 70 (Rome) : 420 p.

Roose E, Smolikowski B (1997) Comparaison de trois techniques de mesure de l'infiltration sur fortes pentes : monocylindre et 2 simulateurs de pluies. Application à un versant de la vallée de Godim au Cap Vert. Bull. Réseau Erosion 17, ORSTOM, Montpellier, France : pp 282-296.

Rose CV, Williams JR, Sander GC, Barry DA (1983) A mathematical model of soil erosion and deposition process. I. Theory for a plane element. Soil Sci Soc Am J 47:991–995.

Rozos D, Skilodimou HD, Loupasakis C, Bathrellos GD (2013) Application of the revised universal soil loss equation model on landslide prevention. An example from N. Euboea (Evia) Island, Greece. Environ Earth Sci DOI 10.1007/s12665-013-2390-3.

Sabir M, Roose E, Ouagga T, Bensalah N, Dore L (2007) Utilisations des terres et risques de ruissellement et d'érosion dans les montagnes au Maroc, Actes des JSIRAUF, Hanoi, 6-9 novembre 2007, 6p.

Sabir M, Barthès B, Roose E (2004) Recherche d'indicateurs des risques de ruissellement et d'érosion sur les principaux sols des montagnes méditerranéennes du Rif occidental (Maroc). Sécheresse 2004 ; 15. pp : 105-110.

Sabir M (1986) Ressources en Eau et Aménagement. L'érosion hydrique et sa quantification. Mémoire de DEA, Université de Paris, France, 145 p.

Sadiki A., Faleh A., Zezerze J.L. (2009) Quantification de l'erosion en nappe dans le bassin versant de l'Oued Sahla, Rif occidental Maroc. Cahiers géographiques, N6, 59-70.

Sadiki A, Faleh A, Navas A, Bouhlassa S (2007) Assessing soil erosion and control factors by the radiometric technique in the Boussouab catchment, Eastern Rif, Morocco. Catena 71 (1), 13-20.

Sadiki A, Bouhlassa S, Auajjar J, Faleh A and Macaire J (2004) Utilisation d'un SIG pour l'évaluation et la cartographie des risques d'érosion par l'Equation universelle des pertes en sol dans le Rif oriental (Maroc) : cas du bassin versant de l'oued Boussouab, Bulletin de l'Institut Scientifique, Rabat, section Sciences de la Terre, 26, 2004, 69-79.

Saygin SD, Ozcan AU, Basaran M, Timur OB, Dolarslan M, Yilman FE, Erpul G (2014) The combined RUSLE/SDR approach integrated with GIS and geostatistics to estimate annual sediment flux rates in the semi-arid catchment, Turkey. Environ Earth Sci 71:1605-1618.

Sarkar S, Kanungo D, Patra A, Kumar P (2006) Disaster mitigation of debris flows, slope failures and landslides. GIS based landslide susceptibility mapping- a case study in Indian Himalaya. Universal Academy Press, Tokyo, Japan, pp 617-624.

Schmidt J (1991) A mathematical model to simulate rainfall erosion. Erosion, transport and deposition processes-theories and models. Catena 19:101–109.

Schmitter P, Dercon G, Hilger T, Thi Le Ha T, Huu Thanh N, Lam N, Duc Vien T, Cadisch G (2010) Sediment induced soil spatial variation in paddy fields of Northwest Vietnam. Geoderma 158, 298-307.

Schmitt LK (2009) Developing and applying a soil erosion model in a data-poor context to an island in the rural Philippines, Environ. Dev. Sustain., 11, 19–42.

Schoorl JM, Boix Fayos C, de Meijer RJ, Van der Graaf ER, Veldkamp A (2004) The 137Cs technique applied to step Mediterranean slopes (Part I), the effects of lithology, slope morphology and land use. Catena 57, 15–35.

Shakhashiro A, Mabit L (2009) Results of an IAEA inter-comparison exercise to assess 137Cs and total 210Pb analytical performance in soil. Appl. Radiat. Isot. 67 (1), 139-146.

She D, Fei Y, Liu Z, Liu D & Shao G (2014) Soil erosion characteristics of ditch banks during reclamation of a saline/sodic soil in a coastal region of China: field investigation and rainfall simulation. Catena, 121, 176-185.

Shin GJ (1999) The analysis of soil erosion analysis in watershed using GIS", Ph.D. Dissertation, Department of Civil Engineering, Gang-won National University.

Sogon S. (1999). Erosion des sols cultivés et transport des matières en suspension dans le bassin versant de Brie (Application des traceurs radioactifs naturels et magnétiques).Thèse de Doct. Université de Paris I-Panthéon-Sorbonne, U.F.R. de Géographie.304p.

Smith RE, Goodrich DC, Quinton JN (1995) Dynamic, distributed simulation of watershed erosion: the KINEROS2 and EUROSEM models. J Soil Water Conserv 50:517–520.

Stewart B, Woolhiser D, Wischmeier W, Caro J, Frere MH (1975) Control of water pollution from cropland, United States Department of Agriculture, United States.

Sutherland RA (1996) Caesium-137 soil sampling and inventory variability in reference locations: a literature review. Hydrological Proceedings 10, 43-53.

Suzen ML, Doyuran V (2003) A comparison of the GIS based landslide susceptibility assessment methods: multivariate versus bivariate. Environ Geol 45:665-679.

Tahiri M., Tabyaoui H., El Hammichi F. (2014) Evaluation et Quantification de l'Erosion et la Sédimentation à Partir des Modèles RUSLE, MUSLE et Déposition Intégrés dans un

SIG. Application au Sous-Bassin de l'Oued Sania (Bassin de Tahaddart, Rif nord occidental, Maroc). European Journal of Scientific Research, Vol. 125, No 2, 157-178.

Tamene L, Park SJ, Dikau R, Vlek PLG (2006) Analysis of factors determining sediment yield variability in the highlands of northern Ethiopia. Geomorphology 76: 76-91.

Tesfahunegn G B (2013) Soil quality indicators response to land use and soil management systems in northern Ethiopia's catchment, Land Degrad. Dev., doi:10.1002/ldr.2245.

Thieken AH, Lucke A, Diekkruger B, Richter O (1999) Scaling input data by GIS for hydrological modeling. Hydrol. Proc. 13, 611–630.

Tian YC, Zhou YM, Wu BF, Zhou WF (2009) Risk Assessment of Water Soil Erosion in Upper Basin of Miyun Reservoir, vol. 57. Environmental Geology, Beijing, China, pp. 937-942.

Tiessen, K.H.D., Li, S., Lobb, D.A., Mehuys, G.R., Rees, H.W., Chow, T.L., 2009. Using repeated measurements of 137Cs and modeling to identify spatial patterns of tillage and water erosion within potato production in Atlantic Canada. Geoderma 153, 104-118.

Torri, D., Santi, E., Marignani, M., Rossi, M., Borselli, L., Maccherini, S. (2012) The recurring cycles of biancana badlands: erosion, vegetation and human impact. Catena 90, 76–86.

Tribak A., El Garouani A. & Abachour M. (2012) Water erosion in tertiary marl series of the Oriental Prérif (Morocco): agents, processes and quantitative evaluation. Rev. Mar. Sci. Agron. Vét. 1 :47-52.

Valentin C, Agus F, Alamban R, Boosaner A, Bricquet GP, Chaplot V, de Guzman T, de Rouw A, Janeau JL, Orange D, Phachomphonh K, Do Duy Phai, Podwojewski P, Ribolzi O, Silbera N, Subagyono K, Thiébaux JP, Tran Duc Toan, Vadari T (2008) Runoff and sediment losses from 27 upland catchments in Southeast Asia: impact of rapid land use changes and conservation practices. Agriculture, Ecosystems and Environment 128, 225–238.

Valentin C, Poesen J, Yong L (2005) Gully erosion: impacts, factors and control. Catena 63:132–153.

Vanwalleghem T, Poesen J, Van Den Eeckhaut M, Nachtergaele J, Deckers J (2005) Reconstructing rainfall and land use conditions leading to the development of old gullies. The Holocene 15 (3), 378- 386.

Van der Knijff JM, Jones RJA and Montanarella L (2000) Soil Erosion Risk Assessment in Europe, EUR 19044 EN, 34p.

Van Westen CJ (1993) Application of geographic information systems to landslide hazard zonation. ITC publ. no. 15, Int. Ins. for Aerospace and Earth Res. Surv, Enschede, The Netherlands, p 245.

Vezena K, Bonn F (2006) Modélisation et analyse de la dynamique spatio-temporelle des relations société − érosion et pollution diffuse en milieu agricole − étude de cas en Vietnam et au Québec ; Interaction Nature-Société, analyse et modèles. UMR6554 LETG, LaBaule, 6p.

Visser H, de Nijs T (2006) The Map Comparison Kit. Environmental Modeling & Software 21, 346-358.

Vrieling A (2006) Satellite remote sensing for water erosion assessment: A review, CATENA, pp. 2-18.

Wachal DJ (2007) Integrating GIS and erosion modeling − A tool for watershed management, ESRI international user conference, Paper N° UC1038, 11p.

Walkley A, Black I.A (1934) An examination of the Degtjareff method for determining soil organic matter and a proposed modification of the chromic acid titration method. Soil Sci., 34, pp: 29-38.

Wallbrink P.J., Murray A.S. (1993). Use of fallout nuclides as indicators of erosion processes, Hydrol. Process. 7:297–304.

Wang Q, Wang S, Yu X (2011) Decline of soil fertility during forest conversion of secondary forest to Chinese fir plantations in subtropical China, Land Degrad. Dev., 22, 444–452.

Walling DE, He Q, Zhang Y (2014) Conversion models and related software. In: Guidelines for Using Fallout Radionuclides to Assess Erosion and Effectiveness of Soil Conservation Strategies. IAEA-TECDOC-1741. IAEA Publication, Vienna, Austria, pp. 125-148.

Walling DE, He Q, Appleby PG (2002) Conversion models for use in soilerosion, soil-redistribution and sedimentation investigations. In: Zapata, F. (Ed.), Handbook for the Assessment of Soil Erosion and Sedimentation using Environmental Radionuclides. Kluwer, Dordrecht, The Netherlands, 111–164.

Walling DE, Quine TA (1995) The use of fallout radionuclide measurements in soil erosion investigations. In: IAEA (Ed.), Nuclear Techniques in Soil-Plant Studies for Sustainable Agriculture and Environmental Preservation. Proc. FAO/IAEA Int. Symp. Vienna, October 17-21, 1994. IAEA Proc. Series STI/PUB/947, Vienna, Austria, 597–619.

Wang H, Sassa K (2005) Comparative evaluation of landslide susceptibility in Minamata area, Japan. Environ Geol 47:956-966.

Wang G, Gertner G, Fang S, Anderson AB (2003) Mapping multiple variables for predicting soil loss by geostatistical methods with TM images and a slope map. Photogrammetric Engineering and Remote Sensing 69: 889–898.

Wang X, Yin ZY (1998) A comparison of drainage networks derived from digital elevation models at two scales. J. Hydrol. 210, 221–241.

Williams JR, Jones CA, Dyke PT (1984) A modelling approach determining the relationship between erosion and soil productivity. Tran ASAE 27:129–144.

Williams JR (1978) A sediment graph model based on an instantaneous unit sediment graph. Water Resour Res 14:659–664

Wilson JP, Lorang MS (2000) Spatial models of soil erosion and GIS. In Spatial Models and GIS: New Potential and New Models, Fotheringham AS, Wegener M (eds). Taylor & Francis: Philadelphia, PA; 83–108.

Wischmeier WH, Smith DD (1978) Predicting rainfall erosion losses: a guide to conservation planning. USDA Handbook 537, Washington.

Wemple BC, Jones JA and Grant GE (1996) Channel Network Extension by Logging Roads in two Basins, Western Cascades. Water Resources Bulletin 32 (6): 1195- 1207.

Xiaojun N, Xiaodan W, Suzhen L, Shixian G & Haijun L (2010) ^{137}Cs tracing dynamics of soil erosion, organic carbon and nitrogen in sloping farmland converted from original grassland in Tibetan plateau. Applied Radiation and Isotopes, 68(9), 1650-1655.

Xu YQ, Luo D, Peng J (2011) Land use change and soil erosion in the Maotiao River watershed of Guizhou Province. J Geogr Sci 21:243-253.

Yair A, Bryan RB, Lavee H, Schwanghart W, Kuhn NJ (2013) The resilience of a badland area to climate change in an arid environment. Catena 106, 12–21.

Yalcin A (2008) GIS-based landslide susceptibility mapping using analytical hierarchy process and bivariate statistics in Ardesen (Turkey): comparisons of results and confirmations. Catena 72, 1-12.

Yesilnacar EK (2005) The application of computational intelligence to landslide susceptibility mapping in Turkey. Ph.D Thesis Department of Geomatics the University of Melbourne, p 423.

Yjjou M, Bouabid R, El Hmaidi A, Essahlaoui A et El Abassi M (2014) Modélisation de l'érosion hydrique via les SIG et l'équation universelle des pertes en sol au niveau du bassin versant de l'Oum Er-Rbia. The International Journal Of Engineering And Science (IJES), Volume 3, Issue 8, Pages, pp: 83-91.

Yjjou M, Bouabid R, El Hmaidi A et Essahlaoui A (2012) Caractérisation topographique et climatique via le SIG du bassin versant du haut Oum Er-Rbia en amont du barrage El Hansali (SW du Moyen Atlas, Maroc), Journal of Hydrocarbons Mines and Environmental Research, 3, 2, 104-109.

Young RA, Onstad CA, Bosch DD, Andersen WP (1989) AGNPS: a nonpoint-source pollution model for evaluating agricultural watersheds. J Soil Water Conserv 44:168–173.

Zapata F (Ed.) (2002) Handbook for the Assessment of Soil Erosion and Sedimentation Using Environment Radionuclides. Kluwer Academic Publishers, The Netherlands, p. 219.

Zezere J (2002) Landslide susceptibility assessment considering landslide typology. A case study in the area north of Lisbon (Portugal). Nat Hazard Earth Syst Sci 2:73-82.

Zhang H, Yang Q, Li R, Liu Q, Moore D, He P, Ritsema CJ & Geissen V (2013). Extension of a GIS procedure for calculating the RUSLE equation LS factor. Comput. Geosci., 52, 177-188.

Zhang J H, Ni SJ & Su ZA (2012) Dual roles of tillage erosion in lateral SOC movement in the landscape. European journal of soil science, 63(2), 165-176.

Zhang JH, Su ZA & Nie XJ (2009) An investigation of soil translocation and erosion by conservation hoeing tillage on steep lands using a magnetic tracer. Soil Tillage & Research, 105, 177–183.

Zhang JH, Quine TA, Ni SJ & Ge FL (2006) Stocks and dynamics of SOC in relation to soil redistribution by water and tillage erosion. Global Change Biology, 12, 1834–1841.

Zhang XB, Higgitt DL, Walling DE (1990) A preliminary assessment of the potential for using caesium-137 to estimate rates of soil erosion in the Loess Plateau of China, Hydrol. Sci. J. 35 (1990) 267–276.

Zhang W, Montgomery DR (1994) Digital elevation model grid size, landscape representation, and hydrological simulations. Water Resour. Res. 30, 1019–1028.

Zhou P, Luukkanen O, Tokola T, Nieminen J (2008) Effect of vegetation cover on soil erosion in a mountainous watershed. CATENA 75 (3), 319-325.

Zupanc V & Mabit L (2010) Nuclear techniques support to assess erosion and sedimentation processes: preliminary results of the use of 137 Cs as soil tracer in Slovenia. *Dela*, 33(2), 21-36.